Thermoplastic Elastomers based on Polyester Recycled Tire Fibers and Ground Tire Rubber

Thèse

Siavosh Moghaddamzadeh

Doctorat en génie chimique
Philosophiae doctor (Ph.D.)

Québec, Canada

Thermoplastic Elastomers based on Polyester Recycled Tire Fibers and Ground Tire Rubber

Thèse

Siavosh Moghaddamzadeh

Sous la direction de :

Denis Rodrigue, directeur de recherche

Résumé

Ce projet porte sur la production et la caractérisation de composites hybrides basés sur un polymère thermoplastique (polyéthylène linéaire de basse densité, LLDPE) avec des fibres de polyester de pneus recyclés (RTF) mélangées avec le caoutchouc des pneus usés (GTR) avec et sans styrène-éthylène-butylène-styrène greffé d'anhydride maléique (SEBS-g-MA) comme compatibilisant. L'étude vise à améliorer les propriétés du LLDPE avec le RTF, GTR et SEBS-g-MA.

La première étape de l'étude est composée de deux parties principales. La première partie porte sur la caractérisation des RTF par spectroscopie infrarouge à transformée de Fourier (FTIR), spectroscopie des photoélectrons X (XPS), analyse thermogravimétrique (TGA), calorimétrie différentielle à balayage (DSC), microscopie électronique (SEM) et densité; tandis que la deuxième partie rapporte la morphologie des composites fabriqués à partir de différentes conditions. En particulier, l'effet de la concentration de RTF (10, 25 et 50% en poids) avec et sans 10% poids de SEBS-g-MA à différentes vitesses de vis (110, 180 et 250 rpm) en-dessous (LT) et au-dessus (HT) de la température de fusion du RTF (253°C) est étudié par extrusion double-vis suivie du moulage par injection. Les résultats montrent une meilleure distribution des particules GTR (intégrées au RTF) dans la matrice (LLDPE) avec l'augmentation du contenu en RTF dans les mélanges compatibilisés. En outre, l'augmentation de la vitesse des vis entraîne une réduction de la longueur des RTF et de la taille des GTR. Cependant, un profil HT mène à la dégradation de la matrice et du GTR.

Dans la deuxième étape du travail, une série complète de caractérisation physique (densité et dureté) et mécanique (tension, flexion et impact) des échantillons produits dans la première partie est présentée. Malgré la diminution des modules et des contraintes maximales, la résistance au choc Charpy augmente de 50% avec 50% de FTR compatibilisées et une amélioration supplémentaire de 56% à haute vitesse de rotation des vis (250 rpm). Cependant, le profil HT diminue toutes les propriétés physico-mécaniques des mélanges.

Finalement, les propriétés rhéologiques des échantillons produits lors de la première partie ont été rhéologiquement caractérisés à l'état fondu (cisaillement oscillatoire de faible

amplitude, SAOS) et solide (analyse mécanique dynamique, DMA) afin de déterminer les relations entre la mise en œuvre, la morphologie et les propriétés macroscopiques. Les résultats montrent une augmentation de l'élasticité des mélanges avec l'augmentation du contenu en RTF en présence de SEBS-g-MA surtout à des vitesses de vis élevées. Néanmoins, le profil HT présente une diminution de l'élasticité à l'état fondu, tandis que la DMA montre une augmentation de l'élasticité pour le profil LT.

Abstract

This project focuses on the production and characterization of hybrid composites based on a thermoplastic polymer (linear low-density polyethylene, LLDPE) and polyester recycled tire fibers (RTF) mixed with ground tire rubber (GTR) with and without styrene-ethylene-butylene-styrene grafted maleic anhydride (SEBS-g-MA) as a compatibilizer. The study aims at improving the properties of LLDPE using RTF, GTR and SEBS-g-MA.

The first step is composed of two main parts. The first part is the characterization of RTF via Fourier transform infrared spectroscopy (FTIR), X-ray photoelectron spectroscopy (XPS), thermogravimetric analysis (TGA), differential scanning calorimetry (DSC), scanning electron microscopy (SEM), and density; while the second part is to report on the morphology from different processing parameters. In particular, the effect of RTF concentration (10, 25 and 50 wt.%) with and without 10 wt.% SEBS-g-MA at different screw speeds (110, 180 and 250 rpm) processed below (LT) and above (HT) the RTF melting temperature (253°C) are investigated for samples produced via twin-screw extrusion followed by injection molding. The results show better GTR particles distribution (imbedded in RTF) in the matrix (LLDPE) with increasing RTF content in the compatibilized compounds. Also, increasing the screw speed leads to a reduction of RTF length and GTR sizes. However, HT profiles produced degradation of the matrix and GTR particles.

In the second step, a complete series of physical (density and hardness) and mechanical (tension, flexion and impact) characterization was performed on the samples produced in the first step. Despite lower moduli and strength, Charpy impact strength increases by 50% for compatibilized 50% RTF compounds with an additional 56% improvement at higher screw speed (250 rpm). However, HT profiles decrease all physico-mechanical properties of the samples.

Finally, the rheological properties of the samples produced in the first step are investigated in both the melt (small amplitude oscillatory shear, SAOS) and solid (dynamic mechanical analysis, DMA) states to understand the relations between processing, morphology and macroscopic properties. The results show increased elasticity with increasing RTF content

with SEBS-g-MA, especially at higher extrusion screw speeds. HT profiles lead to lower elasticity in the melt state, while DMA results show higher elasticity for LT profiles.

Table of contents

List of Tables

List of Figures

Abbreviations

AAm	Acrylamide
BR	Butadiene rubber
COPE	Copolyester
DCP	Dicumyl peroxide
DMA	Dynamic mechanical analysis
DSC	Differential scanning calorimetry
EG	Ethylene glycol
E-GMA	Ethylene glycidyl methacrylate
E-MA-GMA	Ethylene methyl acrylate glycidyl methacrylate
EPDM	Ethylene-propylene-diene-monomer
EVA	Ethylene vinyl acetate
FTIR	Fourier transform infrared spectroscopy
GTR	Ground tire rubber
HDPE	High density polyethylene
HIPS	High impact polystyrene
HMW-PE	High molecular weight polyethylene
HT	High temperature
LDPE	Low density polyethylene
LLDPE	Linear low density polyethylene
LLE	α-olefin modified linear low density polyethylene
LT	Low temperature
MA	Maleic anhydride
MA	Methyl acrylate

MAH	Maleic anhydride
MAHPP	Polypropylene grafted maleic anhydride
MAPE	Maleated polyethylene
MDPE	Medium density polyethylene
MDPE-g-GMA	Medium density polyethylene grafted glycidyl methacrylate
NR	Natural rubber
OTR	Off the road
PE	Polyethylene
PET	Polyethylene terephthalate
PET-g-PMA	Polyethylene terephthalate grafted poly (methyl acrylate)
PMDI	Polymeric methylene diphenyl di-isocyanate
PO	Polyolefin
POE	Ethylene octylene
POE	Poly(ethylene-octene)
POE-g-GMA	Polyolefin grafted glycidyl methacrylate
PP	Polypropylene
PP-g-GMA	Polypropylene grafted glycidyl methacrylate
PP-g-MA	Polypropylene grafted maleic anhydride
PS	Polystyrene
PTW	Ethylene-butyl methacrylate-glycidyl methacrylate
r-EPDM	Recycled ethylene propylene diene monomer
RPE	Recycled polyethylene
R-PET	Recycled polyethylene terephthalate
RR	Reclaimed rubber
RTF	Recycled tire fiber

RTR	Reclaimed tire rubber
SAOS	Small amplitude oscillatory shear
SBR	Styrene butadiene rubber
SBS	Styrene butadiene styrene
SEBS	Styrene ethylene butylene styrene
SEBS-g-MA	Styrene ethylene butylene styrene grafted maleic anhydride
SEBS-g-GMA	Styrene ethylene butylene styrene grafted glycidyl methacrylate
SEM	Scanning electron microscopy
SRP	Scrap rubber powder
TDF	Tire derived fuel
TGA	Thermogravimetric analysis
TMPTA	Trimethylolpropane triacylate
TPA	Terephthalic acid
TPE	Thermoplastic elastomer
TPV	Thermoplastic vulcanizate
UHMW-PE	Ultra high molecular weight polyethylene
VLDPE	Very low density polyethylene
WGRT	Waste ground rubber tire
WGTR	Waste ground tire rubber
W-PA	Waste polyamide
WPE	Waste high density polyethylene
W-PET	Waste polyethylene terephthalate
XLPE	Crosslinked polyethylene
XPS	X-ray photoelectron spectroscopy

Symbols

A	Consistency index (kPa s^m rad^{1-m})
E'	Storage modulus (MPa)
G^*	Complex modulus (MPa)
G'	Dynamic elastic modulus (MPa)
G''	Dynamic loss modulus (MPa)
m	Power law exponent (-)
n	Cross model exponent (-)
$tan\ \delta$	Tangent δ (-)
T_g	Glass transition temperature (°C)
T_α	α transition temperature (°C)
T_β	β transition temperature (°C)
α	α transition (°C)
β	β transition (°C)
γ	γ transition (°C)
δ	Phase angle (°)
δ_{max}	Phase angle maximum (°)
η	Viscosity (Pa.s)
η^*	Complex viscosity (Pa.s)
η_0	Zero shear viscosity (Pa.s)
λ	Relaxation time (s/rad)
ω	Angular frequency (rad/s)
ω_c	Crossover frequency (rad/s)

Dedication

To my beloved family,

for their unique LOVE!

To get something you never had,

You have to do something you never did …

José N. Harris!

Acknowledgments

I would like to take this opportunity to thank God for all the help and support I received from all the people without whom I would not have been able to complete this period of my life in a foreign country.

My first and sincere gratitude goes to my genius supervisor, Professor Denis Rodrigue, for his vast knowledge, inspiring guidance, his kind behavior and patience like a father when I faced troubles during my project. This PhD would never have been completed without his potent leadership.

Most importantly, I would like to express my love and gratitude to my beloved family, my mother, father and brother who encouraged and supported me to enter a new level in my life. I would also like to especially express my gratitude to my lovely wife, *Fereshteh*, for all her mental and physical support when I became disappointed about my work.

I also would like to thank my friends, colleagues and staff in the chemical engineering department at Université Laval for their collaboration, nice attitude and moral support which made my stay and studies more enjoyable.

Finally, I acknowledge the Natural Sciences and Engineering Research Council of Canada (NSERC), the Centre de Recherche sur les Matériaux Avancés (CERMA), Centre Québécois sur les Matériaux Fonctionnels (CQMF) and Center for Applied Research on Polymers and Composites (CREPEC) for technical and financial help. The technical help of our group technician, Mr. Yann Giroux, was also much appreciated.

Forewords

This PhD dissertation is mainly based on three journal papers and consists of five chapters:

In the first chapter, a general introduction on tire structure, worn tires, tire recycling, fibers in tire structure, recycled tire fibers applications and thermoplastic elastomers as well as a brief general introduction about the materials used in this work are presented. Also, a more comprehensive study on polyolefins/polyethylene terephthalate (PO/PET) blends followed by GTR filled thermoplastic elastomers is extensively discussed by reviewing the literature. The objectives of this research work are also specified at the end of this chapter.

The following three chapters present the experimental results of the work in the forms of three accepted papers. My contributions in these papers are performing the experimental works, collecting and analyzing the data and writing the manuscripts as the first author.

In chapter two, as a first step, a complete study on polyester recycled tire fibers (RTF) mixed with ground tire rubber (GTR) is presented based on Fourier transform infrared spectroscopy (FTIR), thermogravimetric analysis (TGA), differential scanning calorimetry (DSC), scanning electron microscopy (SEM) and density. Then, a series of morphological observations are investigated for linear low density polyethylene (LLDPE)/RTF mixed with GTR compounds produced through a twin-screw extruder followed by injection molding based on different processing parameters including RTF content (10, 25 and 50 wt.%), compounding screw speed (110, 180 and 250 rpm), temperature profiles for extrusion and injection molding below (LT) and above (HT) the RTF melting temperature, as well as compatibilizer (styrene-ethylene-butylene-styrene grafted maleic anhydride or SEBS-g-MA) concentration (0 and 10 wt.%). The results show well distributed GTR particles for compatibilized blends with higher GTR content and lower particles size (higher screw speed), as well as lower RTF length and GTR particles size with increase in extruder screw speed at LT profiles. However, HT profiles presented changes in the composites overall texture. This paper was accepted as:

Moghaddamzadeh S. and Rodrigue D., *"The effect of polyester recycled tire fibers mixed with ground tire rubber on polyethylene composites Part I: Morphological analysis", Progress in Rubber, Plastics and Recycling Technology*, **accepted** (2017).

In chapter three, a comprehensive study on the mechanical (tension, flexion and impact) and physical (hardness and density) properties of the produced composites mentioned in chapter two is discussed to better understand the obtained morphological results in chapter two. The mechanical results indicate that despite the decrease in all properties, Charpy impact strength improves by 50% for the compatibilized 50 wt.% RTF at an extruder screw speed of 110 rpm. Increase in compounding screw speed from 110 to 250 rpm shows improvement in tensile (13%) and Charpy impact strengths (56%) due to higher shear and lower GTR particles size at LT profiles. However, HT profiles exhibit reduction in all compounds properties due to GTR and LLDPE degradation. This paper was accepted as:

Moghaddamzadeh S. and Rodrigue D., *"The effect of polyester recycled tire fibers mixed with ground tire rubber on polyethylene composites Part II: Physico-mechanical analysis", Progress in Rubber, Plastics and Recycling Technology*, **accepted** (2017).

Chapter four is devoted to explain the processing and to relate the morphology to the macroscopic properties of all the composites produced with their rheological properties in the melt (small amplitude oscillatory shear or SAOS) and solid (dynamic mechanical analysis or DMA) states. The results show that for both states, elasticity increases with increasing GTR content, but at lower particles size (higher compounding screw speed) for compatibilized samples compared to uncompatibilized ones at LT profiles. In the case of HT profiles, the samples present more rigidity in the solid state compared to the melt state. This paper is currently submitted as:

Moghaddamzadeh S. and Rodrigue D., *"Rheological characterization of polyethylene/polyester recycled tire fibers/ground tire rubber composites"*, **accepted** (2018).

Finally, the fifth chapter contains a general conclusion of the aforementioned works followed by recommendations for future works.

Chapter 1

1. Introduction

1.1 Tire and its components

Tires are well-known as complex engineered products made from different components giving them a wide range of properties. This is coming from a combination of several dissimilar ingredients used to build the different component in a tire structure (Ramarad, Khalid, Ratnam, Chuah, & Rashmi, 2015). Around 12 components are used in a passenger (automobile) tire, while a truck tire has about 20 (Rodgers & Waddell, 2011). The main part in a tire is the rubber which is divided in two general categories: natural rubber (NR) and synthetic rubber. Synthetic rubber can be of different types such as styrene butadiene rubber (SBR), butadiene rubber (BR) and ethylene-propylene-diene-monomer rubber (EPDM). Generally, SBR is used in passenger tires, while NR is the main rubber in truck tires (Fukumori et al., 2002). Table 1.1 presents typical compositions of different tire structures.

Table 1.1. Composition (wt.%) of different tire structures (Ramarad et al., 2015).

Component	Passenger cars	Trucks/buses
Rubber/elastomer	41-48	41-45
Carbon black	22-28	20-28
Metal/steel	13-16	20-27
Textile	4-6	0-10
Additives	10-12	7-10

Tires are made from different compounds consisting of a mixture of rubbers, curing agents, processing aids and reinforcing components that are vulcanized together. Rubber crosslinking using sulphur is called vulcanization which is an irreversible chemical process discovered by Charles Goodyear in 1839 (Akiba, 1997; Rajan, Dierkes, Joseph, & Noordermeer, 2006). The crosslinked structure of rubber is formed by vulcanization when transverse bonds are connecting different rubber chains. This 3D network makes the tires elastic but insoluble (thermoset), so they cannot be reprocessed. Moreover, the presence of different elements like stabilizers, anti-ozonants and anti-oxidants make tires extremely stable and resistant to high temperatures, biodegradation and chemical reagents (Akiba, 1997; Ferrão, Ribeiro, & Silva, 2008; Roche, Ichchou, Salvia, & Chettah, 2011).

1.2 Worn tires

Increasing number of vehicles on the roads has substantially increased the number of used tires. About 800 million tires are discarded in the world annually and this is estimated to increase by 2% each year (van Beukering & Janssen, 2001). In 2015, about 279 million worn tires, the equivalent of 4653 thousand tons, were discarded in the United States alone ("2015 U. S. Scrap Tire Management Summary," 2015). Worn tires are very prone to make environmental, health and safety hazards. Landfilling was used in the past as a simple and common way to dispose of these wastes. However, this procedure was an unsatisfactory way due to the shape and impermeability of used tires which helped to hold water for a long time. Deadly diseases like malaria and dengue have been reported in this case. Also, environmental pollution by leaching toxic materials like stabilizers in water or wet soil led to bacteriological issues (Adhikari, De, & Maiti, 2000; Ferrão et al., 2008). Moreover, each worn tire has about 75% of void space which makes it difficult to either extinguish fires with water or cut off the oxygen supply (Jang, Yoo, Oh, & Iwasaki, 1998). For example, in February 1990, a high stockpile of discarded tires at the Tire King Recycling facilities in Hagersville (Ontario, Canada) caught fire and continued for 17 days before it was completely extinguished (Yang, 1993). This episode released a high amount of toxic products through the air, soil and water.

1.3 Tire recycling

In contrast to landfilling, which has now been banned by most governments, several useful methods have been used to manage waste tires. In general, waste tires are divided in two main categories: 1) the worn parts including reusable and retreaded tires, and 2) end of life tires. Recycling, energy recovery and pyrolysis are three main ways to dispose of waste end of life tires (Ramarad et al., 2015). Tire recycling is known as a promising way to dispose of scrap tires. Different procedures including ambient grinding, cryogenic grinding, wet grinding, extrusion, and abrasion methods are used to shred whole worn tires into crumbs. The conditions used in each method highly affect the average particle size, particle size distribution, and particle shape (Karger-Kocsis, Mészáros, & Bárány, 2013; Sienkiewicz, Kucinska-Lipka, Janik, & Balas, 2012). Ground tire rubber (GTR), recycled tire fiber (RTF) and steel/metal are the three main products of tire recycling. About 65% (crumb rubber), 20% (steel) and 15% (RTF or waste fluff) of the tires by weight are recovered (Anthony, 2005). Generally, GTR refers to ultrafine rubber powders having a diameter of less than 1 mm. Other denomination for GTR can be found in the literature as scrap tire powder, particulate tire rubber, crumb tire rubber, etc. (Karger-Kocsis et al., 2013). Since 50 wt.% of the whole tire is made of rubbers, it is beneficial to compound this polymer waste with other polymers to reduce the final cost of products (Ramarad et al., 2015). In this case, GTR is massively used in rubber/plastic industries to produce athletic tracks, playground surfaces and sport mats (Ferrão et al., 2008), automotive parts and new tires (Anthony, 2005), as well as different civil engineering applications (Sunthonpagasit & Duffey, 2004). Steel/metal is removed by magnets during the recycling process and has its own market (De, Isayev, & Khait, 2005; Ferrão et al., 2008), while RTF is separated by density from rubber crumb (Ferrão et al., 2008). In general, the latter is a mixture of polyester/nylon fibers and fine GTR particles which cannot be separated in tire recycling plants and represents the so-called “fluff” (Anthony, 2005). Hence, RTF wastes is contaminated by fine rubber particles which affect the fibers’ properties.

1.4 Fibers in tire structure

1.4.1 General view

The general function of textile fibres in tires is to provide stable motor vehicle performances over the required operating conditions (Pehlken & Essadiqi, 2005). They also reinforce the overall tire structure. In fact, tire cords help the tire to keep the air pressure inside and give strength to the other tire parts such as the tread and sidewall. Some specifications are essential for tire cords such as: high tensile strength, high resistance to cut and puncture, high impact resistance, good heat resistance, ability to strongly bond with rubber, low elongation, high dimensional stability and high tensile modulus. Generally, tire cords are made from polyester, aramid, rayon, steel and Nylon, where Nylon can be Nylon 6 and Nylon 66 (Gent & Walter, 2006). Generally, the fibers for a passenger tire are made of polyester (98 wt.%) and rayon (2 wt.%), while it is a mixture of polyester (61 wt.%), Nylon (2 wt.%) and steel (37 wt.%) for a truck tire (Pehlken & Essadiqi, 2005). In 1993, the ratio of consumed tire cords in North America were 55% polyester, 43% Nylon and 2% rayon (Smith, 1994). As there are different types of tires (regarding the size and use), each type of tire contains at least one type of these fibers in its structure depending on the intrinsic behavior and specification of that tire cord (Gent & Walter, 2006). Tables 1.2 and 1.3 present different types of tires and tire cords with their respective properties.

Table 1.2. Different types of tires based on their reinforcing fibers (Gent & Walter, 2006).

Tire cord	Tire type
Rayon	Racing
Nylon	Truck Heavy duty (Off The Road or OTR) Aircraft
Polyester	Radial passenger Radial light truck
Steel	Radial truck
Aramid	Radial aircraft

Table 1.3. Properties of different tire cords (Gent & Walter, 2006).

Tire cord	Advantages	Disadvantages
Rayon	High dimensional stability Low shrinkage Good handling (steering) High modulus	Expensive Environmental concerns
Nylon	Low heat generation High strength Impact resistance	Flat spotting Medium moisture absorption
Polyester	High strength Good dimensional stability Low shrinkage Inexpensive	Low heat dissipation
Steel	High strength High modulus Low elongation	High weight Possible moisture corrosion
Aramid	High strength High modulus	Very expensive

1.4.2 Polyester fiber (PET)

Polyethylene terephthalate (PET) is the most common thermoplastic resin of the polyester family which is produced by the condensation polymerization of ethylene glycol (EG) and terephthalic acid (TPA) (Gent & Walter, 2006), as described in Figure 1.1.

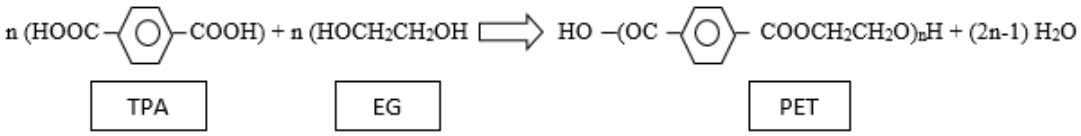

Figure 1.1. Formation of a PET macromolecule.

As discussed earlier, polyester fibers are used in radial passenger and light truck tires. In 2001, more than 99% of the used radial passenger tires and around 98% of light truck tires in the United States contained 98% polyester in their structure (Gent & Walter, 2006). In 2013 in the United States, the total amount of scrap light duty tires including passenger and light truck tires was about 240.5 million, which is the equivalent of 2705.5 thousand tons. This amount was 89.5% of the total market for scrap tires. Moreover, the total amount of disposed tires for this market increased by up to around 13% from 2005 to 2013 which reduced the amount of tire going to landfilling by up to 33.3% (“2013 U. S. Scrap Tire Management Summary,” 2013). An average weight of a new passenger tire and a worn one has been reported to be 11 and 9 kg, respectively (Pehlken & Essadiqi, 2005). The ratio between rubber, fiber and steel are different from one tire manufacturer to another. So, the exact ratio between each component, especially for scrap tires, is very difficult to determine. But the amount of fibers in these tires can be estimated as 3-5% by tire weight (Pehlken & Essadiqi, 2005). Table 1.4 presents typical polyester fiber specifications.

Table 1.4. Typical properties of polyester fibers used as tire cord (Gent & Walter, 2006).

Property	Value
Elongation at break (%)	13
Shrinkage (% at 150ºC)	2.0
Moisture regain (% at room temperature)	0.5
Density (g/cm^3)	1.38
Melting temperature (ºC)	250
Glass transition temperature (T_g) (ºC)	80

As mentioned in section 1.4.1, a tire recycling plant can contain different types of tires. As a result, the final RTF will be a mixture of different tire cords. Therefore, prior to recycling, worn tires should be categorized based on their tire cords structure (when possible). In this case, three options can be applied: 1) passenger and light truck tires plant (polyester), 2) heavy truck tire plant (Nylon), and 3) a mixed tire recycling plant (polyester and Nylon).
Identification of an unknown RTF can be done using Fourier transform infrared spectroscopy (FTIR). This method is a very useful procedure to identify the type of bonds inside a molecule by exploring the functional group of the polymer (Acevedo, Fernández, & Barriocanal, 2015). Moreover, with help of different solvents to dissolve the fibers, the unknown fiber can be identified. Based on ASTM D276, the fiber is polyester if it is insoluble in chloroform for 2 minutes at room temperature, or Nylon if it can be dissolved in boiling acetic acid in 2 minutes. Another method to differentiate between polyester and Nylon is based on their T_g, where polyesters have a glass transition temperature of around 80°C, while for Nylon 66 it is close to 55°C (Gent & Walter, 2006).

1.5 RTF applications

Although RTF has good intrinsic properties (Table 1.4), its use alone or as a secondary material in some applications is limited due to contamination with rubber powder. Though landfilling is a common way to dispose of these wastes, which represents about 10 to 50% of the whole tire weight (Anthony, 2005), the main application is TDF (tire derived fuel) as a

common conventional fuel like oil and natural gas due to a very good energy value of these fibers (Pehlken & Essadiqi, 2005).

Ferreira et al. (Ferreira, Perez, Hirayama, & Saron, 2013) studied waste polyamide (W-PA) from scrap tires to reinforce waste PET (W-PET) (25/75 wt.%). Prior to compounding W-PA/W-PET, W-PA was reinforced with different glass fiber contents (0, 5, 15 and 30%). They reported substantial increase in tensile (130%) and impact (126%) strengths at 15 wt.% glass fibers. To improve the W-PET properties, 25 wt.% of reinforced W-PA was used leading to tensile and impact strengths improvement of 18 and 17%, respectively.

Some other studies reported on using these wastes in civil engineering. Bignozzi et al. (Bignozzi, Saccani, & Sandrolini, 2000) worked on a polymer mortar using different wastes such as tire rubber, rubber powder, micronized tire fibers, and pulverized electrical cables in an unsaturated polyester resin as the matrix. Micronized tire fibers were a mixture of 50% polyester, 30% Nylon and 20% rayon. Each blend was prepared with and without 3-glycidoxypropyltrimethoxysilane as a coupling agent. Based on 1.3 wt.% of each filler in the blend, micronized tire fibers showed the lowest elastic modulus even in the presence of a coupling agent. In a work done by Maderuelo-Sanz et al. (Maderuelo-Sanz, Nadal-Gisbert, Crespo-Amorós, & Parres-García, 2012), a sound absorber with RTF at different thicknesses was made. It was reported that RTF was a mixture of 72.4% GTR, 27.2% and 0.1% steel. Improvement in acoustic properties and decrease in the final product cost compared to glass wool was reported.

Martínez-Cruz et al. (Martínez-Cruz, Martínez-Barrera, & Martínez-López, 2013) worked on RTF to reinforce polymer concrete. The blend was a mixture of 70 vol.% of siliceous and 30 vol.% of polyester resin. Different RTF contents (0.3, 0.6, 0.9 and 1.2 vol.% based on sand concentration) were studied, but the addition of 1.2 vol.% RTF increased the compressive (43%) and flexural (54%) strengths, as well as the elastic modulus (18%) of the neat concrete.

Kumaran et al. (Kumaran, Lakshmipathy, & Mushule, 2011) studied the transport properties of RTF reinforced concrete. An investigation was done based on different RTF length (25, 50 and 75 mm), diameter (4, 5 and 6 mm) and concentration (0, 5, 10, 15, 20 and 25 wt.%).

It was found that above 10 wt.% RTF, some properties such as water and acid absorption were improved compared to samples without RTF. Also, at 10 wt.% RTF, the samples are more ductile compared to the ones without RTF which are very brittle. It was also reported that increasing RTF content with an average length of 50 mm increased the impact resistance compared to the control specimen (without RTF), where a substantial increase (47%) was reported at 10% RTF.

1.6 Polyolefins (PO)

Polyolefins (PO) are thermoplastic materials that can melt above a specific temperature and solidify after cooling. Polyethylene (PE) and polypropylene (PP) are the two main classes of PO. PE is known as one of the most commonly used thermoplastics in the world. It has the simplest structure of all polymers and presents some very good properties such as toughness, almost no moisture absorption, good chemical resistance, low cost, ease of processing and low electrical conductivity (Huang et al., 2007). The mechanical and physical properties of PE highly depend on parameters such as the molecular weight distribution, the extent and type of branching and the crystal structure (Khanam & AlMaadeed, 2015). PE is produced in different forms and structures having a range of density and branching. The most used PE grades are high density polyethylene (HDPE), low density polyethylene (LDPE), linear low density polyethylene (LLDPE) and to some extent medium density polyethylene (MDPE). HDPE has long chains without main branching. This results in regular packing and high crystallinity of the polymer structure leading to higher rigidity than LDPE. When the side chains increase in number and length, LDPE is formed. The long branches form irregular packing in the polymer structure decreasing crystallinity. Hence, LDPE becomes more flexible than HDPE resulting in lower tensile and compressive strengths (Klyosov, 2007; Vasile & Pascu, 2005). LLDPE, compared to LDPE, has side chains on the backbone, but they are shorter in length. This phenomenon let branches to slide by one another upon elongation without becoming entangled. Therefore, LLDPE is more flexible than LDPE, but presents higher tensile strength and impact property (Robertson, 2006). MDPE has intermediate properties between LDPE and HDPE. Although it has good impact and better stress cracking resistance than HDPE, it shows lower hardness and rigidity compared to

HDPE. Less branching than LDPE but more than HDPE makes MDPE being softer than HDPE and more rigid than LDPE. Other forms of PE are high molecular weight polyethylene (HMW-PE), ultra high molecular weight polyethylene (UHMW-PE), and very low density polyethylene (VLDPE) (Klyosov, 2007; Vasile & Pascu, 2005). PP is another inexpensive thermoplastic with some good properties such as low density, high thermal stability, easy reprocessing and resistance to corrosion and fatigue. However, it has poor impact strength at low (room) temperature. Nevertheless, PP exhibits higher moduli and strengths than PE (Karger-Kocsis, 1995).

1.7 PO/PET blends

It is known that a binary blend of PO/PET is immiscible due to their structural/chemical differences. PO has a non-polar structure, while PET shows polarity due to its aromatic as well as carboxyl and hydroxyl groups (Moghaddamzadeh & Rodrigue, 2017a). Several studies have reported a two-phase morphology due to low interfacial adhesion (compatibility) between both phases resulting in poor mechanical properties of this binary blend (Lei *et al.*, 2009; Mostofi, Nazockdast and Mohammadigoushki, 2009; Asgari and Masoomi, 2012; Lei and Wu, 2012; van Bruggen *et al.*, 2016). To decrease the interfacial tension and increase the interfacial adhesion between both components, better disperse the minor phase in the matrix and improve the final properties, the presence of a third component (compatibilizer/coupling agent) with a similar structure to both PO and PET is essential. For instance, van Bruggen et al. (van Bruggen et al., 2016) reported that styrene-ethylene-butylene-styrene (SEBS) triblock copolymer can improve the interfacial adhesion between PP and PET because of the possible compatibility between the styrene groups in SEBS with PET and the ethylene-butylene blocks with PP. On the other hand, when a compatibilizer cannot be located at the interface, the possibility to obtain maximum mechanical improvement will be limited. To improve the compatibilization effect, functional groups can be grafted on the molecular chain. Thus physical and/or chemical interactions can be improved resulting in a compatibilized blend (Heino, Kirjava, Hietaoja, & Seppala, 1997; Pracella & Chionna, 2004). Lei and Wu (Lei & Wu, 2012) reported that the addition of 2.5% ethylene-glycidyl methacrylate (E-GMA) into HDPE/PET (75/25) improved the impact

strength (148.5%) and tensile elongation at break (45%), while decreasing the tensile (20%) and flexural (10%) moduli. The reason for the improvements was associated with a possible reaction between the functional epoxy group in E-GMA and the carboxyl group in PET occurring in the melt state (compounding) to form a graft copolymer.

Satapathy et al. (Satapathy, Nando, Jose, & Nag, 2008) worked on short PET fibers (average length of 4-5 mm) to reinforce waste HDPE (WPE). Firstly, the effect of PET fiber content (10, 30, 50 and 80 wt.%) was investigated. They reported increased tensile (2, 11, 33 and 18%) and impact (52, 66, 100 and 20%) strengths, while flexural modulus decreased (47, 34, 23 and 15%) compared to WPE. In the next step, 1% maleic anhydride (MA) in the presence of 0.2% dicumyl peroxide (DCP) was grafted to WPE. For a 50 wt.% PET composite, although no significant change in the impact strength was reported, an increase in flexural modulus (37%) and tensile strength (3%) was observed. The improvement of flexural modulus was attributed to the formation of a trans-crystalline layer around the PET fibers due to the surface crystallization when PET fibers were in presence of MA-g-WPE resulting in higher composite rigidity.

Kayaisang et al. (Kayaisang, Amornsakchai, & Saikrasun, 2013) worked on recycled PET fibers to reinforce HDPE composites and produced cross-ply laminates. To improve the final properties of the blends, 5 wt.% styrene-ethylene-butylene-styrene grafted maleic anhydride (SEBS-g-MA) was used. A 57% increase in break energy, as well as increased tensile (2%) and flexural (3%) moduli were reported. Strong interfacial adhesion between the phases in the presence of SEBS-g-MA was the main reason of the final properties improvement.

In a work done by Zhang et al. (Zhang, Guo, Yu, Li, & Wu, 2007), blends of recycled PET (R-PET) and LLDPE were compatibilized with non-reactive (SEBS) and reactive (SEBS-g-MA) compatibilizers at different contents (5, 10, 15 and 20 wt.%) in R-PET/LLDPE (80/20). As reported, the tensile yield strength, flexural strength and flexural modulus were all decreased in both systems with increasing compatibilizer content. This reduction was associated to the rubbery structure of both SEBS and SEBS-g-MA. On the other hand, Charpy impact strength increased with compatibilizer content in both systems. Improvements as high as 93% (SEBS) and 222% (SEBS-g-MA) were observed at 20 wt.% compatibilizer. It was also reported that the presence of MA groups in SEBS-g-MA were able to react with

the hydroxyl groups of R-PET to form PET-co-SEBS-g-MA copolymers. Thus, increased interfacial adhesion and decreased surface tension between R-PET and LLDPE was higher compared to blends using SEBS, where only physical interactions between the phases were present. Finally, increased impact strength was reported as a result of finely dispersed LLDPE in the PET matrix.

Daneshvar and Masoomi (Daneshvar & Masoomi, 2012) improved the elongation at break (up to 133%) of MDPE/PET (65/25) blends using 10 wt.% glycidyl methacrylate grafted medium density polyethylene (MDPE-g-GMA) as a reactive compatibilizer. Morphological results showed a 300% decrease in the average PET particle size (dispersed phase) in MDPE.

In a work done by Imamura et al. (Imamura et al., 2014), recycled soft drink bottles were used to improve the compatibility between the components. PET is known as the main component of these bottles, while the caps (closures) are made from PE or PP (mainly), and polystyrene (PS) is used for the labels. The material ratio in the blends was 90, 4, 3 and 3 wt.% for PET, PE, PP and PS, respectively. E-GMA and α-olefin modified linear low-density-polyethylene copolymer (LLDPE) were used as compatibilizers. It was reported that while elongation at break and Izod impact strength of the compatibilized compounds with 10 wt.% EGMA improved by 18 and 100% compared to the compatibilized blends with LLE, the tensile modulus decreased by 5%. However, tensile strength was almost constant (40 MPa) for both compounds. This was associated to strong interfacial adhesion between the epoxy groups in EGMA and hydroxyl or carboxyl groups in PET compared to weaker interfacial adhesion between the double bonds (end groups of linear olefin molecules) which have no affinity towards PET.

Some studies used high energy radiation such as γ radiation to increase the compatibility between PET and polyolefins/elastomers. In a work done by Yin et al. (Yin, Liu, Zheng, Shen, & Deng, 2013), the elongation at break of PET/poly(ethylene-octene) (POE) blends (85/15) was improved by 50-80 times using 2 wt.% trimethylolpropane triacylate (TMPTA) with a dose of 50 kGy compared to non-irradiated PET/POE blends. A 3.4 fold increase for impact strength was also reported at lower dose (30 kGy).

Ma et al. (Ma, Wang, & Ge, 2013) performed PET surface treatment using γ-ray induced copolymerization to graft methyl acrylate (MA) monomers onto PET to improve the compatibility of PET/ethylene-methyl acrylate-glycidyl methacrylate random terpolymer (E-MA-GMA) elastomers. Formation of PET-g-poly (methyl acrylate) (PET-g-PMA) copolymer increased the compatibility of PET/E-MA-GMA blend. As reported, a 30% improvement in impact strength of the binary blend using 0.1 wt.% PET-g-PMA without any decrease in tensile strength was reported compared to the uncompatibilized blend.

The addition of inorganic nanoparticles was also shown to improve stiffness, but decreased composites toughness. Ke et al. (Ke, Jiang, Xu, Ji, & Su, 2012) improved the mechanical properties of PP/PET fibers using nano-$CaCO_3$ surface coated with stearic acid and ethylene-butyl methacrylate-glycidyl methacrylate (PTW) as a solubilizer in polymer composites. Despite reduction in flexural strength (4%) and modulus (11%), improvement in tensile strength (6%), tensile strain (56%) and notched impact strength (73%) was observed. Morphological observations showed a ductile fracture (with nanoparticle) instead of a brittle one (without nanoparticle) due to hydrogen bonding interaction between the stearic acid coating of the nano-$CaCO_3$ and PET leading to a fine PET dispersion in the PP matrix.

It was also reported that using a chain extender such as di-isocyanate can help to compensate for the PET molecular weight reduction while processing (Torres, Robin, & Boutevin, 2001). The poly-functional groups of these chain extenders (isocyanate here) can quickly react with the hydroxyl or carboxyl end groups of PET. As reported by Zhang et al. (Zhang, Guo, Zhang, & Wu, 2009), addition of 1.1 wt.% polymeric methylene diphenyl di-isocyanate (PMDI) as chain extender improved the impact strength of R-PET/LLDPE/SEBS-g-MA by 118% compared to compounds without PMDI, while reduction in tensile strength (8%) and flexural modulus (10%) was observed.

1.8 Thermoplastic elastomers (TPE)

Thermoplastic elastomers (TPE) are polymer blends consisting of two different components: at least one elastomer, presenting low rigidity and high elongation, is melt blended with one rigid thermoplastic acting as a link between the soft and flexible regions. This combination

results in new materials presenting the advantages of both phases. On one hand, TPE have mechanical properties similar to elastomers at ambient temperature, while on the other hand, the presence of the thermoplastic phase as the matrix makes them possible to be reprocessed and recycled. Above the melting point of the rigid phase (thermoplastic), a TPE can melt and flow, but behaves like an elastomer below this temperature. Generally, a TPE contains finely divided elastomer particles dispersed in a thermoplastic matrix, where these particles should be crosslinked to promote elasticity (Mandal, Chakraborty, & Siddhanta, 2014). Because of the unique characteristics (processing and properties) of TPE, demands for a wide range of applications in different industries such as automotive, building and construction have increased over the last years.

1.8.1 GTR in thermoplastic elastomers

1.8.1.1 Mechanical properties

1.8.1.1.1 GTR content

One of the best ways to increase the impact strength of a thermoplastic elastomer is by introducing waste rubber (GTR) to a TPE matrix, giving also environmental and economical features. Different aspects of GTR in terms of concentration, type, particle size and matrix adhesion play a strong role on the final properties of GTR filled thermoplastic elastomers (Naskar, De, & Bhowmick, 2002). However, a major concern is the low compatibility (poor adhesion) between GTR and TPE. Also, large GTR particles size are generally responsible for the low properties (mainly mechanical) of GTR filled thermoplastics. A high degree of crosslinking in the GTR particles is responsible for the poor adhesion with a TPE by restricting molecular diffusion through the interface resulting in low blends properties (Oliphant, Rajalingam, & Baker, 1993). Using a third component with a similar structure to both GTR and matrix; i.e. a compatibilizer/coupling agent, is necessary to improve the interfacial adhesion and final blends properties (Moghaddamzadeh & Rodrigue, 2017a). Compatibilization can be done using physical and chemical techniques, where chemical methods can be classified as reactive and non-reactive compatibilizations. To do so, some

studies have been done on the chemical compatibilization of GTR in thermoplastic elastomers using non-reactive compatibilizers as presented next.

Wang et al. (Wang, Lang, Li, Du, & Wang, 2014) worked on the compatibility of HDPE/waste GTR (WGTR) using different contents of styrene-butadiene-styrene (SBS) block copolymers as a non-reactive compatibilizer. It was reported that while the tensile strength of the compatibilized compounds was almost constant for the different SBS concentration studied, hardness (about 90 shore A) and elongation at break (about 360%) were shown to have a maximum around 12 phr SBS in the blends.

In another work done by Wang et al. (Wang, Zhang, Du, & Wang, 2012), thermoplastic elastomers based on high impact polystyrene (HIPS)/ethylene-vinyl acetate copolymer (EVA)/waste ground rubber tire (WGRT) (25/5/70) powder composites were compatibilized by SBS (0, 3, 6, 9, 12 and 18 phr). It was reported that for 12 phr SBS, the tensile strength and elongation at break were improved by 145 and 280%, respectively. Also, a well-defined droplet morphology was observed for this blend.

Formela et al. (Formela, Korol, & Saeb, 2015) studied the compatibility of thermoplastic elastomers based on LDPE/GTR with non-polar elastomers including SBS block copolymers with different topologies (linear/branched) and partially cross-linked butyl rubber as a compatibilizer. It was reported that for the compounds prepared via co-rotating twin-screw extrusion at different LDPE/GTR ratio and constant elastomer content, although the morphological analysis presented GTR particles encapsulated within the elastomer phase, the mechanical properties were increased by strong interfacial interactions between GTR and LDPE in the presence of SBS. But cross-linked butyl rubber exhibited partial compatibility with LDPE and low compatibility with GTR particles.

Magioli et al. (Magioli, Sirqueira, & Soares, 2010) studied the mechanical properties of PP/GTR and PP/styrene-butadiene copolymer/GTR blends. Higher modulus values were obtained for the PP/GTR blends compared to the compatibilized blends with SBR. It was reported that these observations are mainly the result of higher crosslink density in PP/GTR compounds because of the lower amount of rubber, as well as the presence of fillers in GTR.

Besides non-reactive compatibilization, several works have been published on the compatibility of GTR filled thermoplastic elastomers using reactive compatibilization techniques. In this case, the GTR, the thermoplastic or both phases can be functionalized by maleic anhydride (MAH), as well as chemical (peroxide initiator) or irradiation (γ ray) modifications (grafting techniques).

Tolstov et al. (Tolstov et al., 2007) studied the mechanical properties of TPE based composites using recycled HDPE as the matrix and different concentrations of EPDM/GTR as fillers. The polyethylene and rubber components were functionalized with maleic anhydride (MAH) and acrylamide (AAm) respectively, using chemical or irradiation (γ-rays) induced grafting methods. It was reported that compared to uncompatibilized compounds, tensile strength and elongation at break of the chemically grafted compatibilized blends were improved by 86 and 45%, respectively. However, the γ-irradiation technique produced an additional improvement of 16 and 95%, respectively.

Kim et al. (Kim, Lee, & Balasubramanian, 2006) used high GTR content (65%) to prepare GTR/LDPE and GTR/PP-g-MA (PP grafted maleic anhydride) (65/35) via twin-screw extrusion. Addition of SEBS-g-MA as a compatibilizer resulted in improved elongation at break for the GTR/PP-g-MA (70%) and GTR/LDPE (76%) blends. Moreover, morphological observations showed the formation of a dispersed phase with a continuous GTR matrix.

Lu et al. (Lu, Wang, & Yu, 2014) reported that increasing the GTR content in a TPV formulation (blend of PP/EPDM)/GTR led to an overall decrease in tensile and tear strengths, as well as elongation at break. But at 30% GTR with the addition of 5% PP-g-MA, the tensile strength was improved by 33% with a negligible increase in tear strength.

Kakroodi and Rodrigue (Kakroodi & Rodrigue, 2013) worked on the tensile properties of maleated polyethylene (MAPE)/GTR and HDPE/GTR compounds produced via twin-screw extrusion with high GTR concentration (50-90 wt.%). It was reported that GTR addition led to substantial reduction in mechanical properties, but MAPE/GTR blends showed better properties especially at 70% GTR compared to HDPE/GTR even with the addition of 5% MAPE. Lower homogeneity in HDPE/GTR was reported as the main reason for the lower tensile properties.

In a work done by Veilleux and Rodrigue (Veilleux & Rodrigue, 2016), SBR (GTR) (0-94 wt.%) compounds were melt-blended with PS in a co-rotating twin-screw extruder. Prior to compounding, a SBR pre-treatment was applied using a PS in toluene solution to improve compatibility. It was reported that despite reduction in tensile, flexural and hardness (shore D) properties, the density and impact strength of the surface treated composites were improved, especially for SBR concentrations above 50 wt.%.

1.8.1.1.2 GTR particle size

It is well-known that reduction in mechanical properties of GTR filled thermoplastic elastomers are due to two main factors: i) poor adhesion between the GTR and the matrix, and ii) large GTR particles size (Oliphant et al., 1993). In general, it is believed that smaller particle sizes can optimize the blend properties because of higher surface contact area (Hrdlička, Cebriá, Štefan, & Kuta, 2016; Jain, Gupta, & Nagpal, 2000). On the other hand, due to the crosslinked structure of GTR, it is highly difficult to obtain small GTR particle sizes without applying any mechanical stresses (mainly high shear) during grinding or compounding (melt blending) processes.

In a work done by Lu et al. (Lu et al., 2014), the effect of GTR particle sizes (80, 100, 140 and 200 mesh) on the mechanical properties of TPV/GTR compounds was studied. It was reported that both tensile strength and elongation at break gradually improved with decreasing GTR particles size. For example, when 200 mesh GTR (75-58 μm) was used, an increase in tensile strength (16%) and elongation at break (23%) was observed compared to blend contains 80 mesh GTR (200-150 μm). Also, more cavities were observed when the 80 mesh GTR was used compared to 200 mesh. This was explained by larger particles producing less homogeneous blends due to poor dispersion in the matrix compared to smaller particles. Moreover, larger specific surface area for smaller GTR powders was responsible for improved interfacial adhesion and better mechanical properties for the 200 mesh GTR blends.

Tantayanon and Juikham (Tantayanon & Juikham, 2004) reported that the Izod impact strength of neat PP was improved by 20% at 30% reclaimed tire rubber (RTR) concentration using 40 mesh (about 0.42 mm) particles, while only a 6% increase was obtained at 8 mesh (about 2.38 mm) and 16 mesh (about 1.19 mm). This improvement was related to the smaller rubber particles size resulting in higher surface contact area with the matrix.

In a work done by Yazdani et al. (Yazdani, Karrabi, Ghasmi, Azizi, & Bakhshandeh, 2011), the effects of different compounding twin-screw speed (30, 60, 90 and 120 rpm) on the mechanical properties of TPV with 15% reclaimed rubber (RR) was studied. A gradual decrease in tensile strength from about 14 to 11 MPa was reported, while the elongation at break gradually increased from 330 to 380% when the mixing speed increased from 30 to 120 rpm. It was reported that lower tensile strength was related to increased devulcanization level from 65% (30 rpm) to 88% (120 rpm) in the samples, while increased elongation at break was associated to the lower crosslink density of the devulcanized part of the blend after revulcanization.

Kim et al. (Kim, Lee, Paglicawan, & Balasubramanian, 2007) prepared TPV blends based on GTR/PP-g-MA (65/35) via co-rotating twin-screw extrusion to investigate the effect of screw configurations as well as speed (50, 70, 100, 125 and 150 rpm) on the mechanical properties of the compounds. It was reported that for the optimum screw configuration, the best results in terms of tensile strength, elongation at break and 100% modulus was obtained at 100 rpm due to higher shear rate compared to 50 and 70 rpm, as well as higher residence time compared to 125 and 150 rpm. Morphological observation presented well dispersed PP-g-MA in the matrix at 100 rpm. But above this value, the compounds had roughness on their surface. It was concluded that a balance between shear stress and residence time is controlling the dynamic reactions during compounding.

Hrdlička et al. (Hrdlička et al., 2016) studied the tensile strength and elongation at break of LDPE/GTR (50/50) (particles size of 120, 381, 492 and 650 μm) using a laboratory internal mixer. Firstly, they reported that by incorporating smaller GTR particles, both properties were improved; i.e. tensile strength and elongation at break increased by 7 and 27% respectively, for a 120 μm GTR particle size compared to 650 μm. As reported, this was related to the larger specific surface area of smaller rubber particles. Then, to improve the interfacial adhesion between the components and to achieve better properties, half of the GTR was replaced by EPDM and SEBS separately. At 25% EPDM, an improvement in the tensile strength (18%) and elongation at break (811%) was observed for 650 μm particles. But these properties increased by 52% (tensile strength) and 798% (elongation at break) when 120 μm particles were used. In the case of 25% SEBS, the tensile strength and elongation at

break increased by 17 and 377% respectively, for GTR particles size of 650 μm. However, GTR particles size of 120 μm better improved the aforementioned properties by 47 and 488%, respectively. The authors reported that, although both EPDM and SEBS improved the tensile strength in the blends at the same level, the EPDM samples exhibited a more ductile behavior due to their higher elongation at break improvement.

1.8.1.1.3 GTR degradation

Some studies have been done to investigate the effect of GTR degradation on the final properties of GTR filled thermoplastic elastomers. Scaffaro et al. (Scaffaro, Dintcheva, Nocilla, & La Mantia, 2005) worked on blends of GTR and recycled polyethylene (RPE) at different processing parameters in terms of GTR content, mixing speed, mixing time and temperature profile without any compatibilizing agent. They reported that for a constant extruder screw speed of 300 rpm and 50% GTR, a decrease in tensile strength (19%), elongation at break (27%) and tensile modulus (29%) was observed when compounding was done at 300°C compared to 180°C. GTR degradation at higher temperature was reported as the main reason for lower properties.

Si et al. (Si, Chen, & Zhang, 2013) studied the effect of GTR degradation in a revulcanized SBR/(GTR/EPDM) (70/30) blend when the temperature profile in a twin-screw extruder was increased from 180 to 260°C. Firstly, the gel content of the GTR/EPDM (80/20) was investigated. As a result, a 20% decrease in gel content was observed. Then, the binary blend was melt-blended with SBR as the matrix. For the same processing conditions, although a reduction in tensile strength from 19.5 MPa at 180°C to about 18.0 MPa at 260°C was reported, the elongation at break was increased from 380% at 180°C to 425% at 260°C. Lower tensile strength was ascribed to GTR degradation associated to reduced gel content. However, no specific reason was reported for the increased elongation at break.

Sripornsawat et al. (Sripornsawat, Saiwari, Pichaiyut, & Nakason, 2016) studied the effect of devulcanization time and temperature on the tensile properties of TPV. It was reported that for a dynamically cured devulcanized rubber (GTR)/copolyester (COPE), the tensile strength and elongation at break decreased with increasing devulcanization time and

temperature. Breakdown of the rubber structure and scission of the main rubber chains during devulcanization were reported as the reasons for the reduced tensile properties.

Jalilvand et al. (Jalilvand, Ghasemi, Karrabi, & Azizi, 2007) studied the EPDM devulcanization in a co-rotating twin-screw extruder in terms of screw speed and barrel temperature. They reported that at constant screw speed (140 rpm), the tensile strength and hardness (shore A) decreased by 7 and 10% respectively, for samples produced at 220°C compared to the ones produced at 340°C. On the other hand, the elongation at break of these blends was improved by 57% due to a 44% lower crosslink density of the EPDM.

1.8.1.2 Rheological properties

1.8.1.2.1 Melt state (small amplitude oscillatory shear or SAOS)

Addition of GTR in TPE also affects the rheological properties of the blends in both the melt and solid states. Zhang et al. (Zhang, Lu, & Liang, 2011) studied the melt rheology of waste crosslinked polyethylene (XLPE)/GTR (50/50) compounds prepared by mechanical milling (different cycles). They reported that the apparent viscosity decreased with increasing number of milling cycles, mainly due to de-crosslinking of the GTR and XLPE phase during high shear mechanical milling.

Grigoryeva et al. (Grigoryeva et al., 2005) reported that the melt viscosity of HDPE/EPDM/(GTR/bitumen) (40/25/35(1/1)) gradually decreased when the temperature increased from 180 to 200°C, mostly related to GTR degradation.

Jain et al. (Jain et al., 2000) reported that at a constant EPDM content in PP/EPDM blends, smaller EPDM particles produced higher viscosities because of greater surface area.

In a work done by Scaffaro et al. (Scaffaro et al., 2005), the viscosity of recycled PE/GTR blends was found to increase with increasing GTR content from 25 to 50% due to increased amount of crosslinked particles, but a viscosity decrease was observed for compounds produced at 300°C compared to the ones produced at 180°C as a result of GTR degradation.

Kakroodi and Rodrigue (Kakroodi & Rodrigue, 2013) studied the effect of functional groups such as maleic anhydride (MA) in MAPE on the melt rheology of MAPE/GTR compounds

and compared the results with HDPE/GTR blends without any functional groups. They reported that although HDPE has higher viscosity than MAPE, MAPE/GTR compounds presented higher viscosity compared to HDPE/GTR even at similar GTR content. This observation was associated to better interactions between MAPE and GTR particles. It was concluded that blend viscosity strongly depends on compatibility between the matrix and the filler phase.

Kakroodi et al. (Ramezani Kakroodi, Kazemi, & Rodrigue, 2013) reported increased melt viscosity for MAPE/hemp composites with GTR addition because of its crosslinked structure. Increasing GTR content from 5 to 26% increased more the melt viscosity of the blends due to increased crosslinked density in the compounds. Decreasing viscosity with increasing shear rate (pseudo-plastic behavior or shear-thinning) was observed for all the samples.

Al-Malki et al. (Al-Malki, Al-Nasir, Khalaf, & Zidan, 2013) studied the effect of GTR substitution by virgin polybutadiene rubber (BR) in HDPE. The results showed a shear-thinning behavior (decrease in viscosity with increasing shear rate) for both blends, but an increased viscosity for TPV-R (with GTR) compared to TPV-V (with BR) was related to the crosslinked structure of the GTR. Also, they reported that the presence of GTR resulted in less free volume in TPV-R than TPV-V.

Prut et al. (Prut, Kuznetsova, Karger-Kocsis, & Solomatin, 2012) studied the melt rheology of PP/GTR composites at different GTR concentration (5, 10, 15, 20 and 30%) in terms of complex viscosity and dynamic measurements (cross-over frequency or ω_c). They reported that the addition of GTR in PP resulted in higher complex viscosity (shear-thinning behavior) due to the presence of solid GTR particles (crosslinked). Additionally, although blend elasticity gradually increased with GTR addition, ω_c decreased from 63.1 to 1.6 rad/s when the GTR content increased from 5 to 30%.

In a work done by Mahallati et al. (Mahallati, Hassanabadi, Wilhelm, & Rodrigue, 2016), the rheological behavior of PP/recycled EPDM (r-EPDM) (50/50) was studied to determine the effect of twin-screw extrusion feeding strategy. For P-E blends, PP and r-EPDM were fed into the main hopper (zone 1) and side stuffer (zone 4) respectively, but E-P blends were

produced in the reverse order. They reported that although shear storage and loss moduli of both type of compounds were higher than neat PP due to the presence of the dispersed phase and the presence of an interface between both phases, no significant differences between the moduli of both blends were observed. Also, they stated that at 180°C, ω_c decreased from 12 rad/s (PP) to 6.3 rad/s (P-E) and 5.7 rad/s (E-P) indicating a more elastic behavior for E-P blends.

1.8.1.2.2 Solid state (dynamic mechanical analysis or DMA)

In a work done by Kim et al. (Kim, Ryu, & Chang, 2000), dynamic mechanical properties of compatibilized HDPE/GTR (80/20) with MAHPP (polypropylene grafted maleic anhydride) was carried out. The study was done using modified and unmodified GTR surface with acrylamide (AAm) at different GTR concentration (10, 20 and 30 wt.%). They reported that for 20 wt.% GTR, the storage modulus of the blends increased at low temperatures (between -100 and -50°C) and then decreased compared to the neat HDPE. But HDPE/20 wt.% modified GTR showed higher storage modulus compared to the blend with unmodified GTR mainly due to the increased interfacial interaction between the AAm (surface modified GTR) and the MAH (compatibilizer). Furthermore, they reported that while no damping factor peak was observed for the neat HDPE, the rubber powder-filled compounds showed a peak around -55°C related to the T_g of GTR. However, the compound with modified GTR presented lower tan δ compared to the one with unmodified rubber powder indicating less elasticity.

Li et al. (Li, Zhang, & Zahang, 2003) reported that for HDPE/SRP (scrap rubber powder) (100/40) blends, the storage modulus decreased with SRP addition and decreased even more for compounds modified with EPDM/DCP/silicon oil (10/0.2/4 wt.%) because of the presence of SRP and EPDM. Moreover, the damping factor presented two different peaks: one at -44°C (unmodified) and the other at -53°C (modified) as the T_g of the rubber phase is a good indicator of a more elastic behavior of the modified samples resulting from good interactions between SRP and matrix, as well as good dispersion inside HDPE compared to the unmodified one.

In another work done by Li et al. (Li, Zhang, & Zhang, 2004), the effect of polar (EVA) and non-polar (ethylene octylene or POE) matrices on the loss tangent of HDPE/SRP binary

blends was investigated. Firstly, they found a peak in the loss tangent of HDPE/SRP blend at -47°C associated to the T_g of SRP. Then, they reported two tan δ peaks at -47°C (SRP) and -25°C (EVA) for the HDPE/SRP/EVA blend indicating lower SRP effect on the mobility of EVA chains. But for HDPE/SRP/POE compounds, two tan δ peaks at -47°C (SRP) and -12°C (POE) were observed as the T_g of SRP and POE, respectively, showing a 20°C increase in the T_g of POE in HDPE/POE. They reported that this phenomenon was attributed to the restriction in POE chains mobility in the presence of SRP.

Lee et al. (Lee, Balasubramanian, & Kim, 2007a) reported that the addition of 10 phr SEBS and SEBS-g-MA to TPV/PP (65/35) blends, presented two shifts in loss tangent peak from -46.3°C (uncompatibilized blend) to -42.7°C (SEBS) and -40.5°C (SEBS-g-MA) as a result of good adhesion with the dispersed phase.

Magioli et al. (Magioli et al., 2010) reported an increased storage modulus for GTR/PP (70/30) blends compared to GTR/SBR/PP (30/40/30) compounds as a result of increased crosslink density of the rubber phase. Also, they reported lower loss tangent from around 0.23 for PP/SBR/GTR to around 0.18 for PP/GTR with a minor T_g shift of the rubber from -50 to -48°C indicating a restriction of the chain mobility due to the crosslinked GTR structure.

1.9 Thesis objectives and organization

Several studies have been done in the past to produce GTR filled thermoplastic compounds with and without reinforcing agents such as natural fibers, but there is almost no information in the literature on using synthetic fibers to reinforce these composites. A combination of GTR and synthetic fiber can be easily obtained as a direct product of tire recycling, where different types of fibers are used as tire cord in the tire structure for which polyester (namely as PET) is the main one in this case. Although some studies on using these waste materials as filler/reinforcement in civil engineering applications were published, there is very limited information available on the use of RTF as a filler/reinforcement to produce polymer composites. On the other hand, due to the fluffy structure (low weight and high bulk) of these wastes, almost all of them are landfilled which is an unfriendly way to use/dispose them. So,

the main objective of this thesis is to use RTF mixed with GTR as a good substitution of GTR itself as filler/reinforcement/impact modifier in thermoplastic based (here LLDPE) composites. In particular, the objectives of this research are:

1. To determine the possibility to use polyester recycled tire fibers in polymer compounds due to the low cost of production, availability and good intrinsic properties.

2. To produce and characterize polyethylene based composites based on RTF/GTR using industrial processes (extrusion/injection).

3. To quantify the effect of formulation and processing conditions using the following parameters:

    - RTF content (10, 25 and 50 wt.%);
    - compatibilizer content (0 and 10 wt.%);
    - compounding screw speed (110, 180 and 250 rpm) and,
    - temperature profiles in extrusion and injection molding below (LT) and above (HT) the melting temperature of RTF

    on the final (morphological, physical, mechanical and rheological) properties of the composites to better understand the relationships between processing, morphology and macroscopic behavior.

To address these issues, this dissertation consists of five chapters:

Chapter 1 presented general information about the tire structure, discarded tires, tire recycling, different types of fibers as tire cord in the tire structure, recycled tire fiber applications, thermoplastic elastomers and a brief overview of the materials used for this research work. Then, a literature review was presented mainly focusing on the mechanical properties of PET/PO blends, as well as the properties of thermoplastic elastomers based on GTR.

The second chapter, as the first step of the work, studies the polyester structure of RTF and the presence of GTR imbedded in them based on different characterization tools (FTIR, DSC, XPS, TGA, SEM and density). These data are important due to the lack of information (datasheet) for this material. Also, for LLDPE composites based on RTF mixed with GTR and produced by extrusion compounding followed by injection molding, a complete series of morphological observations (RTF and GTR particles size, dispersion, and adhesion) of the fractured surfaces is presented to investigate the effects of different processing parameters including RTF content, compatibilizer concentration, compounding screw speed and temperature profiles in extrusion and injection molding.

In the third chapter, a complete study on the mechanical (tension, flexion and impact) and physical (hardness and density) properties of the composites produced in chapter 2 is reported to relate these properties with the morphological analyses presented.

Chapter 4 investigates the rheological properties of all compounds produced in the second chapter in the melt (small amplitude oscillatory shear or SAOS) and solid (dynamic mechanical analysis or DMA) states to understand the relations between processing, morphology and macroscopic properties.

Finally, the fifth chapter presents a general conclusion based on the main results of this study and proposes some recommendations for future works.

Chapter 2

The effect of polyester recycled tire fibers mixed with ground tire rubber on polyethylene composites

Part I: Morphological analysis

Moghaddamzadeh S. and Rodrigue D., Progress in Rubber, Plastics and Recycling Technology, accepted (2017).

Résumé

L'effet de fibres polyester de pneus recyclés (RTF) mélangées avec le caoutchouc des pneus usés (GTR) dans le polyéthylène linéaire de basse densité (LLDPE) avec et sans styrène-éthylène-butylène-styrène greffés d'anhydride maléique (SEBS-g-MA) a été étudié. En particulier, différentes concentrations de RTF (10, 25 et 50% en poids) et de vitesses des vis d'extrusion (110, 180 et 250 rpm), ainsi que les profils de température (extrusion et moulage par injection) ont été utilisées pour optimiser les conditions de mise en œuvre. Dans cette première partie, une étude complète de la morphologie et des propriétés physiques des fibres RTF et des particules GTR a été effectuée. Les résultats montrent que les mélanges compatibilisés présentent des fibres RTF plus courtes et des tailles de particules GTR plus petites, mais une meilleure dispersion des particules de caoutchouc dans la matrice LLDPE est obtenue. En général, des températures de procédé plus faibles en extrusion et en injection mènent à une meilleure adhésion interfaciale entre les différentes composantes en raison de l'augmentation du cisaillement et de l'énergie mécanique exercée sur les différentes particules.

Abstract

The effect of polyester recycled tire fibers (RTF) mixed with ground tire rubber (GTR) in linear low-density polyethylene (LLDPE) with and without styrene-ethylene-butylene-styrene grafted maleic anhydride (SEBS-g-MA) was studied. In particular, different RTF contents (10, 25 and 50 wt.%) and compounding screw speed (110, 180 and 250 rpm), as well as temperature profiles (extrusion and injection molding) were used to optimize the processing conditions. In this first part, a complete physical and morphological analysis for the RTF fibers and GTR particles was performed. The results show that the compatibilized compounds have lower RTF length and GTR particle size, but better distribution of rubber particles in the LLDPE matrix. Overall, lower processing temperatures used in both extrusion and injection molding showed better interfacial adhesion between the components due to higher shear and mechanical energy imparted on the different particles.

2.1 Introduction

Worn tires are one of the most challenging sources of waste in the world and the amount of used tires generated every year is around 1.2 billion (Sahajwalla et al., 2011). In order to avoid discarding this material in the environment after its end of life (Adhikari et al., 2000; Ferrão et al., 2008; Naskar et al., 2002; Ramarad et al., 2015), tire recycling was developed as the main solution to manage used tires. In general, used tires can be decomposed into three main component: ground tire rubber (GTR), recycled tire fiber (RTF) and steel (Ramarad et al., 2015). Although several studies were published on the use of GTR in several polymer matrices like polyethylene (PE) (Naskar et al., 2002; Sonnier, Leroy, Clerc, Bergeret, & Lopez-Cuesta, 2006; Tolstov et al., 2007; X. Zhang et al., 2011) and polypropylene (PP) (Lee, Balasubramanian, & Kim, 2007b; Magioli et al., 2010; P Mahallati & Rodrigue, 2015; Shanmugharaj, Kim, & Ryu, 2005; W.-K. Wang, Yang, Bao, Xie, & Yang, 2011) to increase some mechanical properties such as impact strength, there is very limited information available on the use of RTF as a filler/reinforcement to produce polymer composites. Although different materials are used as tire cords in the tire structure (Gent & Walter, 2006), polyester (polyethylene terephthalate or PET) is mainly used.

Since polyolefins are non-polar while PET is polar, their blends are immiscible and heterogeneous leading to poor mechanical properties because of low compatibility between both phases (Zhang et al., 2007). To improve the interfacial adhesion and make the minor phase well dispersed in the matrix, the addition of a third component (compatibilizer/coupling agent) with a structure similar to both phases is needed (Ramezani Kakroodi et al., 2013; Zhang et al., 2007). For example, there should be good compatibility between the styrene groups in styrene-ethylene-butylene-styrene (SEBS) triblock copolymer with PET, while the same should occur between the ethylene-butylene blocks and polyethylene (van Bruggen et al., 2016). Additionally, coupling agents having maleic anhydride functional groups can react with both polyethylene and GTR (Ramezani Kakroodi, Bainier, & Rodrigue, 2012; Ramezani Kakroodi et al., 2013), as well as the hydroxyl and carboxylic end groups of PET. So, chemical and physical interactions are expected. Figure 2.1 presents the typical structure of the polymers used.

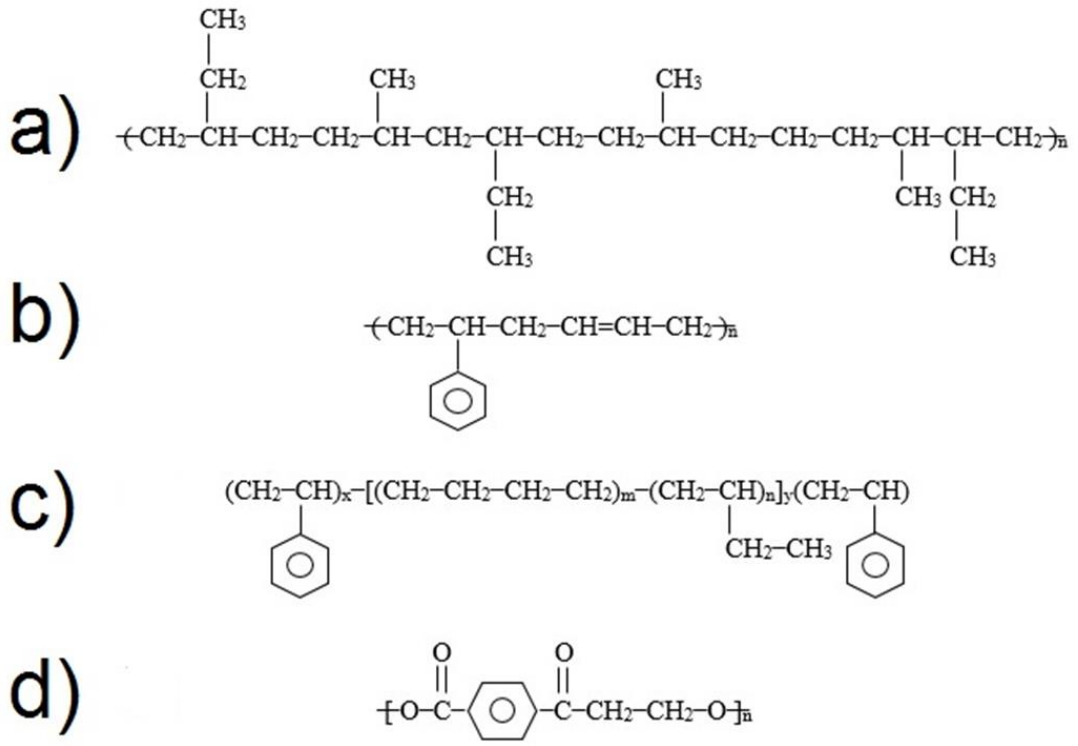

Figure 2.1. Chemical structures of the polymers used: a) LLDPE, b) Styrene Butadiene Rubber (SBR), C) SEBS and d) PET.

Since there is no specific report on the subject, this study investigates the effect of RTF content and processing conditions on the morphological properties of linear low density polyethylene (LLDPE) compounds. In particular, the RTF contains GTR particles which will affect the final properties. So, the main objectives of this first part is to investigate the changes in both uncompatibilized and compatibilized compounds in terms of: 1) GTR particle size distribution, 2) RTF fiber length distribution, and 3) the general homogeneity and physical properties of the final compounds. A complete characterization of the RTF and GTR is also presented to explain the results obtained.

2.2 Experimental

2.2.1 Materials

The matrix used for this study was LLDPE (LL8460 from ExxonMobil, Canada) in a powder form. This polymer has a peak melting temperature of 127ºC, a density of 938 kg/m^3 and a melt index of 3.3 g/10 min (190ºC/2.16 kg). The RTF was supplied by Quebec Transloc (Canada) and represents a mixture of RTF with GTR as shown in Figure 2.2 Its overall density is 1268 ± 1 kg/m^3. SEBS-g-MA (FG1901X from Kraton, USA) with a 30% polystyrene content grafted with 2% maleic anhydride was used as a compatibilizer. Its density is 910 kg/m^3 with a melt index of 22 g/10 min (230ºC/5 kg) and a melting temperature of 124°C.

Figure 2.2. General view of the polyester recycled tire fibers (RTF) mixed with ground tire rubber (GTR) as received.

2.2.2 Processing

RTF was first dried at 80ºC in an oven for 12 hours. All the compounds were melt-blended in a co-rotating twin-screw extruder Leistritz ZSE-27 with a L/D ratio of 40. For all the composites, the amount of compatibilizer was 10 wt.% based on the RTF. Three RTF contents were used: 10, 25 and 50 wt.% For the highest RTF content (50%), the effect of processing conditions on the final blends was studied first. In particular, extruder screw speed (110, 180 and 250 rpm) and temperature profiles (both extrusion compounding and injection molding) were investigated (Table 2.1). The latter was selected as to produce conditions above and below the melting temperature of the fibers (around 253°C). Tables 2.1, 2.2 and 2.3 present all the conditions studied where LT (low temperature) and HT (high temperature) are associated to samples produced below and above the melting temperature of the fibers, respectively. It is worth mentioning that the compatibilized injection molded sample with a HT profile (I-250) was extruded with a LT profile, while the compatibilized compound extruded with a HT profile (E-250) was injection molded with a LT profile.

Table 2.1. Sample coding of the compounds produced at different conditions.

Sample	LLDPE (wt.%)	RTF (wt.%)	Compatibilizer (wt.%)	Screw speed (rpm)	Temperature profile
L-1001	100	0	0	110	LT
L-901	90	10	0	110	LT
L-751	75	25	0	110	LT
L-501	50	50	0	110	LT
L-508	50	50	0	180	LT
L-502	50	50	0	250	LT
LC-901	90	10	10	110	LT
LC-751	75	25	10	110	LT
LC-501	50	50	10	110	LT
LC-508	50	50	10	180	LT
LC-502	50	50	10	250	LT
E-250	50	50	10	250	HT
I-250	50	50	10	250	HT

Table 2.2. Temperature profiles used in the extruder.

Temperature profile	Zone (°C)					
	1 to 5	6	7	8	9	10
LT	170	170	170	170	170	175
HT	170	210	250	250	260	265

Table 2.3. Temperature profiles used for injection molding.

Temperature profile	Zone (°C)			
	Rear	Middle	Front	Nozzle
LT	170	175	180	185
HT	220	260	260	250

Since the fibers were very fluffy (low bulk density), all the materials were previously dry-blending together to get better flowability and control on feeding the extruder in its first zone (main hopper). So, SEBS-g-MA was pulverized before dry-blending. This procedure was made to assure a more constant flow rate from the feeder and distribution of stresses in the extruder, but is expected to produce higher size reduction for the PET fibers and GTR particles (Mahallati & Rodrigue, 2014). At the die (2.7 mm in diameter) exit, the compounds were quenched in a water bath and later pelletized. Finally, the pellets were dried in a convection oven (forced air) for about 4 h at 75ºC to be injection molded on a Nissei PS60E9ASE machine with a mold temperature of 30°C. The mold dimensions were selected to produce directly the geometries needed for mechanical characterization as described in the second part of this study.

2.2.3 Characterization

Fourier transform infrared spectroscopy (FTIR) of RTF was performed on a Nicolet IS50 FT-IR (Thermo Scientific, Madison, USA) equipped with a MCT (mercury cadmium telluride) detector cooled with liquid nitrogen at room temperature. A Golden-Gate™ attenuated total reflection (ATR) module from Specac Ltd. (London, UK) was used to record the spectra on a diamond crystal. Each spectrum was obtained from 64 scans at a resolution of 4 cm^{-1} between 4000 and 850 cm^{-1}.

X-ray photoelectron spectroscopy (XPS) measurements on the RTF were performed on a XSAM800 XPS spectrometer (Kratos, UK) with a monochromatic Al source operated at 300 W. The size of the monochromatic X-ray beam was 800 µm × 300 µm. Survey scans were recorded with a pass energy of 160 eV and a step size of 1 eV. Binding energy scale was calibrated against standard samples: Au $4f_{7/2}$: 83.95 eV; Ag $3d_{5/2}$: 368.2 eV, and Cu $2p_{3/2}$: 932.6 eV.

Thermogravimetric analysis (TGA) of RTF was performed on a TGA Q5000 IR (TA Instruments, USA). About 9 mg of sample was placed in an aluminum pan. The measurements were performed by heating from 50 to 850°C at a rate of 10°C/min in air and nitrogen atmosphere (25 ml/min).

Differential scanning calorimetry (DSC) was done using a DSC7 (Perkin Elmer, USA) equipment under a nitrogen atmosphere. About 7 mg of sample was placed in an aluminum pan and measurements were performed by heating from 50°C to 300°C at 10°C/min in a nitrogen atmosphere, then cooling back to 50°C at 10°C/min.

Density measurement was carried out on a gas (nitrogen) pycnometer model Ultrapyc 1200e (Quantachrome Instruments, USA). The test was repeated five times for each sample.

To characterize the morphology of the raw materials and the compounds (first broken in liquid nitrogen), the surfaces were coated with gold-palladium in vacuum. Then, a scanning electron microscope (SEM) model JSM-840A (JEOL, Japan) was used at 15 kV to take images at different magnifications.

Finally, particle sizes (RTF and GTR) after processing were obtained using the following procedure: 0.5 g of each compound was dissolved in 50 cm^3 of xylene below its boiling point (around 138°C) for about 3 h. Then, the solutions were filtered using vacuum for about 45 min. The extracted materials on the filter papers were used for SEM and image analysis using the *ImageJ* software (National Institute of Health, USA).

2.3 Results and discussion

To confirm that the RTF structure is based on PET, some characterizations were done prior to compounding.

2.3.1 FTIR analysis

Figure 2.3 presents the FTIR results of RTF mixed with GTR. This test was performed to confirm that the RTF is polyester. The main groups in PET structure are carbonyl (C=O), hydroxyl (O−H) and aromatic ring. The peaks at 3410 cm^{-1} and 1711 cm^{-1} represent the hydroxyl and carbonyl groups stretching of PET, respectively, which are close to the values of 3440 and 1720 cm^{-1} reported by Holland and Hey (Holland & Hay, 2002). The peaks at 1632 and 1409 cm^{-1} represent the aromatic skeletal stretching bands. These values are close

to the values reported by Holland and Hey (Holland & Hay, 2002) as 1615 and 1410 cm^{-1}, respectively. Additionally, the peaks at 2917 and 2850 cm^{-1} represent aliphatic C− H stretching in PET and close to the values of 2960 and 2880 for neat PET as reported by Holland and Hey (Holland & Hay, 2002). Another strong peak can be seen at 1239 cm^{-1} which is related to the C(O)−O stretching of ester groups in PET and close to the value of 1270 cm^{-1} reported by Holland and Hey (Holland & Hay, 2002). The other peaks are related to GTR. For instance, the peak at 1632 cm^{-1} is related to non-aromatic C=C bond stretching of GTR reported by Liang et al. (Liang, 2015) at 1644 cm^{-1} and Zhang et al. (Zhang, Zhu, Liang, & Lu, 2009) at 1634 cm^{-1}. According to the results obtained by Miller and Wilkins (Miller & Wilkins, 1952) and Colom et al. (Colom, Andreu-Mateu, Cañavate, Mujal, & Carrillo, 2009), the peaks at 1096 and 1540 cm^{-1} are related to SiO_2 and ZnO in the GTR structure which can be found at 1090 and 1530 cm^{-1}, respectively.

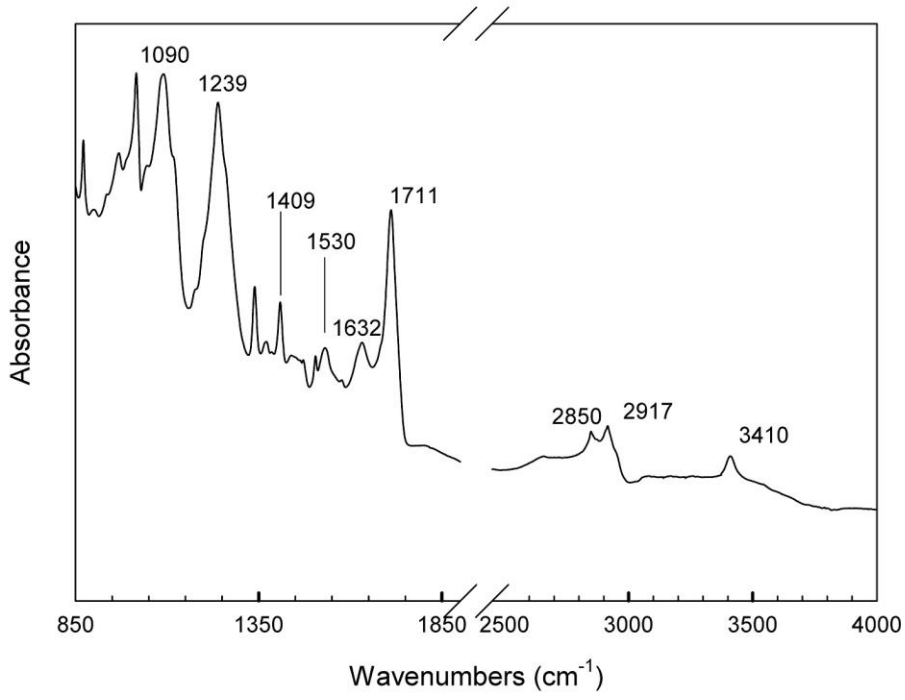

Figure 2.3. Infrared spectrum (FTIR) of the RTF mixed with GTR.

2.3.2 XPS analysis

Figure 2.4 shows the results of the XPS analysis of RTF mixed with GTR. This test was performed to investigate which atoms are present on the RTF surface. Also, this information can support the FTIR results about the presence of inorganic materials like Si and Zn in the RTF structure mixed with GTR in the form of SiO_2 and ZnO, respectively. Furthermore, two very small peaks at 225 and 345 eV can be seen. The first one is related to sulphur (S) in the GTR structure (vulcanizing agent), while the second one belongs to calcium (Ca) which can be related to the presence of calcium carbonate ($CaCO_3$) as a filler or a processing aid in the form of calcium fatty acid salts (Hoffman, 1988).

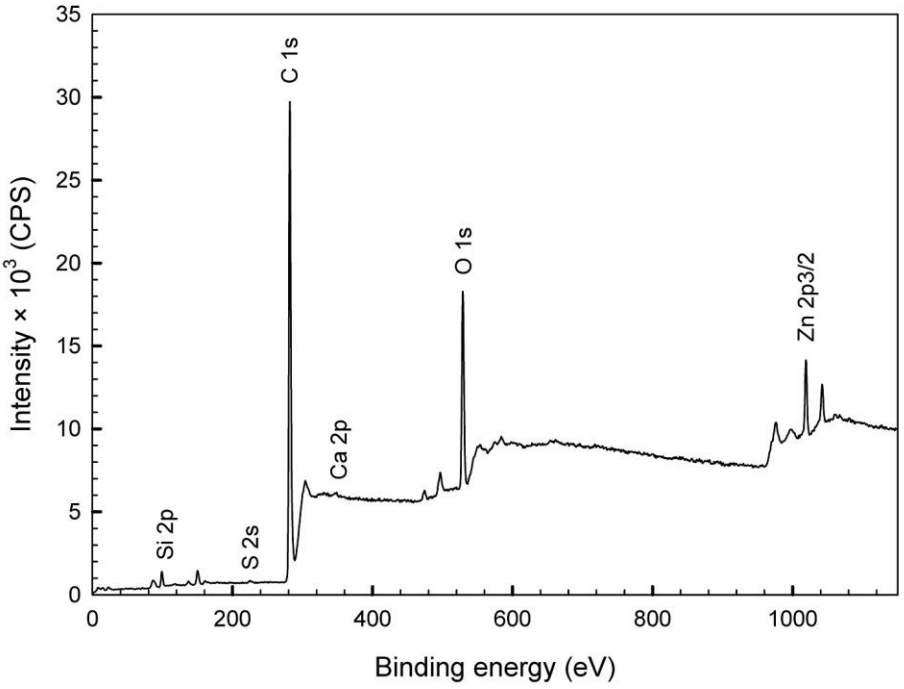

Figure 2.4. XPS analysis of the RTF mixed with GTR.

2.3.3 TGA analysis

Figure 2.5a presents the TGA results in nitrogen of the RTF mixed with GTR. First, the residues are about 29% indicating the presence of inorganic particles in RTF mixed with GTR in an inert atmosphere (nitrogen). Here, the results can be separated in two main parts: RTF and GTR. The small hump around 235°C in the derivative of the weight curve can be associated to GTR degradation. Around 8% GTR can be measured at this point. On the other hand, a wide area can be seen on the derivative curve from 300 to 425°C which is composed of two peaks. The main peak around 375°C can be related to RTF degradation (Girija, Sailaja, & Madras, 2005; Holland & Hay, 2002), while a smaller one around 425°C can be associated with the remaining content of RTF. Based on these data, about 63% RTF can be estimated. To get more information, the TGA tests were also performed in air.

Figure 2.5b reports the TGA results of RTF mixed with GTR under air. In this case, the residual weight is only 4.5%. This result confirms that there are some organic and inorganic materials imbedded in RTF and GTR reacting with oxygen. As seen in the derivative curve, between 200 and 370°C, three steps around 233, 305 and 360°C can be related to GTR decomposition. The highest decomposition temperature might be related to the formation of carbon dioxide from the oxidation of carbon residues produced at lower temperatures (Arockiasamy et al., 2013; Liang, Rodrigue, & Brisson, 2015; Sircar, 1992). Figure 2.5b, also shows that around 5% wt. was lost at 233°C, which can be associated to the amount of GTR in RTF. Also, Liang et al. (Liang, Hardy, Rodrigue, & Brisson, 2014) and Sircar (Sircar, 1992) reported that extra sulphur, organic accelerators and antioxidants in GTR are lost below 300°C. Additionally, two sharp peaks at 395 and 415°C can be related to RTF decomposition in two steps leading to a 37% weight loss. Liang et al. (Liang et al., 2014) reported the presence of inorganic compounds such as calcium, silicon and zinc in the form of $CaCO_3$, SiO_2 and ZnO in GTR, respectively. Hence, a broad peak at 488°C (13.5% weight loss) can be associated to the oxidation of these inorganic materials in GTR. So, the TGA results are in agreement with the FTIR and XPS analyses about the presence of inorganic materials in GTR mixed with RTF.

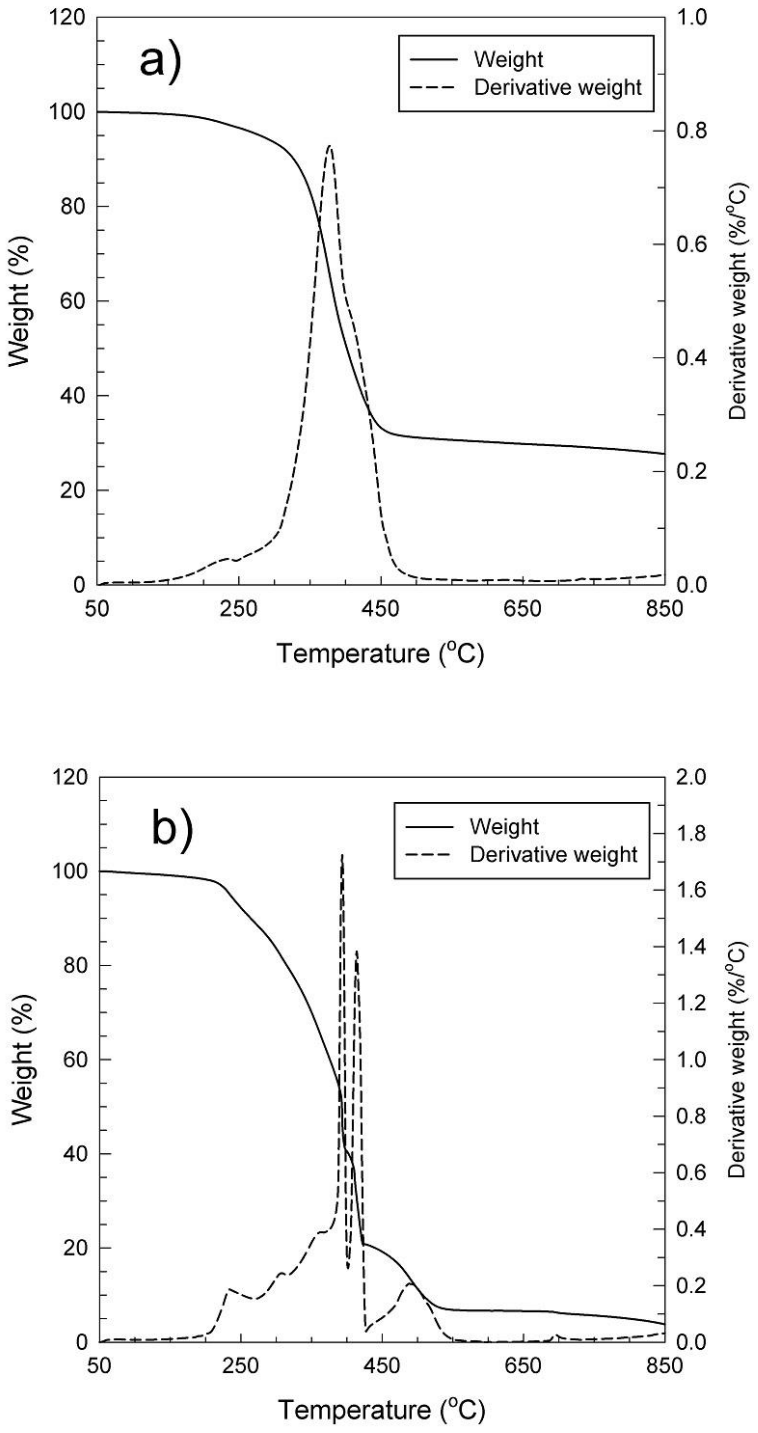

Figure 2.5. TGA results of the RTF mixed with GTR in: a) nitrogen and b) air.

2.3.4 DSC analysis

Figure 2.6 shows the DSC results of RTF mixed with GTR. To perform extrusion and injection molding at LT and HT profiles, both first and second endothermic heating were performed to determine the lower and higher temperatures of the RTF melting peak, respectively. As seen in Figure 2.6, the melting point of RTF is around 253°C which is close to the melting point of PET fibers (255°C) as reported by Gent and Walter (Gent & Walter, 2006) and Zhu et al. (Zhu, Li, Zhang, & Tanimoto, 2006). To further confirm the presence of inorganic compounds in the RTF mixed with GTR as obtained from FTIR, XPS and TGA, the cooling curve was analyzed. Zhu et al. (Zhu et al., 2006) reported in PET/SiO_2 sample prepared by cryo-milling that the crystallization temperature increased from 157 to 212°C compared to neat PET at a cooling rate of 10°C/min due to the nucleation effect of Si. He et al. (He, Shao, Zhang, Deng, & Li, 2009) also reported an increase of the crystallization temperature (from 190 to 205°C) for PET-ZnO nanocomposites compared to neat PET at a cooling rate of 10°C/min due to the nucleation effect of Zn. Hence, both peaks in the crystallization curve at 207 and 227°C can be related to the presence of Zn and Si in the forms of ZnO and SiO_2 acting as nucleating agents in RTF mixed with GTR.

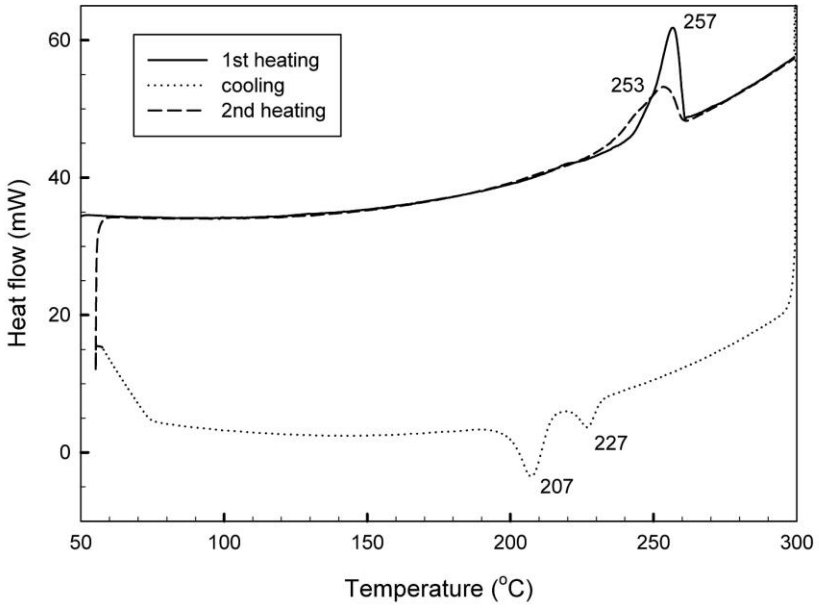

Figure 2.6. DSC results of the RTF mixed with GTR.

2.3.5 Morphological analysis of RTF and GTR

Figure 2.7 presents typical images of the RTF/GTR mixture at different magnifications. It must be mentioned that several steps are involved in the size reduction of a worn tire and each one decreases the size of both RTF and GTR particles. Due to the heterogeneous nature of this recycled material, it is difficult to obtain a specific size and distribution. Nevertheless, image analysis of the SEM images was performed and the results showed that for the material received, the RTF length is 2500 ± 1500 µm (Figures 2.7a and 2.7b) with a diameter of 20 ± 2 µm (Figure 2.7c), while the GTR particles size distribution (Figure 2.7d) is 90 ± 10 µm.

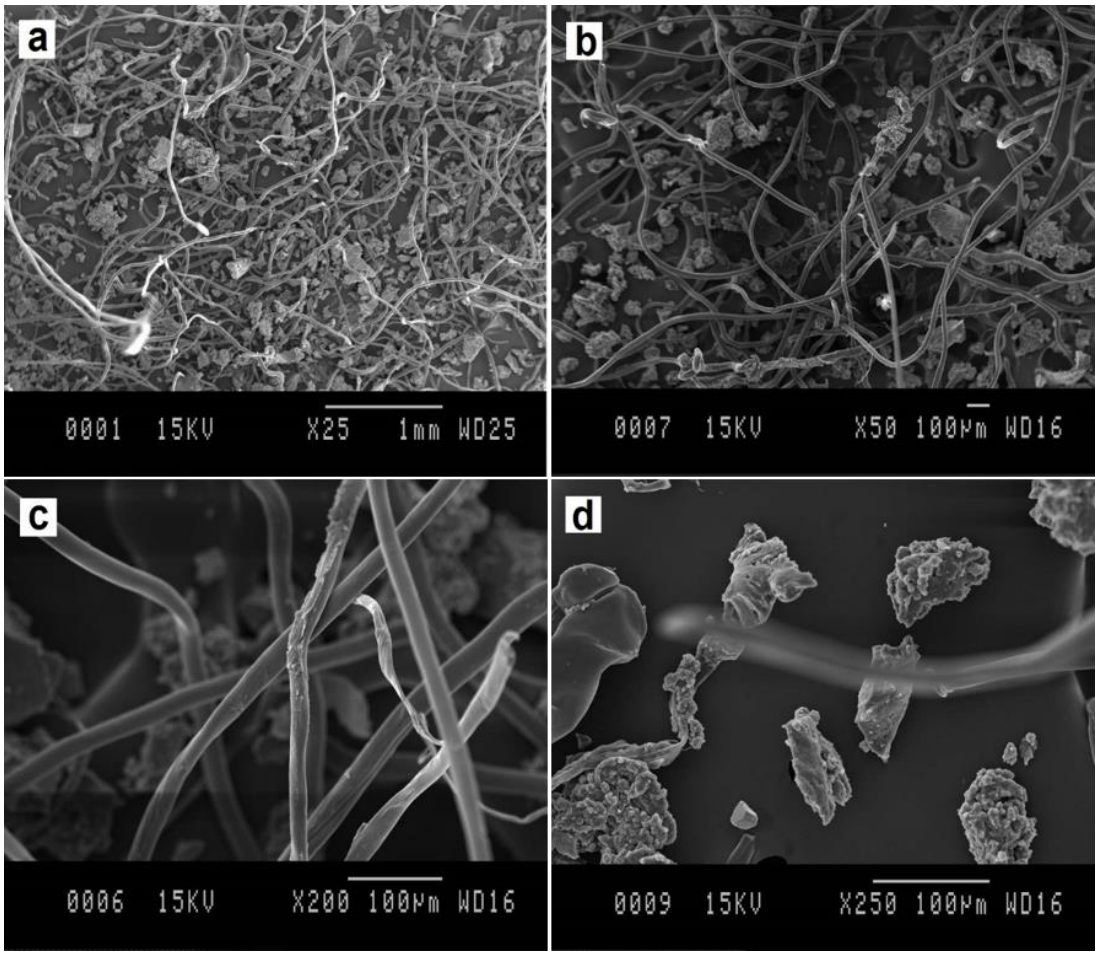

Figure 2.7. Typical SEM images of the RTF mixed with GTR at different magnifications.

2.3.6 Morphological analysis of composites

2.3.6.1 Effect of RTF content

Figure 2.8 presents different RTF content (10, 25 and 50% wt.) for both uncompatibilized and compatibilized compounds produced with an extruder screw speed of 110 rpm. It can be seen that the GTR content also increases with RTF content. Reduction in RTF length and GTR particles size occurred due to their processing (shear and elongational stresses). A comparison with the initial sizes (Figure 2.7) shows that for the compatibilized blends, the general texture of the compounds is different due to better interfacial stress transfer between GTR and LLDPE, but less of an effect for RTF. A more detailed analysis of the size distribution is presented next.

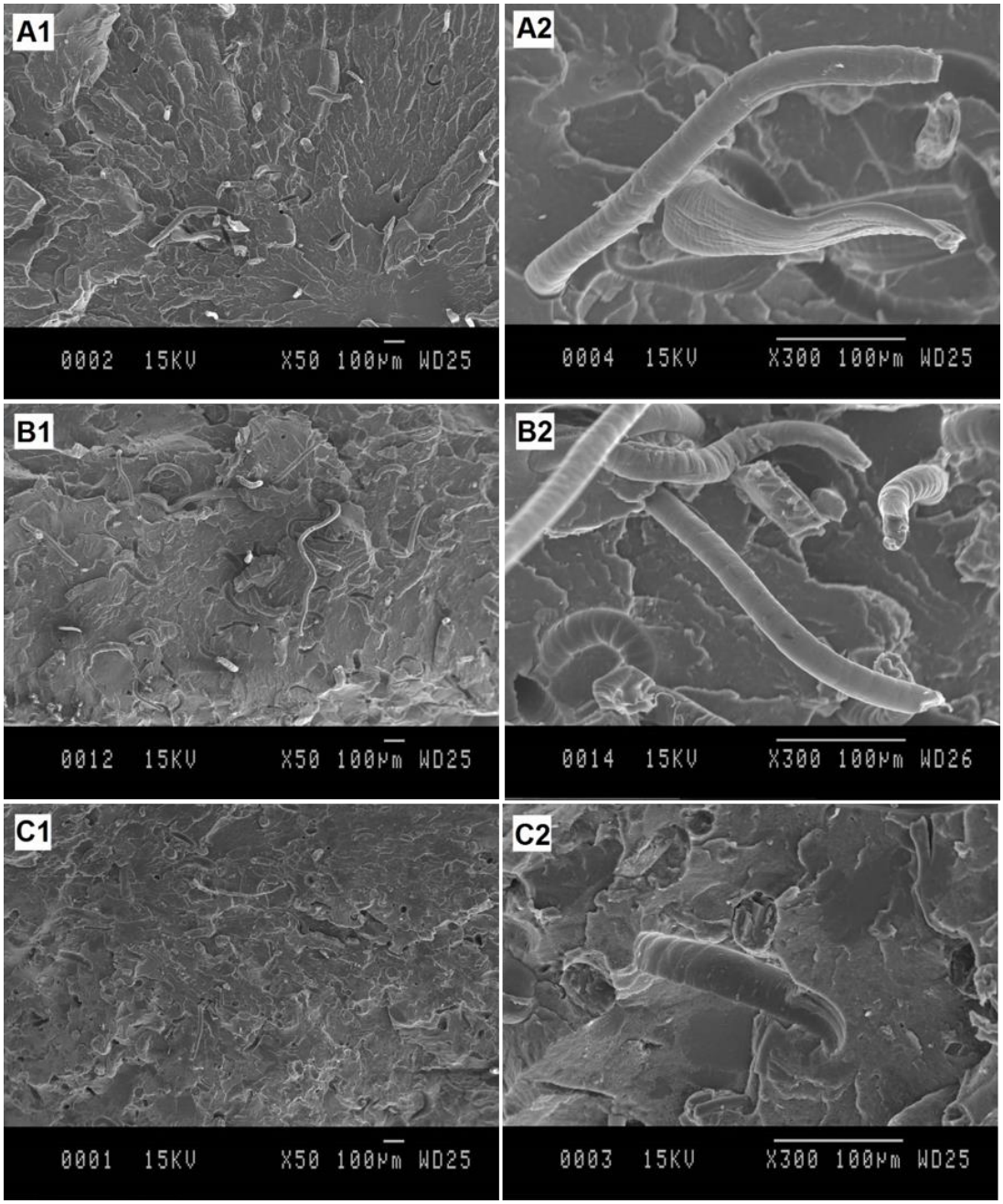
A1
0002 15KV X50 100µm WD25
A2
0004 15KV X300 100µm WD25
B1
0012 15KV X50 100µm WD25
B2
0014 15KV X300 100µm WD26
C1
0001 15KV X50 100µm WD25
C2
0003 15KV X300 100µm WD25

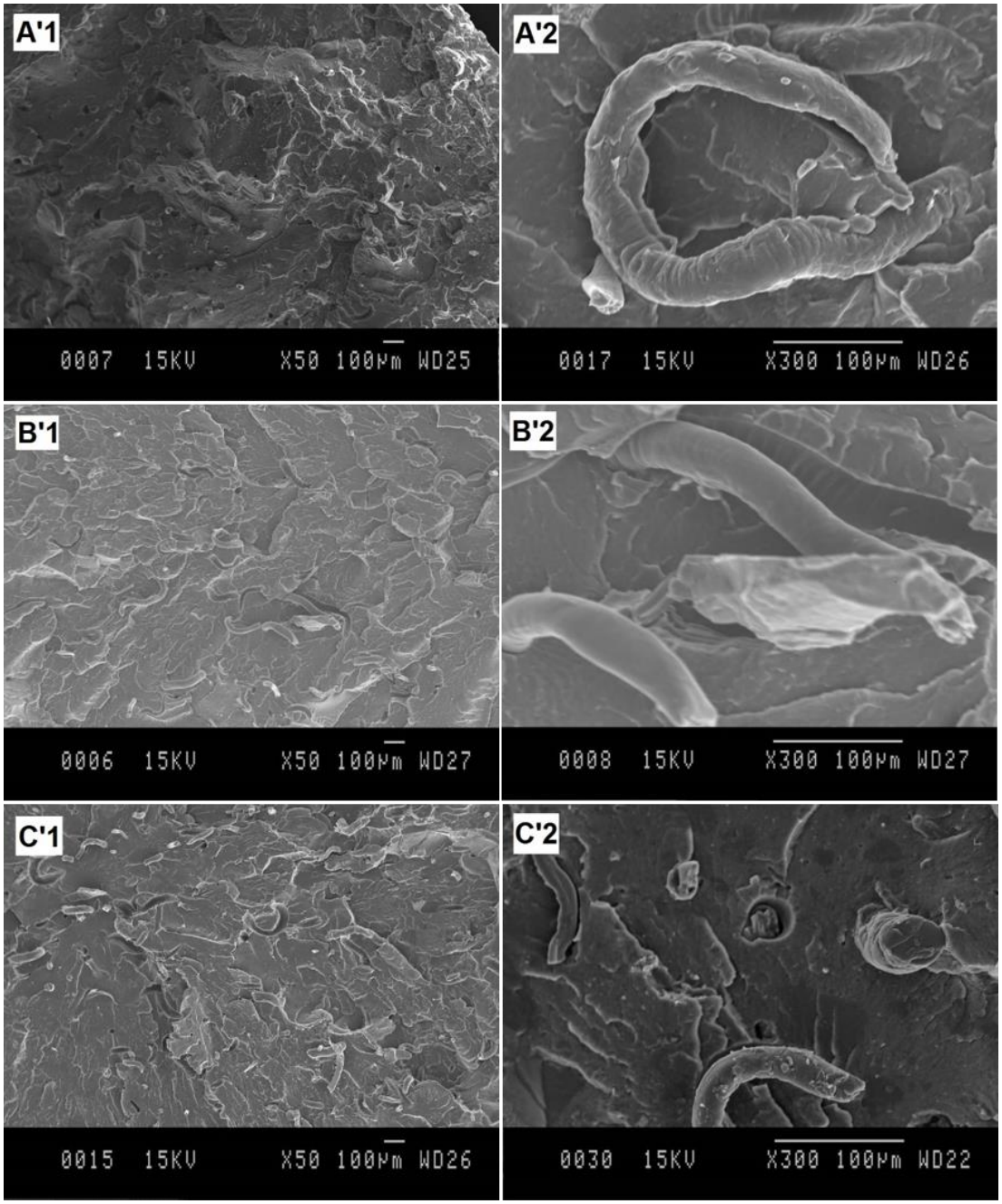

Figure 2.8. SEM images of the uncompatibilized (A, B and C) and compatibilized (A', B' and C') compounds with different RTF contents at different magnifications: A,A') 10%, B,B') 25% and C,C') 50%.

2.3.6.2 Effect of extruder screw speed

As discussed earlier, one of the objectives of this study is use a high amount of RTF as a filler in LLDPE. Figure 2.9 presents SEM images for the uncompatibilized (Figures 2.9A, 2.9B and 2.9C) and compatibilized (Figures 2.9A', 2.9B' and 2.9C') composites with 50% RTF produced at different extruder screw speeds. It is obvious that when a low speed is used (110 rpm), there is poor interfacial adhesion between RTF, GTR and LLDPE (Figure 2.9A) even in the presence of a compatibilizer (Figure 2.9A'): the fibers can be easily seen besides GTR particles. On the other hand, increasing the extruder screw speed to 180 and 250 rpm led to higher reduction in fiber length and as a result, no RTF with the same length as produced at 110 rpm can be detected inside the uncompatibilized (Figures 2.9B and 2.9C) and compatibilized (Figures 2.9B' and 2.9C') compounds produced at higher extruder speeds. Mechanical breakup reduces fiber length because of the high shear produced at higher extruder screw speeds as reported by Wall (Wall, 1989) for polyamide/glass fiber composites produced by twin-screw extrusion. Additionally, applying higher extruder speed can also decrease the size of GTR particles. As a result, better distribution of GTR particles can be seen in both uncompatibilized (Figures 2.9B and 2.9C) and compatibilized (Figures 2.9B' and 2.9C') composites, but better interfacial adhesion between GTR and LLDPE can be seen in Figure 2.9C' compared to the uncompatibilized sample (Figure 2.9C). This can be related to better interfacial adhesion as well as higher specific surface area created by producing smaller particle sizes.

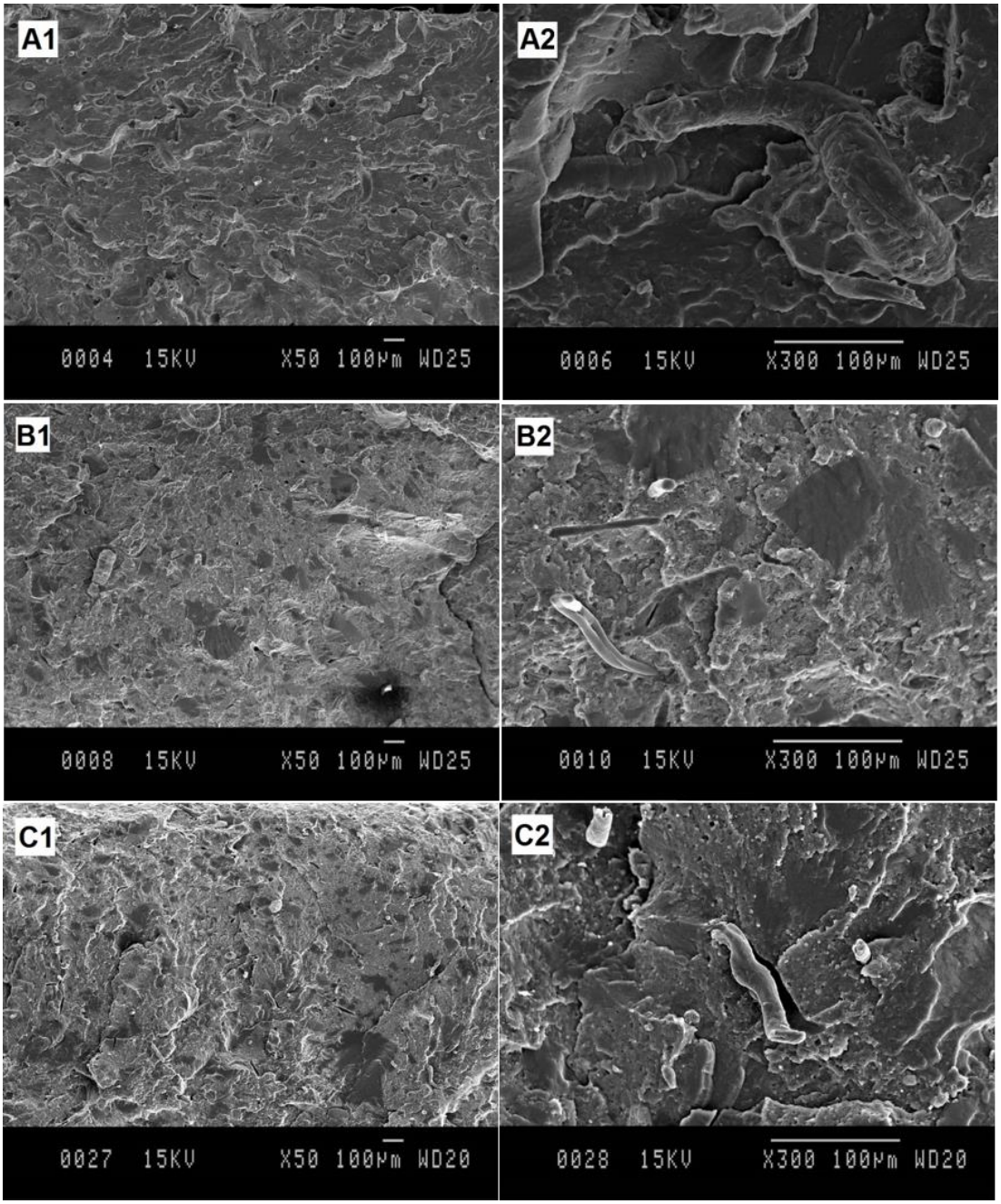
A1
0004 15KV X50 100µm WD25
A2
0006 15KV X300 100µm WD25
B1
0008 15KV X50 100µm WD25
B2
0010 15KV X300 100µm WD25
C1
0027 15KV X50 100µm WD20
C2
0028 15KV X300 100µm WD20

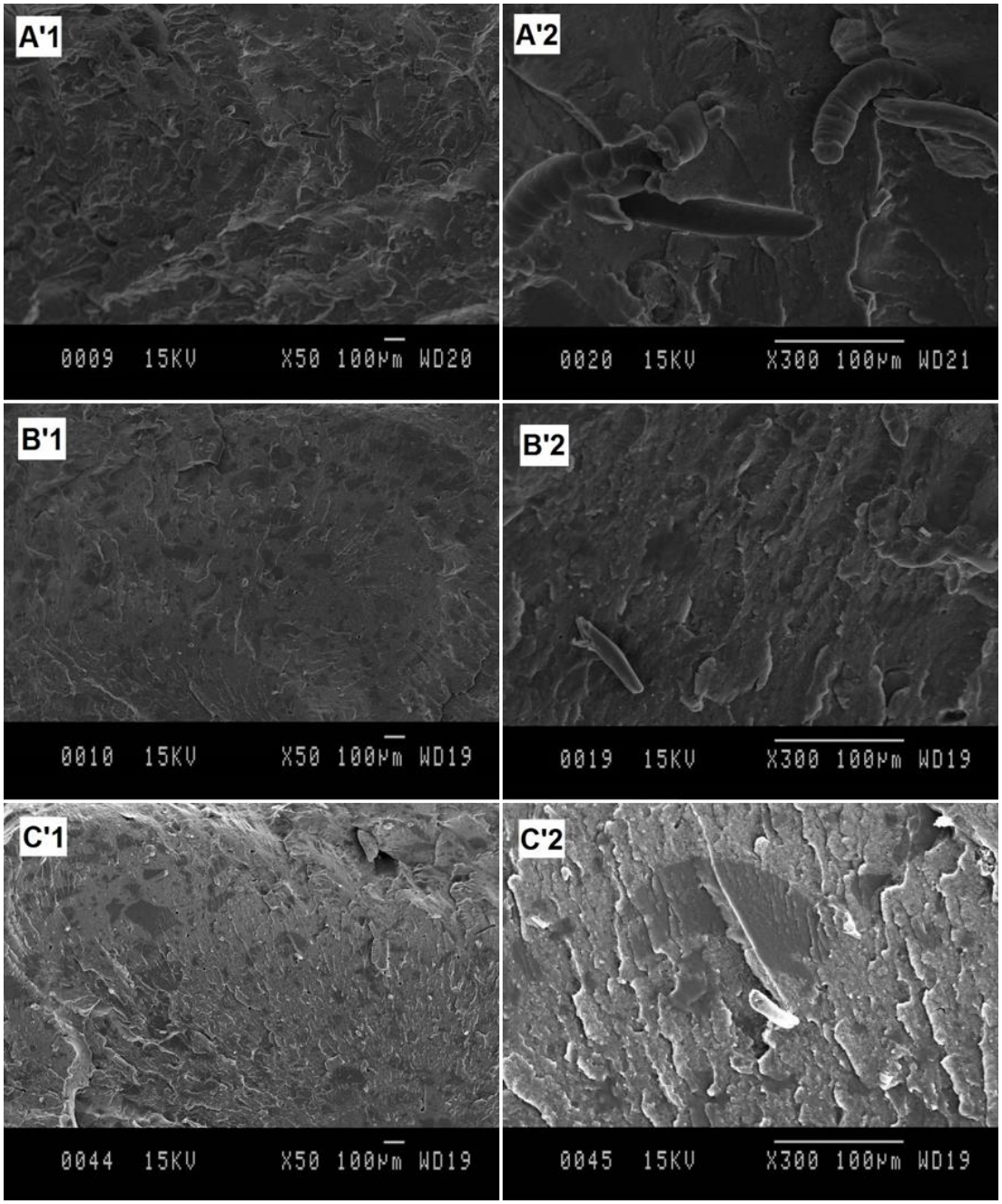

Figure 2.9. SEM images of the uncompatibilized (A, B and C) and compatibilized (A', B' and C') blends with 50% RTF at different extruder screw speeds and different magnifications: A,A') 110 rpm, B,B') 180 rpm and C,C') 250 rpm.

At 110 and 180 rpm, the RTF length of the uncompatibilized compounds is 320 ± 200 µm and 273 ± 121 µm (Figures 2.10A1 and 2.10B1), while it decreases to 188 ± 75 µm and 121

± 32 µm for the compatibilized composites (Figures 2.10A'1 and 2.10B'1), respectively. Increasing the extruder screw speed to 250 rpm led to further fiber length reduction to 169 ± 99 µm for the uncompatibilized (Figure 2.10C1) and 37 ± 5 µm for the compatibilized (Figure 2.10C'1) compounds. Higher fiber length reduction produced at different extruder screw speeds for the compatibilized composites compared to the uncompatibilized ones can be related to better interfacial stress transfer because of the presence of the compatibilizer imposing more stresses on the fibers leading to higher probability of fiber breakup. Generally, these values are much less than the 2500 ± 1500 µm reported for the original fibers. Thus, the RTF length during extrusion decreased by about 87, 89 and 93% (uncompatibilized compounds), and 92, 95 and 99% (compatibilized composites) when the extruder screw speed increased from 110 to 180 and 250 rpm, respectively. Furthermore, when the extruder screw speed increased to 250 rpm, fiber breakup for the compatibilized compounds was more important leading to RTF length smaller than the GTR particles size (Figure 2.7) and losing their "fiber" nature to become more "particles" (Figure 2.10C'1). For GTR, due to their "particle" geometry and rubbery nature (more deformable and more difficult to break), much less size reduction was observed. In general, the texture of the compatibilized GTR particles (Figures 2.10A'2, 2.10B'2 and 2.10C'2) changed compared to the uncompatibilized ones (Figures 2.10A2, 2.10B2 and 2.10C2). At 110 and 180 rpm, the GTR particle sizes of the uncompatibilized samples are 6.3 ± 2.4 µm and 6.1 ± 1.1 µm (Figures 2.10A2 and 2.10B2), while it decreases to 4.3 ± 1.1 µm and 3.8 ± 1.3 µm for the compatibilized ones (Figures 2.10A'2 and 2.10B'2), respectively. Increasing the speed to 250 rpm led to further reduction down to 4.2 ± 1.3 µm for the uncompatibilized (Figure 2.10C2) and 3.4 ± 0.8 µm for the compatibilized (Figure 2.10C'2) compounds. Similar to RTF results, higher GTR particle size reduction was produced for the compatibilized compared to the uncompatibilized blends due to better interfacial stress transfer. Nevertheless, compared to the GTR initial particle size of 90 ± 10 µm (Figure 2.7d), it is obvious that GTR particles size was decreased producing about 93, 93 and 95% (uncompatibilized), and 95, 96 and 96% (compatibilized) size reduction when the extruder screw speed increased from 110 to 180 and 250 rpm, respectively.

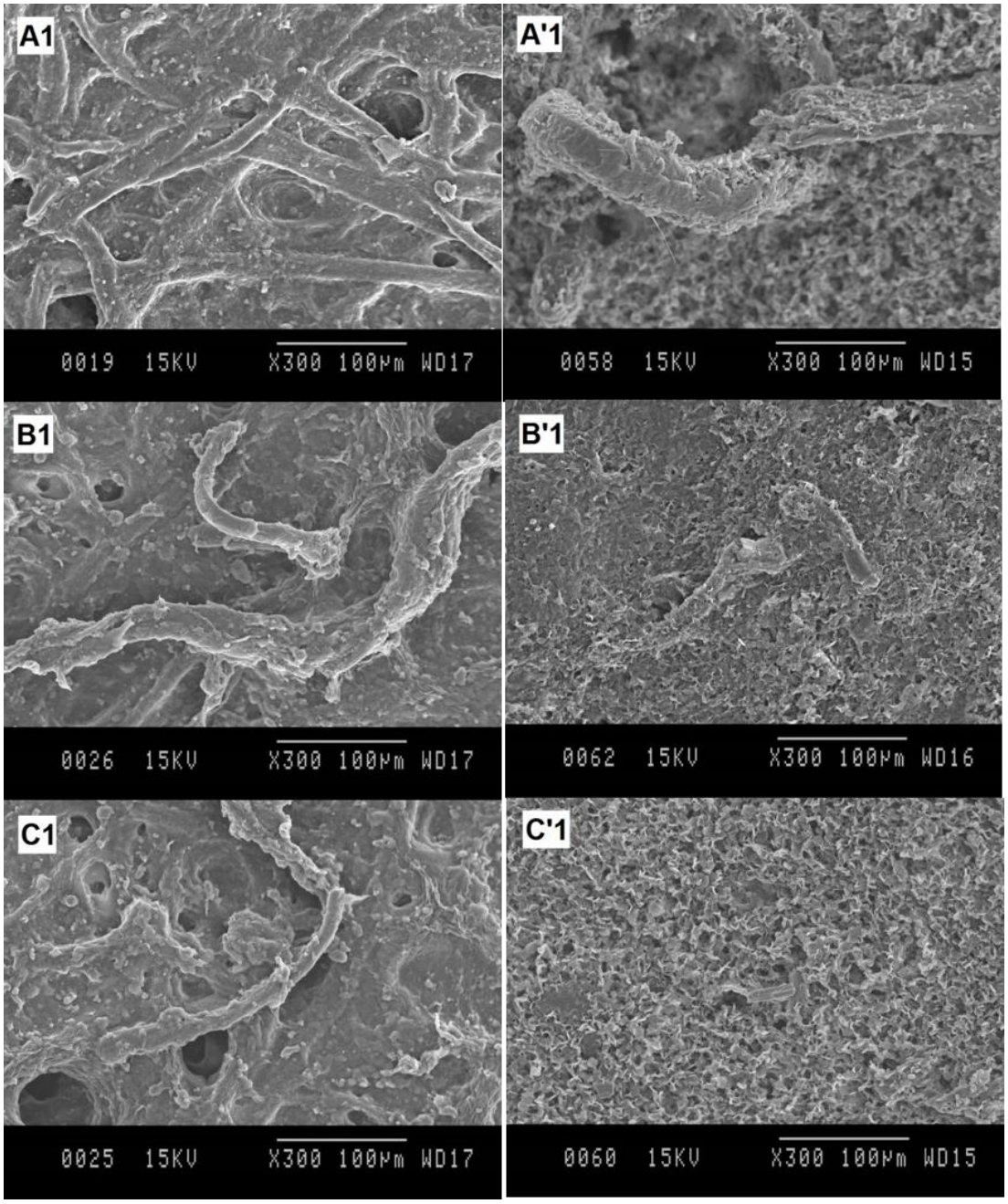
A1
0019 15KV X300 100µm WD17
A'1
0058 15KV X300 100µm WD15
B1
0026 15KV X300 100µm WD17
B'1
0062 15KV X300 100µm WD16
C1
0025 15KV X300 100µm WD17
C'1
0060 15KV X300 100µm WD15

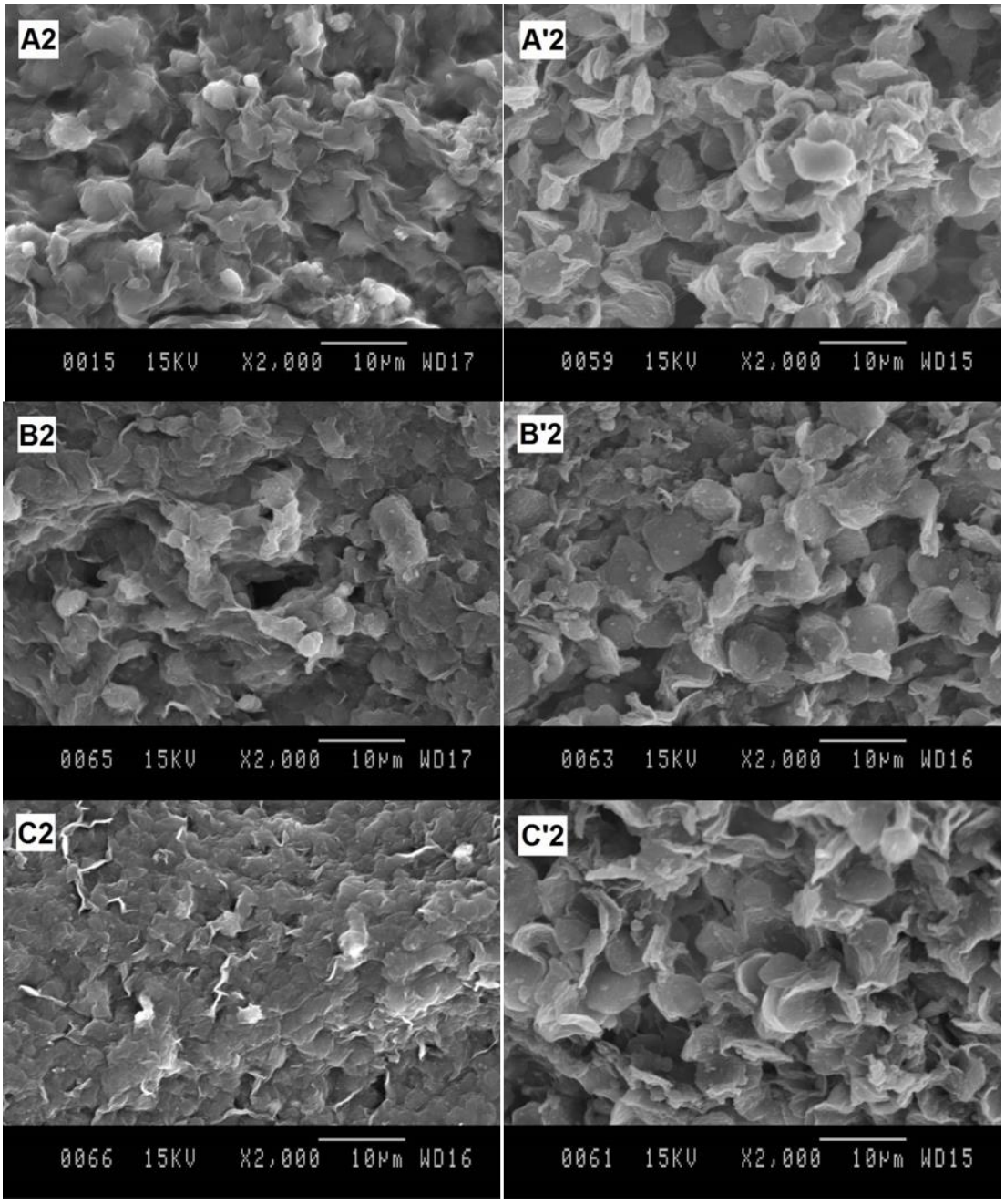

Figure 2.10. SEM images of the uncompatibilized (A, B, C) and compatibilized (A', B', C') RTF and GTR particles after extrusion at different screw speeds and different magnifications: A,A') 110 rpm, B,B') 180 rpm and C,C') 250 rpm.

2.3.6.3 Effect of high temperature (HT) profiles

Figure 2.11 presents typical SEM images of the compatibilized blends of 50% RTF produced with an extruder screw speed of 250 rpm and HT profile in extrusion or injection molding (see Tables 2.1-2.3). A comparison between E-250 (Figures 2.11A1 and 2.11A2) and I-250 (Figures 2.11B1 and 2.11B2) shows that the general texture changed which can be related to possible LLDPE degradation in the presence of air during extrusion starting around 260°C (Figure 2.12b) compared to its degradation in an inert gas (nitrogen) starting around 370°C (Figure 2.12a), as well as the decomposition of the GTR structure (Scaffaro et al., 2005) starting around 210°C (Figure 2.5b). But due to lower residence time in injection molding compared to extrusion, less LLDPE degradation and GTR decomposition occurred in I-250 (Figures 2.11B1 and 2.11B2).

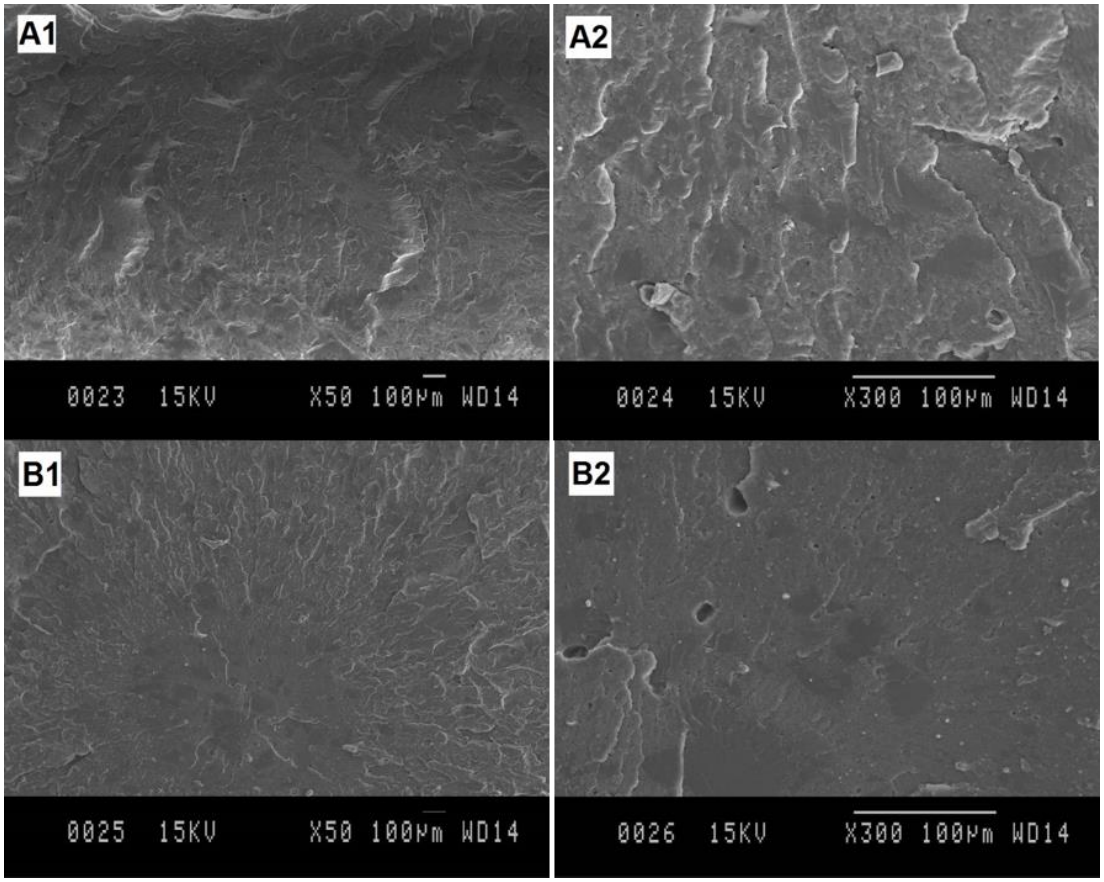

Figure 2.11. SEM images of the compatibilized blends of 50% RTF at 250 rpm extrusion screw speed and HT profiles at different magnifications: A) E-250 and B) I-250.

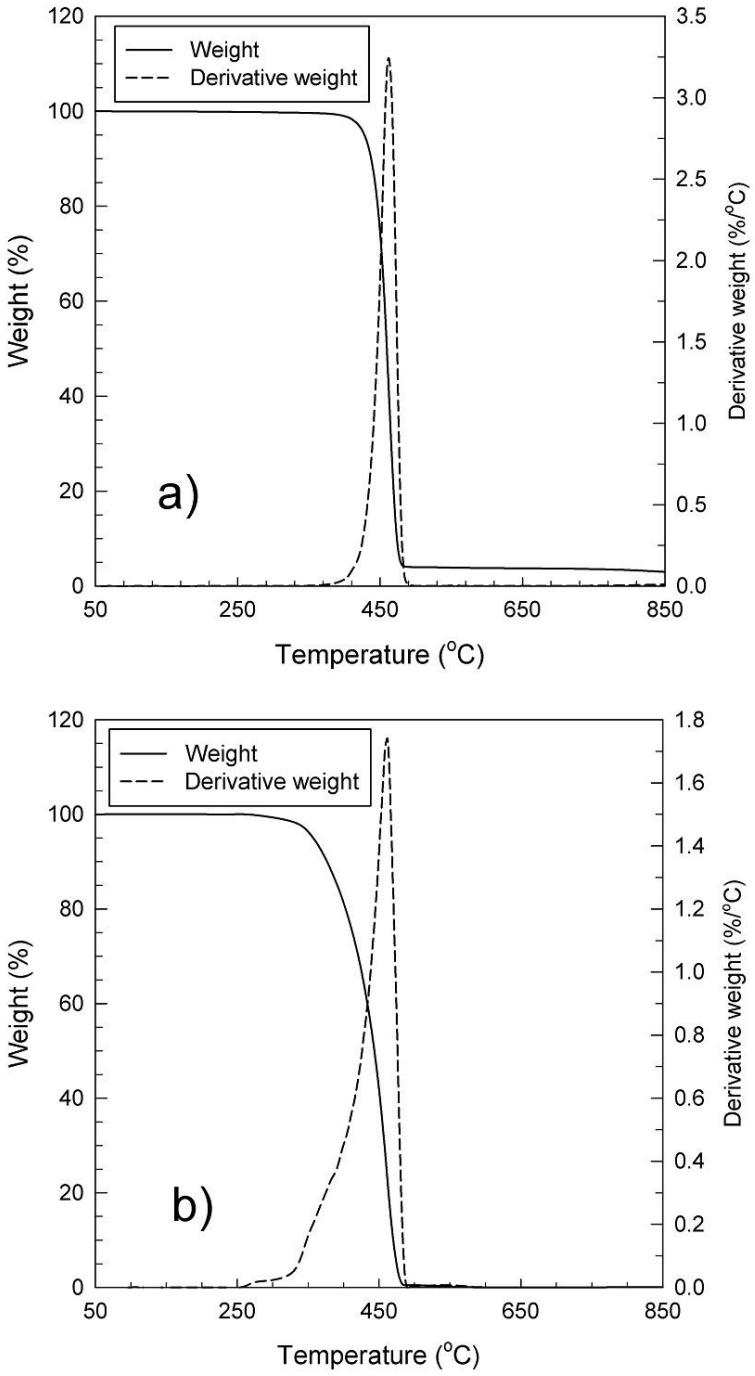

Figure 2.12. TGA results of LLDPE in: a) nitrogen and b) air.

2.4 Conclusion

In the first part of this study, the effect of RTF addition mixed with GTR in LLDPE with and without SEBS-g-MA was investigated. Different contents (10, 25 and 50 wt.%) were used, while the coupling agent content was fixed (10 wt.%) when added. To improve the interfacial adhesion between the components while reducing raw material costs, different processing conditions in extrusion compounding (screw speed of 110, 180 and 250 rpm) and injection molding were applied at low (LT) and high (HT) temperature profiles related to values below or above the melting point of RTF fibers (PET).

The morphological results showed that lower RTF length and GTR particles size occurred with increasing extrusion screw speed, while better distribution was obtained especially for compatibilized compounds (more homogeneous samples). RTF length during extrusion decreased by about 87, 89 and 93% (uncompatibilized compounds), and 92, 95 and 99% (compatibilized composites), as well as decreases in GTR particles sizes of about 93, 93 and 95% (uncompatibilized compounds), and 95, 96 and 96% (compatibilized composites) was observed when the extruder screw speed increased from 110 to 180 and 250 rpm, respectively. In the case of applying HT profiles for extrusion or injection molding, possible LLDPE and GTR degradation was observed leading to changes in the overall texture of the compounds. However, the compounds produced with a HT profile in injection molding have less degradation due to lower residence time compared to a HT profile in extrusion.

Finally, based on the morphological results obtained, this information will be used to relate with the mechanical properties of the compounds that are reported in the second part of this study (Moghaddamzadeh & Rodrigue, 2017b).

Acknowledgments

The authors would like to acknowledge the financial support of the Natural Sciences and Engineering Research Council of Canada (NSERC), material donation for LLDPE (ExxonMobil, Canada) and RTF (Quebec Transloc), as well as the technical support of the

Research Center on Advanced Materials (CERMA), the Quebec Center on Functional Materials (CQMF) and the Research Center for High Performance Polymer and Composite Systems (CREPEC). Also, the technical help of Mr. Yann Giroux for the experiments was highly appreciated.

Chapter 3

The effect of polyester recycled tire fibers mixed with ground tire rubber on polyethylene composites Part II: Physico-mechanical analysis

Moghaddamzadeh S. and Rodrigue D., Progress in Rubber, Plastics and Recycling Technology, accepted (2017).

Résumé

Ce travail présente les propriétés mécaniques (tension, flexion et impact) et physiques (densité et dureté) de composites à base de fibres de polyester de pneus recyclés (RTF) mélangées avec du caoutchouc de pneus usés (GTR) dans le polyéthylène linéaire de basse densité (LLDPE) avec et sans styrène-éthylène-butylène-styrène greffé d'anhydride maléique (SEBS-g-MA) comme agent compatibilisant. En particulier, l'effet de la concentration de RTF (10, 25 et 50% en poids), de la vitesse de rotation des vis d'extrusion (110, 180 et 250 rpm) et les profils de température (extrusion et moulage par injection) a été étudié. Les résultats montrent que les meilleures propriétés ont été obtenues avec un contenu élevé en RTF (50%) et des vitesses de vis élevées (250 rpm) combinés avec un profil de température faible pour l'extrusion et le moulage par injection lorsque l'agent compatibilisant est ajouté.

Abstract

This work reports on the mechanical (tension, flexion and impact) and physical (density and hardness) properties of recycled polyester tire fibers (RTF) mixed with ground tire rubber (GTR) and linear low density polyethylene (LLDPE) with and without styrene-ethylene-butylene-styrene grafted maleic anhydride (SEBS-g-MA) as a compatibilizer. In particular, the effect of RTF content (10, 25 and 50 wt.%), extruder screw speed (110, 180 and 250 rpm) and temperature profiles (extrusion and injection molding) was studied. The results showed that the best properties were obtained at the highest RTF content (50%) and extruder screw speed (250 rpm) combined with the lowest temperature profile in both extrusion and injection molding when the compatibilizer was added.

3.1 Introduction

Polymer wastes have become an important environmental issues in recent years (Nishida, 2011). This is especially the case for worn tires. Although several methods have been developed for tire recycling, scrap tires management is still a problem (Ramarad et al., 2015), especially for one of the main tire components called the "recycled tire fibers" (RTF). Polyester (polyethylene terephthalate or PET) is the main synthetic fibers used in the tire structure (Gent & Walter, 2006), but this material is very difficult to get with high purity level as some ground tire rubber (GTR) particles are present with these fibers due to limitation of the separation process. Nevertheless, RTF can be used as a reinforcing agent in polyolefins like polyethylene (PE) and polypropylene (PP) to improve their properties, as well as reducing the costs. But due to compatibility limitations, a "compatibilizer" having a similar structure with the polyolefin and PET as well as GTR must be added (Moghaddamzadeh & Rodrigue, 2017a). To date, some work can be found on synthetic fibers reinforced composites (Ferreira et al., 2013) and natural fibers reinforced polyolefin/GTR blends (Ramezani Kakroodi et al., 2012; Ramezani Kakroodi et al., 2013). For example, Ferreira et al. (Ferreira et al., 2013) worked on waste polyamide (W-PA) from scrap tires to reinforce waste PET (W-PET) (25/75 wt.%). First, they reinforced W-PA with different glass fiber contents where substantial improvement in tensile (130%) and impact (126%) strengths at 15 wt.% was observed. To improve the W-PET properties, 25 wt.% of reinforced W-PA was used leading to tensile and impact strengths improvement of 18 and 17%, respectively. Kakroodi et al. (Ramezani Kakroodi et al., 2013) studied the compatibility of maleated polyethylene (MAPE)/hemp fiber/GTR composites with different hemp and GTR contents. They reported that while tensile strength of MAPE/hemp blends at 50 and 60 wt.% hemp increased by 80 and 68% respectively, Charpy impact strength decreased by 5% when hemp content increased from 50 to 60 wt.%. To recover some ductility, 10% GTR was added to a 50 wt.% hemp composite resulting in a 50% improvement in Charpy impact strength, while adding 26% GTR led to a 79% improvement. On the other hand, a 44% reduction in tensile strength was observed. A work on the mechanical properties of flax fiber reinforced high density polyethylene (HDPE)/GTR was reported by Kakroodi et al. (Ramezani Kakroodi et

al., 2012) using styrene-ethylene-butylene-styrene grafted maleic anhydride (SEBS-g-MA). It was shown that adding 15 and 30 wt.% of equal contents of flax fiber/GTR as fillers decreased the tensile strength by 25 and 47%, while increasing the Charpy impact strength by 26 and 64%, respectively. These results show that in general, a compromise between ductility and strength must be accepted.

Some studies on improving the compatibility between polyethylene (PE) or polypropylene (PP) and PET using different compatibilizers have been reported. Dobrovszky and Ronkey (Dobrovszky & Ronkay, 2015) reported a 90% decrease in tensile modulus of compatibilized high density polyethylene (HDPE)/PET blends using 4% vol. of SEBS-g-MA when the PET vol.% decreased from 100 to 0%. Asgari and Masoomi (Asgari & Masoomi, 2015) reported that the tensile modulus of compatibilized PP/PET blends using polypropylene grafted glycidyl methacrylate (PP-g-GMA) increased by 63% when the PET fiber content increased to 30 wt.%. Pei et al. (Pei, Evstatiev, & Friedrich, 2012) studied microfibrillar reinforced composites of HDPE/PET and reported that for a 50% PET content, the tensile strength and modulus increased by 82 and 180% compared to neat HDPE, respectively. Pracella et al. (Pracella, Rolla, Chionna, & Galeski, 2002) reported a 21% increase in tensile strength for the compatibilized blend of recycled PET/recycled PE with ethylene glycidyl methacrylate copolymer (E-GMA) associated with a domain size reduction of R-PE in the R-PET matrix. Furthermore, lower tensile strength combined with higher Charpy impact strength of compatibilized PP/PET blends using two different compatibilizers such as PP-g-GMA and polypropylene grafted maleic anhydride (PP-g-MA) was reported by Asgari and Masoomi (Asgari & Masoomi, 2012). At 30 wt.% of PET fibers, the tensile strength of the compatibilized blends decreased by 26 and 50% for PP-g-GMA and PP-g-MA compared to the neat PP, respectively. In contrast, Charpy impact strength increased by 36% for both compatibilizers. Similarly, van Bruggen et al. (van Bruggen et al., 2016) investigated the compatibility of PP/PET (85/15) based on different compatibilizers (SEBS-g-MA, SEBS-g-GMA) and polyolefin grafted glycidyl methacrylate (POE-g-GMA) processed under different temperature profiles in extrusion and injection molding (250, 270 and 300°C). It was found that applying higher temperature (300°C), besides using SEBS-g-GMA, was useful to improve the mechanical properties by reducing the surface tension and increasing the interfacial adhesion between both phases. The addition of 2.5% of SEBS-g-GMA

increased the Izod impact strength by up to 58% compared to SEBS-g-MA and POE-g-GMA when the ternary blends were melt blended at 300°C.

In the first part of this study, a complete characterization of the RTF and its compounds with linear low density polyethylene (LLDPE) was presented using different processing conditions (Moghaddamzadeh & Rodrigue, 2017a). From the samples produced, a morphological analysis was performed to get a clear picture of the final materials structure (particle size and dispersion). Here, an analysis is made on the effect of RTF content (mixed with GTR particles) on the physical and mechanical properties of these samples.

3.2 Experimental

3.2.1 Materials

Table 3.1 presents an overview of the materials used for this study.

Table 3.1. Specification and properties of the materials used.

Material	LLDPE	RTF	SEBS-g-MA
Commercial name	LL8460	-	FG1901X
Producer/supplier	ExxonMobil (Canada)	Quebec Transloc (Canada)	Kraton (USA)
Density (kg/m^3)	938	1268 ± 1	910
Melting point (°C)	127	253	124
Melt index	3.3 g/10 min (190ºC/2.16 kg)	-	22 g/10 min (230ºC/5 kg)
Form (appearance)	Powder	Fibers/Fluffy	Pellet
Remarks	-	Mixed with GTR	Contains 30% of polystyrene and grafted with 2% of maleic anhydride

3.2.2 Processing

First, the RTF was oven-dried for 12 hours at 80°C. Due to the RTF fluffy nature and its low bulk density, all the components were dry-blended together for better feeding (constant/stable rate) into the first zone of a co-rotating twin-screw extruder Leistritz ZSE-27 with a L/D ratio of 40. To do so, SEBS-g-MA was pulverized. Based on preliminary results, the amount of compatibilizer was fixed at 10 wt.% of the RTF content (10, 25 and 50 wt.%.) in all cases. Different processing conditions including compounding screw speed (110, 180 and 250 rpm) as well as low temperature (LT) and high temperature (HT) profiles in extrusion (10 zones)

and injection molding (4 zones) were selected to produce the samples with the highest amount of RTF. These different processing conditions were used to study the effects of RTF final length and GTR particle sizes, as well as possible materials degradation below and above the RTF melting point (253°C) on the physico-mechanical properties of these composites. The compounds out of a 2.7 mm extrusion die were quenched in a water bath and then pelletized. The pellets were dried in a forced air circular dryer for about 4 h at 75°C before being fed to a Nissei PS60E9ASE injection molding machine. The mold was fixed at 30°C and the samples were prepared to the specific dimensions required for mechanical characterization as described later. Tables 3.2-3.4 present the different processing conditions used. It should be noticed that sample E-250 was first extruded using a HT profile and then injection molded using a LT profile, which is the reverse case for I-250. More information on sample preparation can be found in the first part of this study (Moghaddamzadeh & Rodrigue, 2017a).

Table 3.2. Composition of the compounds with their respective processing conditions.

Composite	LLDPE (wt.%)	RTF (wt.%)	SEBS-g-MA (wt.%)	Screw speed (rpm)	Temperature profile
L-1001	100	0	0	110	LT
L-901	90	10	0	110	LT
L-751	75	25	0	110	LT
L-501	50	50	0	110	LT
L-508	50	50	0	180	LT
L-502	50	50	0	250	LT
LC-901	90	10	10	110	LT
LC-751	75	25	10	110	LT
LC-501	50	50	10	110	LT
LC-508	50	50	10	180	LT
LC-502	50	50	10	250	LT
E-250	50	50	10	250	HT
I-250	50	50	10	250	HT

Table 3.3. Extrusion temperature profiles.

Temperature profile	Zone (°C)					
	1 to 5	6	7	8	9	10
LT	170	170	170	170	170	175
HT	170	210	250	250	260	265

Table 3.4. Injection molding temperature profiles.

Temperature profile	Zone (°C)			
	Rear	Middle	Front	Nozzle
LT	170	175	180	185
HT	220	260	260	250

3.3 Characterization

Tensile tests were done according to ASTM D638 (type IV and thickness of 3.2 mm) using at least 5 specimens for each compound. The tests were performed at room temperature using a 500 N load cell at a strain rate of 10 mm/min on an Instron (Instron, USA) universal mechanical tester model 5565.

Flexural tests were done on an Instron (Instron, USA) model 5565 according to ASTM D790 at room temperature. At least 5 rectangular specimens with dimensions of 80×12.7×3.2 mm^3 were tested in a three-point bending mode (span length of 60 mm) at a crosshead speed of 2 mm/min with a 50 N cell.

Notched Charpy impact tests were performed according to ASTM D256. For each composition, 10 rectangular samples with dimensions of 127×12.7×3.2 mm^3 were tested on a Tinius Olsen (Tinius Olsen, USA) model 104 at room temperature. The samples were notched with an automatic sample notcher model ASN 120m (Dynisco, USA).

Density measurement of the compounds was performed using a gas (nitrogen) pycnometer model Ultrapyc 1200e (Quantachrome Instruments, USA). For each sample, the test was repeated five times.

Hardness measurement was done according to the shore D scale (thermoplastics) using a model 307L durometer (PTC Instruments, USA). The reported values are the average of at least 15 measurements for each composition.

3.4 Results and discussion

3.4.1 Mechanical properties

3.4.1.1 Effect of RTF content

Figure 3.1 presents the tensile and flexural properties as a function of RTF content for a screw speed of 110 rpm. For uncompatibilized blends, all the mechanical properties are lower than neat LLDPE and decreasing with RTF content. This trend can be related to poor interfacial adhesion of the binary blends (polar and non-polar materials) (Moghaddamzadeh & Rodrigue, 2017a). Also, the compatibilized blends produced even lower mechanical properties than the uncompatibilized samples. This behavior is associated to the low rigidity of the rubbery structure of SEBS-g-MA (Dobrovszky & Ronkay, 2015; Moghaddamzadeh & Rodrigue, 2017a; Zhang et al., 2007), as well as the presence of GTR (Mahallati & Rodrigue, 2014). As seen in Figure 3.1, better compatibility between LLDPE and GTR with the addition of SEBS-g-MA leads to better stress transfer from the matrix to the rubber particles leading to lower overall rigidity of the compounds. In this case, all the mechanical properties of the compatibilized blends decreased even more with increasing RTF content. For instance, when 50% RTF was used, the tensile and flexural strengths, as well as tensile and flexural moduli, decreased by 2, 10, 14 and 11%, respectively. Furthermore, a substantial decrease in the elongation at break occurred when the RTF reached its highest content (50%) resulting in a 97% (uncompatibilized) and 94% (compatibilized) decrease when compared to neat LLDPE. This can be related to two different phenomena: limited interfacial adhesion between RTF and LLDPE even in the presence of the compatibilizer (Moghaddamzadeh & Rodrigue, 2017a), and limited chain mobility of GTR particles due to their crosslinked nature. Nevertheless, the rubbery structure of the compatibilizer led to higher tensile strain at break overall.

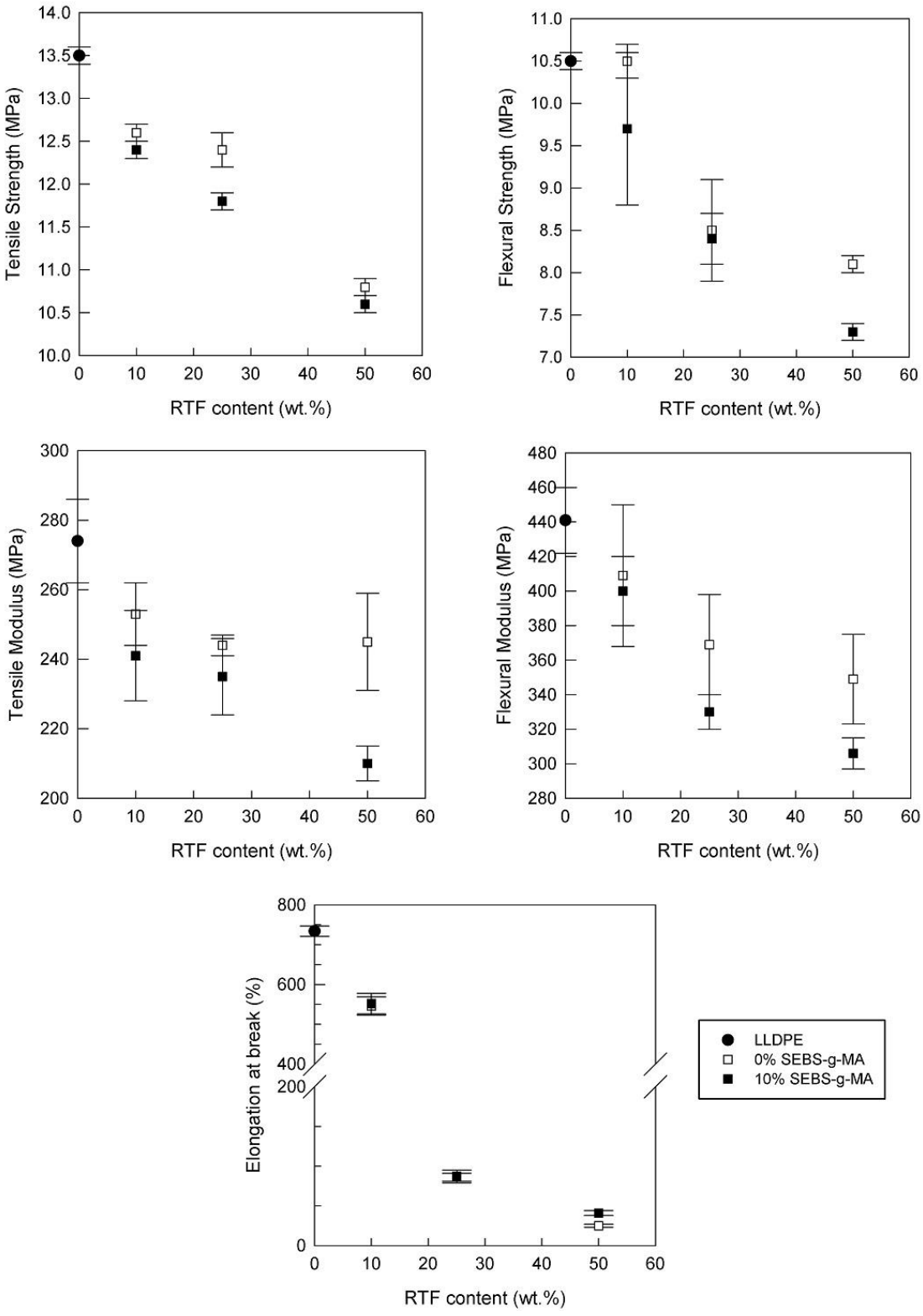

Figure 3.1. Tensile and flexural properties as a function of RTF content.

Figure 3.2 presents the Charpy impact strength as a function of RTF content at low screw speed (110 rpm). The impact strength for the uncompatibilized blends is almost constant over the whole range of concentration studied. On the other hand, adding the compatibilizer led to substantial Charpy impact strength increase from 211 to 248 (18%), 214 to 276 (29%) and 208 to 312 J/m (50%) at 10, 25 and 50% RTF, respectively. This behavior is related to a higher amount of GTR, but mainly to better interfacial stress transfer making the compounds more ductile; i.e. better energy absorption through elastic deformation of the rubbery GTR particles (Mahallati & Rodrigue, 2014). Again, the rubbery structure of SEBS-g-MA itself can increase the elasticity and Charpy impact strength of the compounds (Zhang et al., 2007).

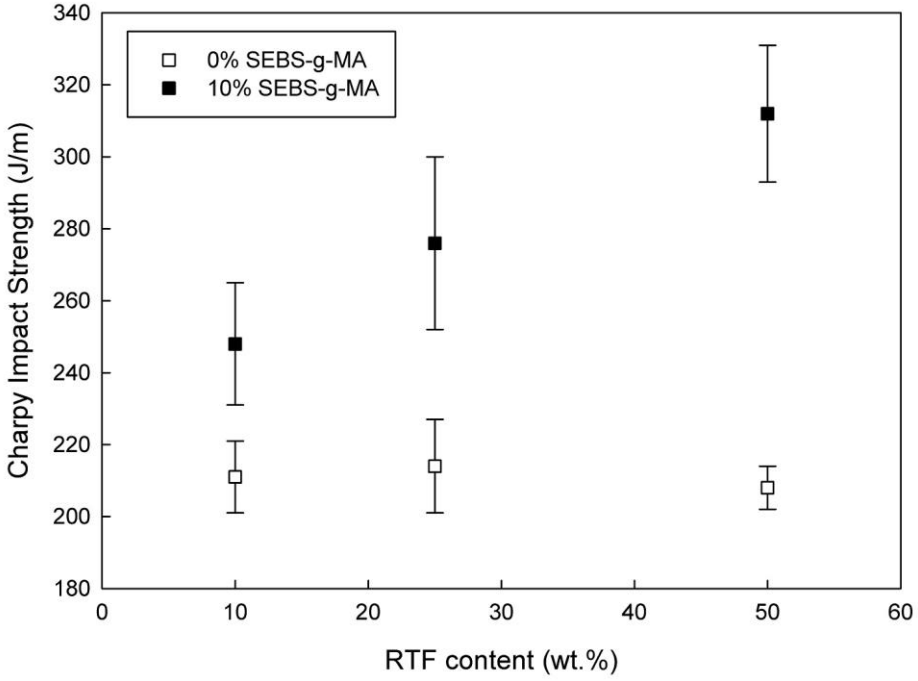

Figure 3.2. Charpy impact strength as a function of RTF content.

Figure 3.3 presents the density and hardness (shore D) of the composites as a function of RTF content for an extruder screw speed of 110 rpm. As seen in Figure 3.3, the density of all the composites increased due to the higher density of RTF (1268 kg/m^3) compared to LLDPE (938 kg/m^3) and SEBS-g-MA (910 kg/m^3). In fact, increasing the amount of RTF in the blends also led to higher GTR (1252 ± 11 kg/m^3) [5] content resulting in density increase, but

no significant difference was observed between the uncompatibilized and compatibilized systems. Overall, the compounds density increased by about 2, 6 and 12% compared to LLDPE for 10, 25 and 50% RTF, respectively. For hardness, the values decreased with RTF content as more GTR particles as well as compatibilizer (softer materials) are present inside the composites. Again, no significant difference between uncompatibilized and compatibilized samples. The hardness decrease compared to the matrix (63.1 shore D) by about 4, 7 and 9% when RTF content increased from 10 to 25 and 50%, respectively.

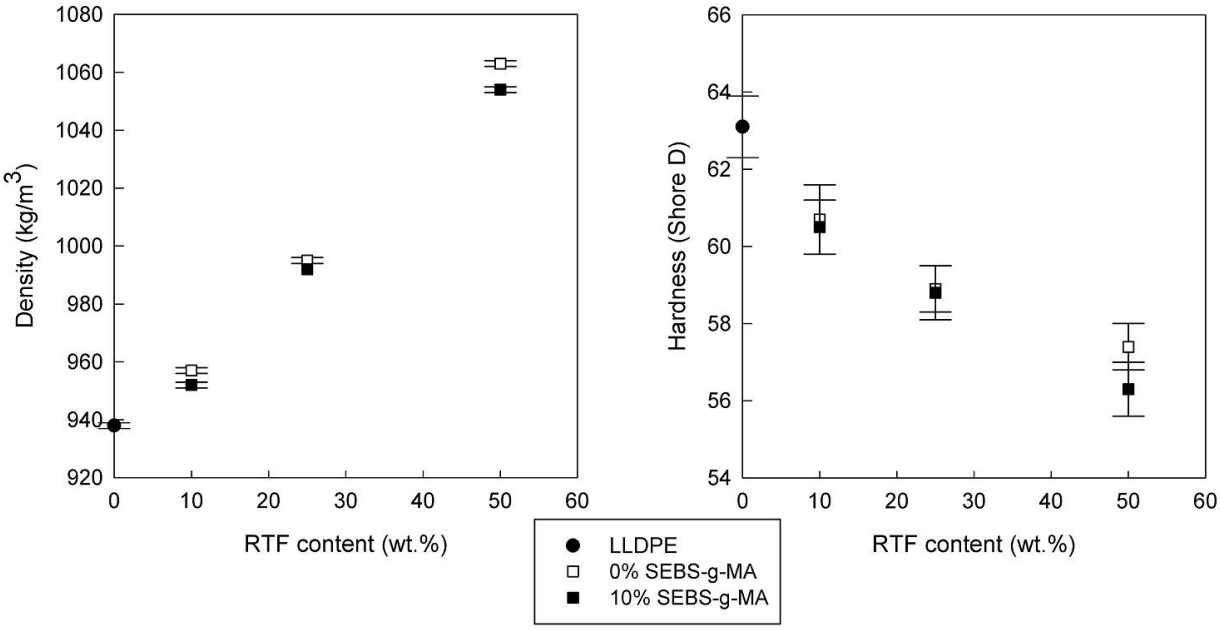

Figure 3.3. Density and hardness as a function of RTF content.

3.4.1.2 Effect of screw speed

Some studies reported better mechanical properties using higher screw speed for composites based on natural (Joseph, Joseph, & Thomas, 1999) and synthetic (Yilmazer & Cansever, 2002) fibers. Joseph et al. (Joseph et al., 1999) reported that tensile strength and tensile modulus of PP/sisal fiber composites increased by 13% and 4% respectively, when the rotor speed of an internal batch mixer increased from 30 to 50 rpm. In a work done by Yilmazer

and Cancever (Yilmazer & Cansever, 2002), the Izod impact strength increased by 20% when the screw speed of a co-rotating twin-screw extruder increased from 250 to 300 rpm for Nylon 6/glass fiber (70/30) composites. Scaffaro et al. (Scaffaro et al., 2005) investigated the effect of different mixing speeds and GTR content on the binary blend of recycled PE and GTR in a twin-screw extruder. As a result, tensile strength decreased by 10% while the tensile modulus increased by 14% when 25% GTR was used for injection molded samples. Based on these limited information, both uncompatibilized and compatibilized blends with 50% RTF were produced at different extruder screw speed (180 and 250 rpm) to determine the effect of higher mixing intensity on the mechanical properties of the resulting compounds.

Figure 3.4 presents the tensile and flexural properties of 50% RTF at different extruder screw speeds. It can be seen that while the tensile strength of the compatibilized blend at the lowest screw speed is lower than the uncompatibilized one, increasing the extruder screw speed to 180 and 250 rpm led to improved tensile strength from 10.3 to 11.7 MPa (14%) and 10.8 to 12.2 MPa (13%), respectively. In addition, tensile strength increased from 11.7 to 12.2 MPa (4%) when the screw speed increased from 180 to 250 rpm for the compatibilized blends. This can be associated to GTR particles size reduction resulting in higher surface contact area with the matrix (Joseph et al., 1999; Moghaddamzadeh & Rodrigue, 2017a; Yilmazer & Cansever, 2002). This is even more noticeable in the presence of SEBS-g-MA leading to increased tensile strength due to better stress transfer from LLDPE to GTR. Furthermore, the tensile strength of 50% RTF compatibilized blend produced at 250 rpm (12.2 MPa) is about the same as the tensile strength of 10% RTF compatibilized blend produced at 110 rpm (12.4 MPa). This behavior is related to the reduction of GTR particle size produced at higher extrusion speed resulting in better stress transfer from the matrix to the rubber particles (Moghaddamzadeh & Rodrigue, 2017a).

When the speed increased from 110 to 180 and 250 rpm, the rubber particles have smaller sizes due to high mechanical stresses (mainly shear) (Moghaddamzadeh & Rodrigue, 2017a). So, finer GTR particles are responsible for higher elasticity and impact strength of the blends (Mehrabzadeh & Nia, 1999), but also leading to rigidity loss. This reduction is also a result of better compatibility between the matrix and rubber particles in the presence of the compatibilizer leading to better stress transfer from LLDPE to GTR (Ramezani

Kakroodi et al., 2012). Also, the rubbery structure of the compatibilizer affected this reduction (Dobrovszky & Ronkay, 2015; Zhang et al., 2007). Despite limited losses of about 7% and 10% (flexural strength), as well as 9% and 14% (flexural modulus) for the compatibilized compounds produced at 180 and 250 rpm compared to 110 rpm, increasing the extruder screw speed did not change the tensile modulus of both uncompatibilized and compatibilized compounds, as well as the flexural properties of the uncompatibilized blends when 50% RTF was used.

In the case of tensile strain at break, although there is negligible differences between the samples produced at different extruder screw speed, higher values are obtained for the compatibilized compounds due to rubbery structure of SEBS-g-MA (Dobrovszky & Ronkay, 2015; Zhang et al., 2007).

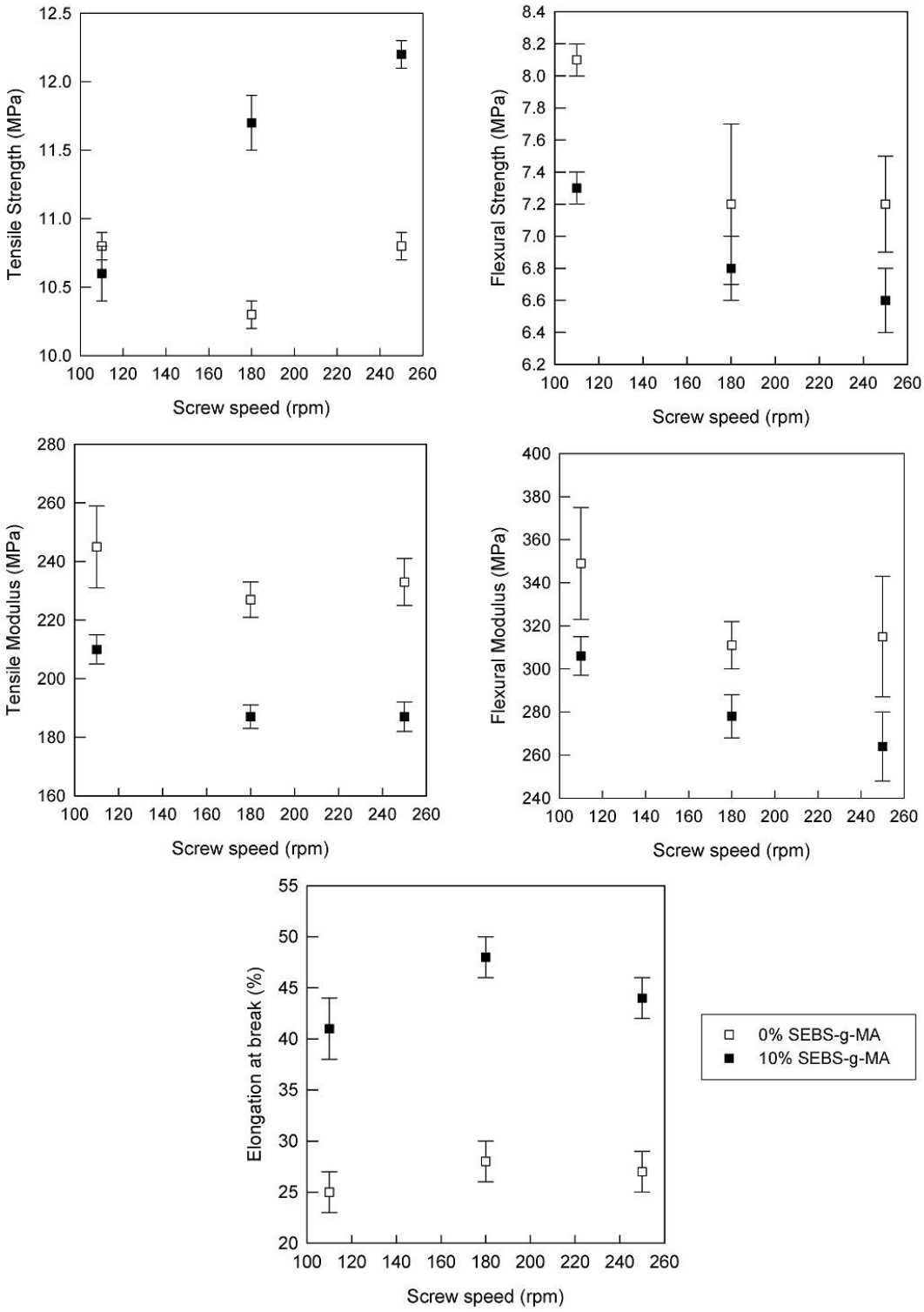

Figure 3.4. Tensile and flexural properties of the 50% RTF compounds at different extrusion screw speeds.

Figure 3.5 presents the Charpy impact strength of 50% RTF at different extrusion screw speed. It is obvious that impact strength for the uncompatibilized blends is constant, while increasing with extrusion screw speed for the compatibilized samples. Charpy impact strength increased from 208 to 312 J/m (50%), 229 to 482 J/m (110%) and 230 to 486 J/m (111%) when the screw speed was 110, 180 and 250 rpm, respectively. On the other hand, increasing the extruder screw speed from 110 to 180 and 250 rpm led to increased Charpy impact strength of the compatibilized samples from 312 to 482 J/m (54%) and 312 to 486 J/m (56%), respectively. This behavior can be related to several phenomena: 1) higher GTR content at 50% RTF (compared to 10 and 25% RTF), 2) GTR particles size reduction leading to increased surface contact area with the matrix (Joseph et al., 1999; Moghaddamzadeh & Rodrigue, 2017a; Yilmazer & Cansever, 2002), and 3) the rubbery structure of SEBS-g-MA (Dobrovszky & Ronkay, 2015; Zhang et al., 2007). These factors make the composite more elastic leading to better energy absorption through elastic deformation (Mahallati & Rodrigue, 2014) especially when better stress transfer from the matrix to the GTR particles is produced with a compatibilizer.

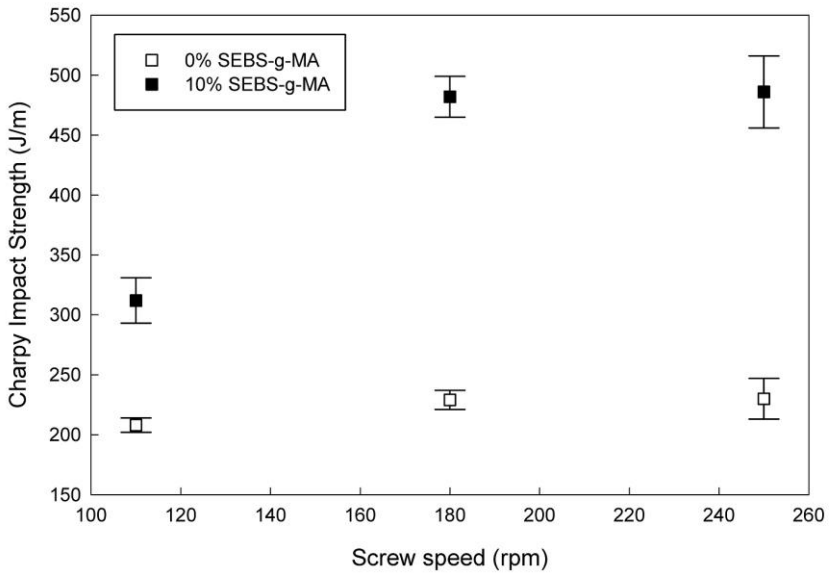

Figure 3.5. Charpy impact strength at 50% RTF for different extrusion screw speed.

Figure 3.6 presents the density and hardness (shore D) of the 50% RTF compounds produced at different extruder screw speed. It can be seen that the density of the compatibilized samples is around 1050 kg/m^3 and slightly lower than the uncompatibilized compounds (around 1060 kg/m^3 order) due to presence of the compatibilizer having a lower density (910 kg/m^3). It is clear that the reduction in RTF length and GTR particles size produced at different extrusion speeds (Moghaddamzadeh & Rodrigue, 2017a) did not change the overall density. On the other hand, the hardness of the compounds decreased with increasing extruder screw speed. But higher decrease is observed for the compatibilized composites due to the presence of a soft compatibilizer and finer GTR particles size (Moghaddamzadeh & Rodrigue, 2017a) leading to more elastic compounds. In fact, hardness decreased from 57.4 (uncompatibilized) to 55.3 shore D (compatibilized) which represents a 4% decrease when the extruder screw speed increased from 110 rpm to 250 rpm.

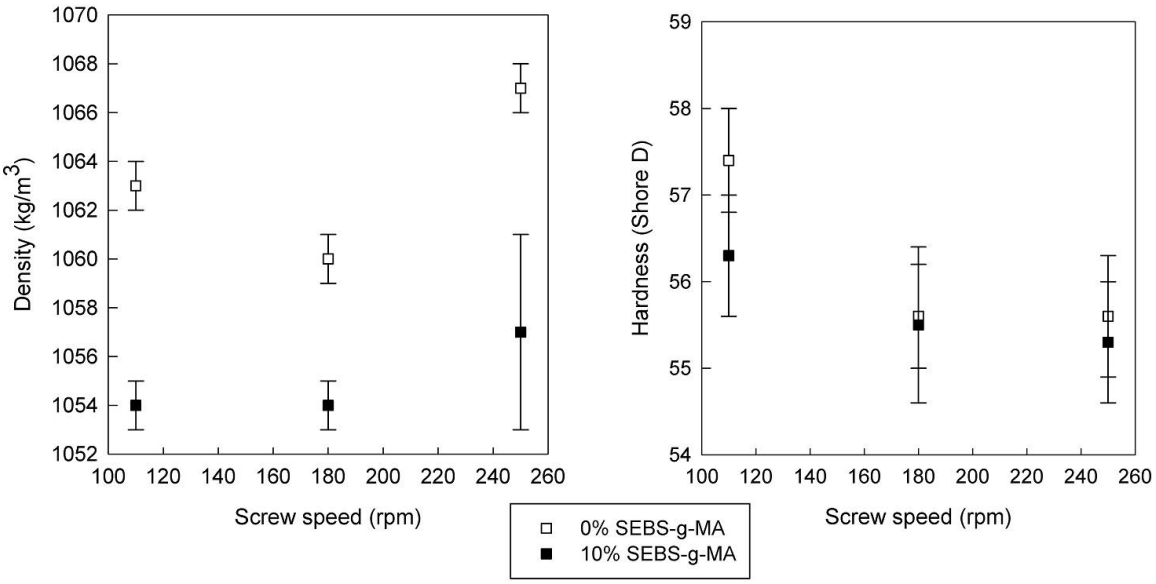

Figure 3.6. Density and hardness at 50% RTF for different extrusion screw speed.

3.4.1.3 Effect of high temperature (HT) profiles

Since it was found that using the highest amount of RTF (50%) and the highest extrusion screw speed (250 rpm) can increase the Charpy impact strength of the compatibilized LLDPE/RTF compounds, higher temperature profiles were applied in both extrusion and injection molding to process above the melting point of the RTF according to the DSC results obtained in the first part of this study (Moghaddamzadeh & Rodrigue, 2017a). Figure 3.7 shows that substantial decreases were observed when higher temperatures were used in both steps (E-250 and I-250) with the exception of the elongation at break. These decreases are related to possible degradation of the LLDPE and decomposition of the GTR structure according to TGA results, as well as SEM images reported in our previous study (Moghaddamzadeh & Rodrigue, 2017a). Also, the mechanical properties of E-250 are lower than I-250 which can be related to lower residence time in injection molding resulting in less LLDPE degradation and GTR decomposition compared to extrusion (Moghaddamzadeh & Rodrigue, 2017a). In this case, while tensile and flexural strengths, as well as tensile and flexural moduli of E-250 decreased by 34, 12, 18 and 3%, respectively, a more important decrease in Charpy impact strength (about 50%) was observed compared to LC-502.

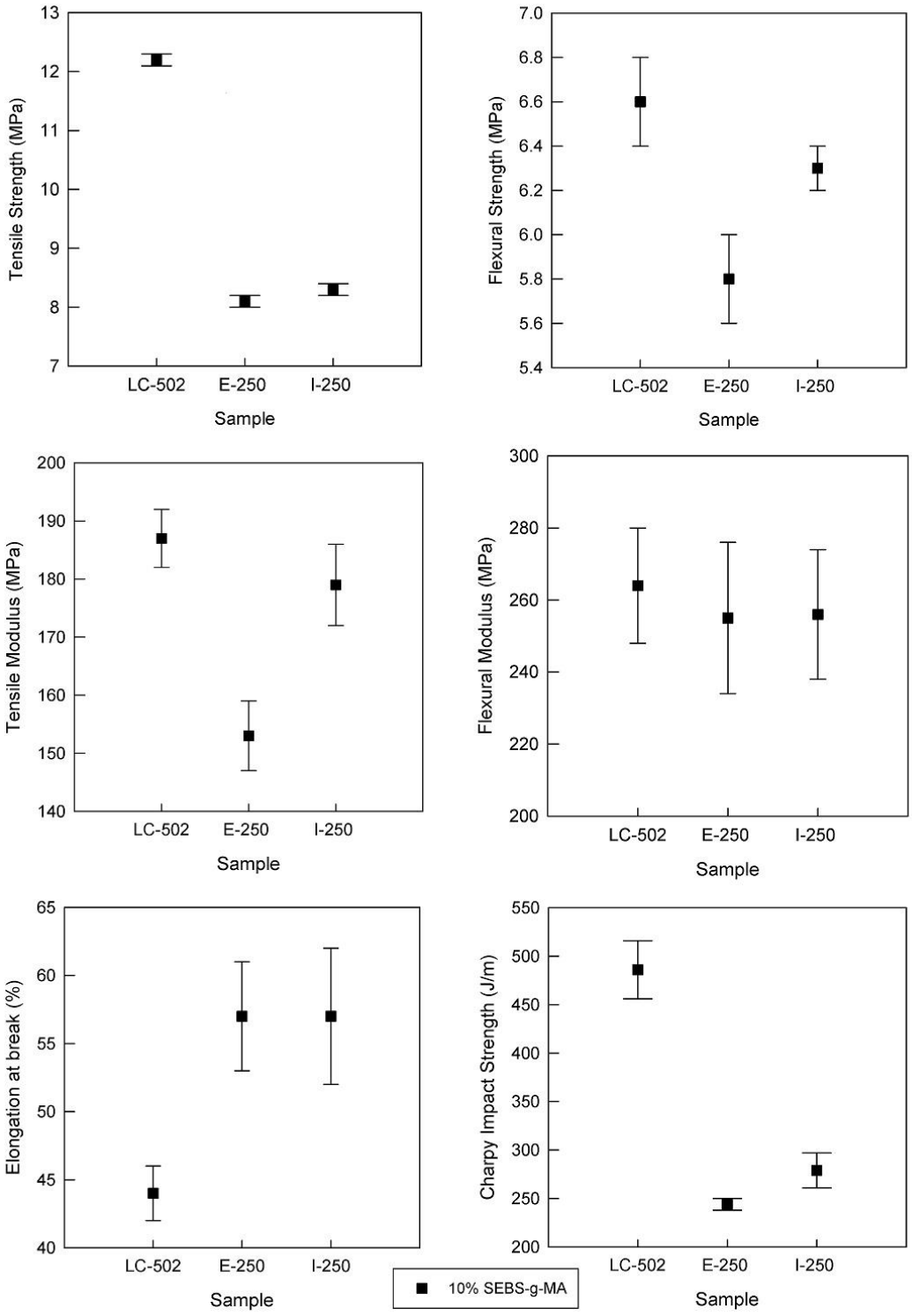

Figure 3.7. Mechanical properties of the compatibilized 50% RTF compounds at different temperature profile.

Figure 3.8 presents the density and hardness of the compatibilized composites produced with the highest RTF content (50%) and the highest extruder screw speed (250 rpm) at different temperature profiles. It can be seen that the density of E-250 (1049 kg/m^3) is slightly lower than LC-502 (1057 kg/m^3). This can be related to more GTR degradation (starting around 200°C in air according to the TGA results (Moghaddamzadeh & Rodrigue, 2017a)) for HT profiles leading to GTR mass loss leading to lower final density. Also, due to the higher residence time in the extruder compared to injection molding, the density of E-250 (1049 kg/m^3) slightly decreased compared to I-250 (1051 kg/m^3) as well. Nevertheless, the hardness of all the composites did not significantly change and decreased from 55.3 shore D (LC-502) to 54.8 shore D (I-250) and 54.2 shore D (E-250).

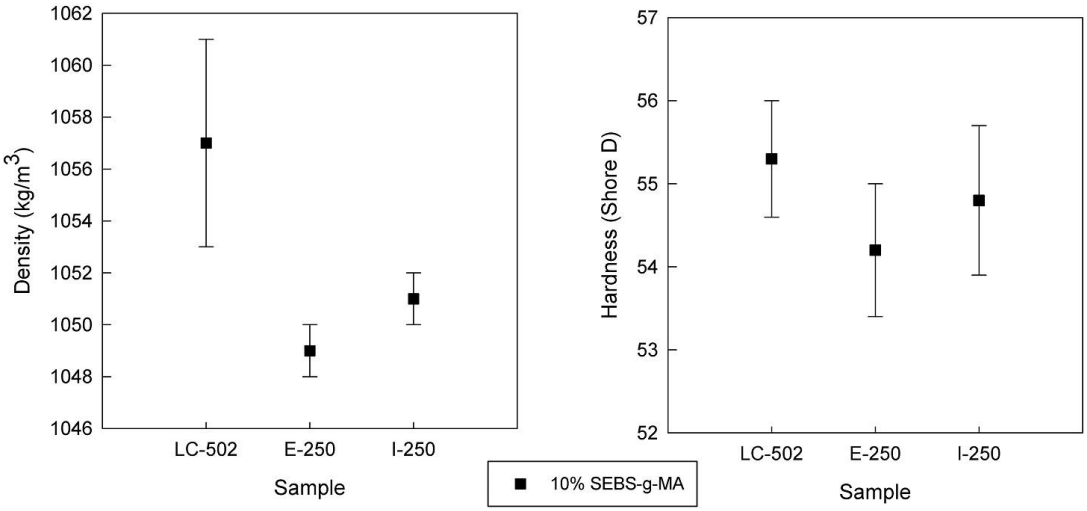

Figure 3.8. Density and hardness of the compatibilized 50% RTF compounds at different temperature profile.

3.5 Conclusion

In this study, the mechanical and physical properties of melt blended recycled tire fibers (RTF) mixed with ground tire rubber (GTR) as fillers in linear low density polyethylene (LLDPE) with and without 10 wt.% styrene-ethylene-butylene-styrene grafted maleic

anhydride (SEBS-g-MA) as a compatibilizer was studied. The investigation focused on the effect of three parameters: RTF content (10, 25 and 50%), extrusion screw (110, 180 and 250 rpm) speed and temperature profiles (above and below RTF melting point).

Firstly, the effect of RTF content was determined at the lowest extruder screw speed (110 rpm). The results showed a decrease of all mechanical properties except for Charpy impact strength of the compatibilized compounds by about 18, 29 and 50% at 10, 25 and 50% RTF, respectively. In the case of physical properties, while density and hardness of both uncompatibilized and compatibilized blends did not significantly change, density increased by about 2, 6 and 12%, while hardness (shore D) decreased by 4, 7 and 9% when the RTF content increased from 10 to 25 and 50%.

In the second step of the work, the effect of extrusion screw speed (110, 180 and 250 rpm) on the physico-mechanical properties of the 50% RTF was investigated. This was done as to add the highest RTF content and decrease the final costs. As a result, increase in tensile strength (14 and 13%) and Charpy impact strength (54 and 56%) of the compatibilized 50% RTF occurred when the extruder screw speed was increased to 180 and 250 rpm, respectively. Also, while hardness (shore D) of the compatibilized 50% RTF decreased by 4% at 250 rpm compared to 110 rpm, density was almost constant for all the compounds.

Finally, the effect of different temperature profiles selected below (LT) and above (HT) RTF melting point (253°C) on the final properties of the compatibilized 50% RTF composites produced at the highest extruder screw speed (250 rpm) was studied. As a result, all the mechanical properties of E-250 and I-250 (HT) decreased when compared to LC-502 (LT). But the decrease was more important for E-250 in Charpy impact strength (50%) due to the longer residence time of the materials in the extruder compared to the injection molding machine leading to higher LLDPE and GTR degradation level resulting in lower density. Nevertheless, the hardness of the compounds produced at HT profiles did not significantly change.

Acknowledgments

The authors would like to acknowledge the financial support of the Natural Sciences and Engineering Research Council of Canada (NSERC), material donation for LLDPE (ExxonMobil, Canada) and RTF (Quebec Transloc), as well as the technical support of the Research Center on Advanced Materials (CERMA), the Quebec Center on Functional Materials (CQMF) and the Research Center for High Performance Polymer and Composite Systems (CREPEC). Also, the technical help of Mr. Yann Giroux for the experiments was highly appreciated.

Chapter 4

Rheological characterization of polyethylene/polyester recycled tire fibers/ground tire rubber composites

Moghaddamzadeh S. and Rodrigue D., Journal of Applied Polymer Science, accepted (2018). DOI: 10.1002/app.46563

Résumé

Le comportement rhéologique des fibres de polyester recyclées (RTF) mélangées à du caoutchouc de pneu broyé (GTR) et du polyéthylène linéaire de basse densité (LLDPE) avec et sans anhydride maléique greffé de styrène-éthylène-butylène-styrène (SEBS-g-MA) comme agent compatibilisant a été étudié dans les états fondu (cisaillement oscillatoire de faible amplitude ou SAOS) et solide (analyse mécanique dynamique ou DMA). En particulier, l'effet de la teneur en RTF (10, 25 et 50% en poids), de la vitesse de la vis d'extrusion (110, 180 et 250 rpm) et des profils de température (extrusion et injection) ont été étudiés. En général, il a été constaté que les propriétés rhéologiques à l'état fondu (module et viscosité) des échantillons non-compatibilisés augmentaient avec la teneur en RTF, mais des valeurs plus élevées étaient obtenues lorsque le SEBS-g-MA était ajouté en raison d'un meilleur couplage interfacial. Bien que des résultats similaires aient été obtenus à l'état solide, il a été montré que la rhéologie à l’état fondu peut mieux expliquer les variations car les mesures sont plus sensibles à la qualité de l'interface puisque la contribution de la matrice est moins importante.

Abstract

The rheological behavior of polyester recycled tire fibers (RTF) mixed with ground tire rubber (GTR) and linear low density polyethylene (LLDPE) with and without styrene-ethylene-butylene-styrene grafted maleic anhydride (SEBS-g-MA) as a compatibilizer was investigated in the melt (small amplitude oscillatory shear or SAOS) and solid (dynamic mechanical analysis or DMA) states. In particular, the effect of RTF content (10, 25 and 50 wt.%), extrusion screw speed (110, 180 and 250 rpm) and temperature profiles (extrusion and injection molding) was studied. In general, it was found that the rheological properties in the melt state (modulus and viscosity) of the uncompatibilized samples increased with RTF content, but higher values were obtained when SEBS-g-MA was added due to better interfacial coupling. Although similar results were obtained in the solid state, it was shown that melt rheology can better explain the variations as the measurements are more sensitive to the interface quality since the matrix contribution is less important.

4.1 Introduction

Polymer wastes are an important environmental issue and discarded (scarp) tires are one of the most hazardous sources of these wastes. With increasing demands for transportation, the tire production rate significantly increased over the years leading to the consumption of more than 17 million tons of rubbers (Al-Malki et al., 2013). This is why tire recycling is important and different methods were proposed to reduce the important volume of worn tires as a waste going into the environment and leading to chemical contamination (Ramarad et al., 2015). Ground tire rubber (GTR) is a very well-known product of tire recycling which has been widely used in thermoplastics, mainly polyolefins (PO) like polyethylene (PE) and polypropylene (PP), to produce thermoplastic elastomers (TPE) (Oliphant & Baker, 1993; Phinyocheep, Axtell, & Laosee, 2002; Rajalingam & Baker, 1992; Rajalingam, Sharpe, & Baker, 1993; Tantayanon & Juikham, 2004). The main advantages of these compounds is their good processability (melt processing), good mechanical properties (high elasticity) especially at low temperatures (Mahallati et al., 2016), as well as lower costs. Also, some studies reported on the incorporation of crosslinked GTR in thermoplastics to produce thermoplastic vulcanizates (TPV) (Jacob et al., 2001; Magioli, Sirqueira and Soares, 2010; Cañavate et al., 2011; Zhang, Lu and Liang, 2011). Moreover, to understand the processing and relate the morphology to macroscopic properties, several studies used melt rheology for PE/GTR (Ramezani Kakroodi et al., 2013; Lima, Magalhães Da Silva, Oliveira, & Costa, 2015; Scaffaro et al., 2005) and PP/GTR (Han, Van Den Weghe, Shete, & Haw, 1981; Lima et al., 2015; Prut et al., 2012; Zhang, Zhang, Kang, Bang, & Kim, 2008), as well as their rheological behavior in the solid state via dynamic mechanical analysis (DMA) for PE/GTR (Grigoryeva et al., 2005; Kim et al., 2000; Li et al., 2003, 2004) and PP/GTR (Lee, Balasubramanian and Kim, 2007a; Magioli, Sirqueira and Soares, 2010) . On the other hand, recycled tire fibers (RTF) is another main component of the tire recycling process (Moghaddamzadeh & Rodrigue, 2017a) which can have different structures but mostly made from polyester (PET) (Gent & Walter, 2006). But RTF has not been used frequently as reinforcement for composite production. Furthermore, no study reported on the rheological behavior of RTF mixed with GTR as fillers in PO based composites.

Since rheological characterizations are known to be useful tools to investigate the relationships between structural properties (morphology), processability and mechanical behavior, this work investigates the rheological properties in both the melt and solid states for RTF/GTR filled linear low density polyethylene (LLDPE) composites. In the first parts of this study (Moghaddamzadeh & Rodrigue, 2017a, 2017b), the morphological and mechanical properties were reported for three different processing parameters including RTF/GTR content (total filler content), compounding screw speed (resulting in different final particle sizes) and different temperature profiles (above and below PET melting temperature). Here, shear rheology is combined with DMA to get more information on the effect of morphology and interfacial adhesion between the phases and better explain the mechanical results reported in previous papers.

4.2 Experimental

4.2.1 Materials

As the matrix, linear low density polyethylene (LL8460, ExxonMobil, Sarnia, Canada) in a powder form (M_w = 94 kg/mol) was used. This LLDPE has a melting point of 127ºC, a density of 0.938 g/cm^3 and a melt index of 3.3 g/10 min (190ºC/2.16 kg). As the filler, RTF (Quebec Transloc, Lévis, Canada) was used. This waste material is mixed with GTR (5-8 wt.%) and has a density of 1.27 ± 0.01 g/cm^3. To improve compatibility, SEBS-g-MA (FG1901X, Kraton, Houston, USA) was selected. This compatibilizer is in a pellet form and contains 30% polystyrene grafted with 2% maleic anhydride. It has a melting temperature of 124°C, a melt index of 22 g/10 min (230ºC/5 kg) and a density of 0.91 g/cm^3. More details on the materials can be found in our previous studies (Moghaddamzadeh & Rodrigue, 2017a, 2017b).

4.2.2 Processing

Firstly, RTF was oven dried at 80°C for 12 h. Then, compounding was done using a co-rotating twin-screw extruder Leistritz ZSE-27 (L/D = 40). The studied parameters were RTF

content (10, 25 and 50 wt.%), as well as screw speed (110, 180 and 250 rpm) with low temperature (LT) and high temperature (HT) profiles in both extrusion and injection molding based on the RTF melting point (253°C). When added, 10 wt.% SEBS-g-MA (based on RTF) after pulverizing (pellet to powder) was applied. Due to the fluffy texture of the RTF (Moghaddamzadeh & Rodrigue, 2017a), all the materials were dry-blended together before feeding to the extruder main hopper to get a constant feeding flow rate. The compounds passed through a die (diameter of 2.7 mm), quenched in a water bath and pelletized. Then, the pellets were dried at 75ºC for 4 h before being injection molded on a Nissei PS60E9ASE machine (Japan) with a fixed mold temperature (30°C). Finally, the samples were cut directly from the injection molded parts for each characterization. Tables 4.1-4.3 present an overview of the experimental conditions, and more details can be found in our previous publications (Moghaddamzadeh & Rodrigue, 2017a, 2017b).

Table 4.1. Sample coding of the compounds produced at different conditions.

Sample	LLDPE (wt.%)	RTF (wt.%)	Compatibilizer (wt.%)	Screw speed (rpm)	Temperature profile
L-1001	100	0	0	110	LT
L-901	90	10	0	110	LT
L-751	75	25	0	110	LT
L-501	50	50	0	110	LT
L-508	50	50	0	180	LT
L-502	50	50	0	250	LT
LC-901	90	10	10	110	LT
LC-751	75	25	10	110	LT
LC-501	50	50	10	110	LT
LC-508	50	50	10	180	LT
LC-502	50	50	10	250	LT
E-250[a]	50	50	10	250	HT
I-250[a]	50	50	10	250	HT

[a] Composite E-250 was melt blended with LT profile and injection molded with HT profile, while sample I-250 has reversed production conditions.

Table 4.2. Temperature profiles in extrusion.

Temperature Profile	Zone 1 (°C)	Zone 2 (°C)	Zone 3 (°C)	Zone 4 (°C)	Zone 5 (°C)	Zone 6 (°C)	Zone 7 (°C)	Zone 8 (°C)	Zone 9 (°C)	Zone 10 (°C)
LT	170	170	170	170	170	170	170	170	170	175
HT	170	170	170	170	170	210	250	250	260	265

Table 4.3. Temperature profiles in injection molding.

Temperature Profile	Rear (°C)	Middle (°C)	Front (°C)	Nozzle (°C)
LT	170	175	180	185
HT	220	260	260	250

4.3 Characterization

Viscoelastic characterization in the melt state was carried out using an ARES (TA Instruments, USA) rheometer with 25 mm discs and 3 mm gap. All the tests were performed at 180°C under nitrogen. To determine the linear viscoelastic region of the compounds, strain sweeps were done in the range of 0.08-100% at 1 Hz. Then, dynamic frequency sweeps were performed over an angular frequency range of 0.1-193 rad/s. SigmaPlot v.12 (Systat Software, USA) was used to fit the experimental data with rheological models. All the fitted parameters have p-values below 0.0001. For each sample, the characterization included the dynamic elastic modulus, complex viscosity, van Gurp-Palmen plot and tan δ (damping factor) to investigate the elasticity of the compounds.

Dynamic mechanical analysis (DMA) was done on a RSA3 (TA Instruments, USA) using rectangular specimens having dimensions of 45×12.5×3.15 mm^3 in the three-point bending mode (span of 40 mm). According to the linear viscoelastic range of the compounds, a deformation of 0.01% at a rate of 2°C/min and a frequency of 1 Hz within the temperature range of 30-110°C was applied. The results are presented in terms of storage modulus and damping factor to investigate again the samples elasticity and to compare with the results in the melt state.

4.4 Results and Discussion

For the sake of paper length, only new results are presented and discussed here while more details about interfacial adhesion improvement, stress-transfer mechanism and, degradation

can be found in our previous papers reporting on morphology (Moghaddamzadeh & Rodrigue, 2017a) and mechanical properties (Moghaddamzadeh & Rodrigue, 2017b).

4.4.1 Melt rheology

Figure 4.1 shows the dynamic elastic modulus (G') as a function of angular frequency for different RTF content (Figure 4.1a), compounding screw speed (Figure 4.1b) and temperature profiles (Figure 4.1c). As seen in Figure 4.1a, G' for uncompatibilized composites is higher than for the neat LLDPE. This is associated with the presence of RTF and the interface (Mahallati et al., 2016) which is increasing with RTF content. On the other hand, increasing the mixing speed at constant filler content (Figure 4.1b) decreased the RTF aspect ratio and GTR sizes (Moghaddamzadeh & Rodrigue, 2017a) (because of higher shear). Hence, due to larger surface area created, smaller rubber particles impart higher elasticity (Moghaddamzadeh & Rodrigue, 2017b). This explains the higher G' values for L-502 compared to L-501 and L-508. But the addition of SEBS-g-MA (Figures 4.1a and 4.1b) improves the interfacial stress transfer resulting in higher elasticity of the compatibilized samples compared to uncompatibilized systems (Moghaddamzadeh & Rodrigue, 2017b). In fact, for uncompatibilized systems, only physical interactions are present between the phases. On the other hand, the addition of a compatibilizer like SEBS-g-MA improves the interaction due to the reactivity of the maleic anhydride (MA) groups having strong polarity and resulting in lower surface tension and increased interfacial adhesion between the phases. Furthermore, as seen in Figure 4.1c, samples E-250 and I-250 produced with HT profiles have lower shear storage modulus than LC-502 related to the degradation of rubber particles as well as the matrix (Moghaddamzadeh & Rodrigue, 2017a). However, less degradation occurred in sample I-250 compared to E-250 due to lower material residence time in injection molding at HT profile (Moghaddamzadeh & Rodrigue, 2017a, 2017b).

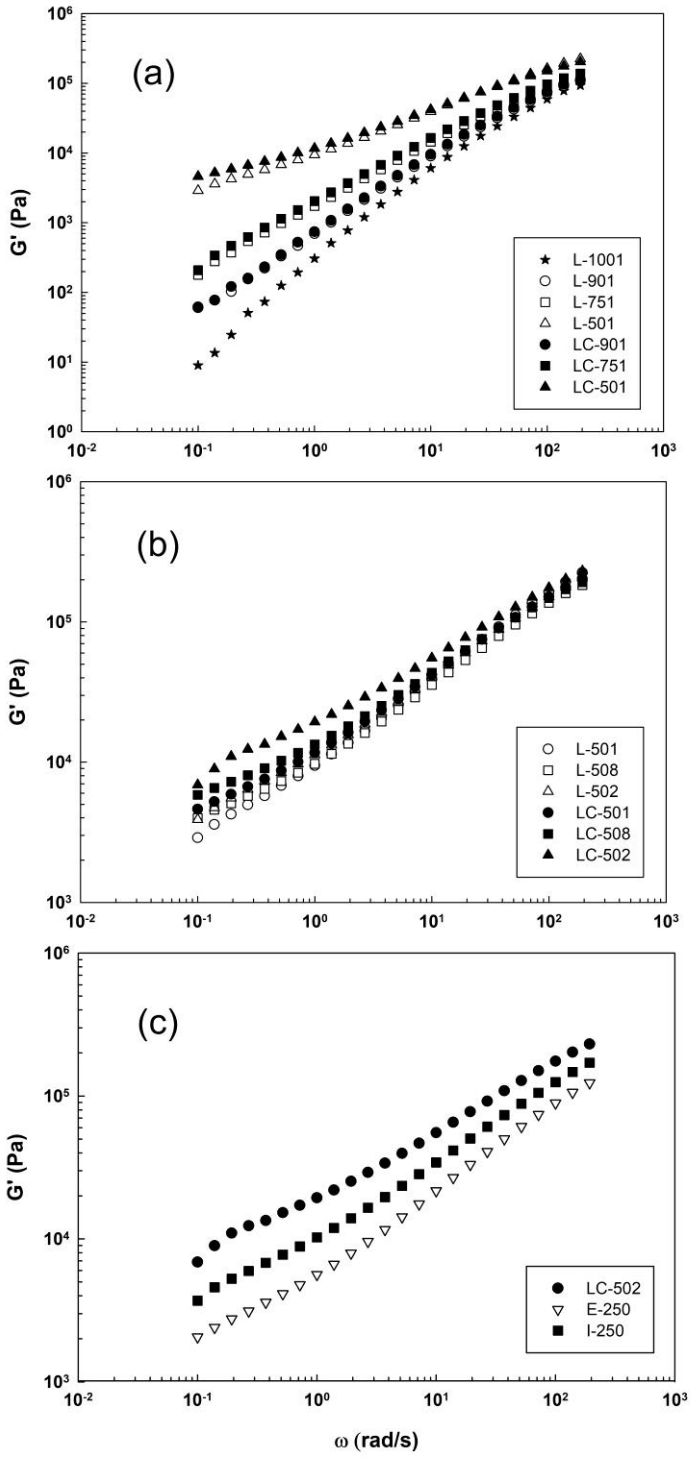

Figure 4.1. Dynamic elastic modulus as a function of angular frequency (180°C) to determine the effect of: a) RTF content, b) extruder screw speed, and c) temperature profiles.

Figure 4.2 shows the complex viscosity (η^*) of the composites as a function of angular frequency for different RTF content (Figure 4.2a), mixing speed (Figure 4.2b) and temperature profiles (Figure 4.2c). It is obvious that the presence of rubber particles embedded in the RTF increased the complex viscosity due to the cross-linked structure of GTR (Jain et al., 2000; Ramezani Kakroodi et al., 2013; Lima et al., 2015) and the effect increases with increasing RTF content (Figure 4.2a). Moreover, it is known that for a fixed GTR content, finer rubber particles impart higher viscosities due to higher surface contact area (Jain et al., 2000). The same trend is observed in Figure 4.2b. Sample L-501 has the largest fiber/particle size (Moghaddamzadeh & Rodrigue, 2017a) presenting the lowest viscosity, while L-502 has the smallest fiber/particles size producing the highest viscosity compared to L-501 and L-508. On the other hand, the addition of SEBS-g-MA increases the viscosity (Ezzati, Ghasemi, Karrabi, & Azizi, 2008) due to better interfacial adhesion between the matrix and GTR resulting in better stress transfer from LLDPE to rubber particles (Moghaddamzadeh & Rodrigue, 2017b) (Figures 4.2a and 4.2b). Hence, LC-502 presents the highest viscosity.

Furthermore, as seen in Figure 4.2c, the samples produced with HT profiles have lower complex viscosity. This is associated with GTR and LLDPE degradation at higher temperatures (Moghaddamzadeh & Rodrigue, 2017b; Scaffaro et al., 2005). However, sample I-250 shows higher viscosity than E-250 mostly due to lower degradation associated to lower residence time in injection (4 zones) compared to extrusion (10 zones) (Moghaddamzadeh & Rodrigue, 2017a, 2017b). For all the composites, a shear-thinning behavior (pseudo-plastic) was observed as the viscosity decreases with increasing shear rate.

Two different models were used to fit the data: the Cross model at low RTF concentrations (0-25%) and the power-law at higher RTF content (50%). Neat LLDPE presents a Newtonian plateau at low frequency (10^{-1} to 10^{0} rad/s) that can also be seen for composites with RTF < 50 wt.%, but this trend cannot be seen for composite with RTF = 50 wt.% indicating a tendency toward a yield point due to the presence of RTF. So, the Cross model better fits with RTF < 50% and the Power-law model fits well with RTF = 50%.

The Cross viscosity model can be written as (Chimeni, Dubois, & Rodrigue, 2017):

$$\eta_{(\omega)=}\frac{\eta_0}{1+(\lambda\omega)^{1-n}} \quad (4.1)$$

where η_0 is the zero-shear viscosity, λ is a material time constant (related to the melt relaxation time), and *n* is controlling the slope of the shear-thinning zone. Also, the simple power-law equation can be written as (Ramezani Kakroodi et al., 2013):

$$\eta^* = A\,\omega^{m-1} \quad (4.2)$$

where *A* is the consistency index and *m* is the power-law exponent. Table 4.4 shows that with increase in RTF content, *A*, η_o, λ, and *n* increases, while *m* decreases (power-law). It is obvious that the Cross model fits better at low RTF content < 50%. Note that the parameters for the Cross model were not reported for L-501 and LC-501 due to inappropriate R^2 and p-values ($R^2 << 1$ and $p > 0.0001$).

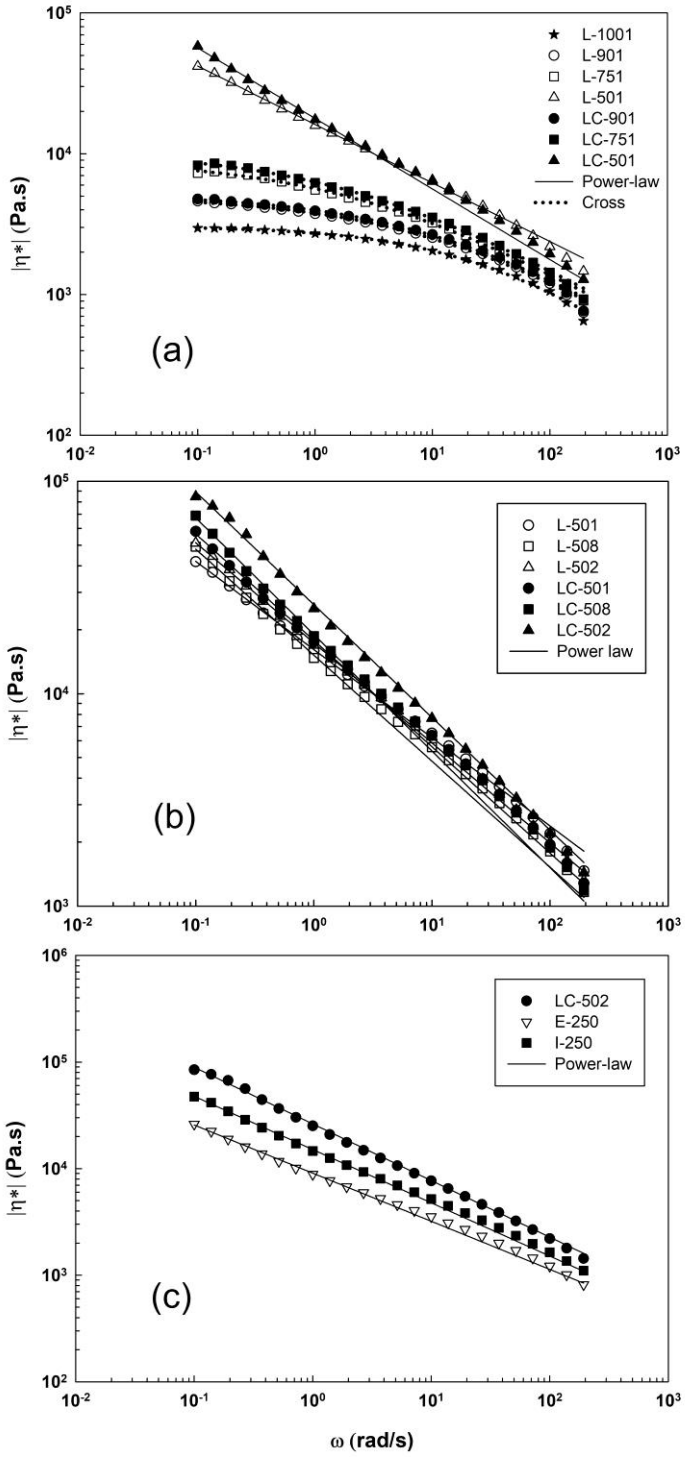

Figure 4.2. Complex viscosity as a function of angular frequency (180°C) to determine the effect of: a) RTF content, b) compounding screw speed, and c) temperatures profiles. The lines are regression to eq. (1-2) with the parameters of Table 4.4.

Table 4.4. Parameters of the Cross (eq.1) and power-law (eq.2) viscosity models for compounds (180°C).

Sample	Cross model				Power-law model		
	η_0 (kPa.s)	λ (s/rad)	n (-)	R^2	A (kPa s^m rad^{1-m})	m (-)	R^2
L-1001	3.07	0.031	0.401	0.997	2.51	0.869	0.873
L-901	4.97	0.091	0.492	0.998	3.46	0.832	0.933
LC-901	5.14	0.098	0.494	0.997	3.62	0.833	0.929
L-751	9.12	0.361	0.520	0.997	5.14	0.787	0.957
LC-751	10.5	0.429	0.524	0.998	5.73	0.778	0.959
L-501	N/A	N/A	N/A	N/A	16.1	0.585	0.999
LC-501	N/A	N/A	N/A	N/A	17.8	0.500	0.998
L-508	N/A	N/A	N/A	N/A	15.2	0.501	0.997
LC-508	N/A	N/A	N/A	N/A	19.0	0.451	0.998
L-502	N/A	N/A	N/A	N/A	17.4	0.529	0.999
LC-502	N/A	N/A	N/A	N/A	26.3	0.469	0.996
E-250	N/A	N/A	N/A	N/A	9.06	0.549	0.998
I-250	N/A	N/A	N/A	N/A	15.1	0.501	0.999

Figure 4.3 presents the van Gurp-Palmen plots of the samples produced with different RTF content (Figure 4.3a), extruder screw speed (Figure 4.3b) and temperature profiles (Figure 4.3c). These plots can be used to determine the samples elastic properties by plotting the phase angle (δ) as a function of the complex modulus (G^*). When $\delta < 45°$, the sample mainly has an elastic behavior as (Ezzati et al., 2008):

$$\delta < 45° \rightarrow \tan\delta < 1 \rightarrow G''/G' < 1 \rightarrow G'' < G' \quad (3)$$

As expected, the van Gurp-Palmen plot of the neat matrix (homogeneous linear polymer) reaches a plateau close to 90° when the complex modulus (G^*) decreases (Chimeni, Toupe, Dubois, & Rodrigue, 2016; Trinkle, Walter, & Friedrich, 2002) (Figure 4.3a). But when RTF is added (especially at higher content), a maximum is observed in the plots (Figure 4.3a). This is associated with the improved interfacial adhesion between the matrix and the rubber

particles leading to higher elasticity resulting in particle-matrix morphology (Li, Yu, & Zhou, 2006b). For example, at 50 wt.% RTF, a peak is seen for both uncompatibilized and compatibilized samples, but the compatibilizer produced a shift from 54.8 to 50.1° in δ_{max} and from 35.8 to 36.6 kPa in $|G^*_{\delta max}|$ for L-501 and LC-501, respectively. This shift is related to the presence of SEBS-g-MA and indicates improved interfacial adhesion in the blends (Moghaddamzadeh & Rodrigue, 2017b). This phenomenon has also been reported for polymer blends having a droplet morphology (Ezzati et al., 2008; Li et al., 2006b; Li, Yu, & Zhou, 2006a). Nevertheless, for the range of conditions tested, no maximum was observed for RTF < 50 wt.%.

Moreover, as the mixing speed increased from 110 to 180 and 250 rpm (Figure 4.3b), all the samples showed a maximum in the curves associated to the presence of an interface. For all compatibilized blends, the maximum is shifted to higher $|G^*_{\delta max}|$ values indicating better interfacial stress transfer. The shift is even more important as higher screw speeds were used leading to higher surface area created as reported by Ezzati et al. (Ezzati et al., 2008). Table 4.5 presents all the data for the samples produced with different mixing speed. As seen in Figure 4.3c, compatibilized 50% RTF samples produced at different temperature profiles present significant differences between the curves. The maximum complex modulus ($|G^*_{\delta max}|$) for LC-502 (65.0 kPa) is higher than E-250 (19.5 kPa) and I-250 (36.0 kPa), while it has lower δ_{max} (44.1°) compared to E-250 (53.4°) and I-250 (49.2°). These shifts indicate higher elasticity of LC-502 associated with stronger interfacial adhesion for LT profile compared to the GTR/LLDPE degradation for HT profile (Moghaddamzadeh & Rodrigue, 2017a).

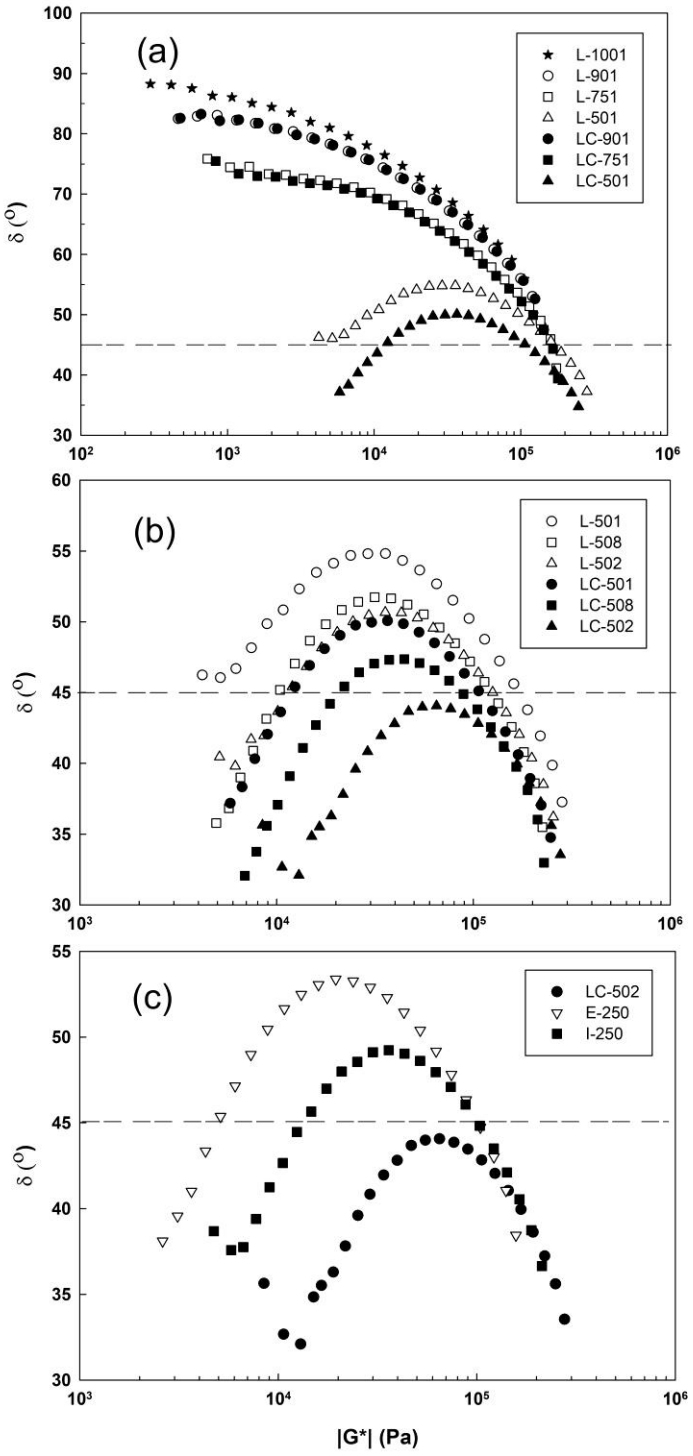

Figure 4.3. van Gurp-Palmen plots (180°C) to determine the effect of: a) RTF content, b) extruder screw speed, and c) temperature profiles.

Table 4.5. Complex modulus at the maximum phase angle and its corresponding phase angle from van Gurp-Palmen plots (180°C) for samples produced with different extruder screw speed.

Sample	L-501	L-508	L-502	LC-501	LC-508	LC-502
δ_{max} (^{o})	54.8	51.7	50.7	50.1	47.4	44.1
$\lvert G^*_{\delta max} \rvert$ (kPa)	35.8	31.5	35.7	36.6	44.6	65.0

Figure 4.4 presents the tan δ (damping factor) results as a function of frequency for samples produced with different RTF content (Figure 4.4a), compounding screw speed (Figure 4.4b) and temperature profiles (Figure 4.4c), while Table 4.6 presents all the values of interest. As seen in Figure 4.4a, the crossover frequency (ω_c) (related to tan δ = G"/G' = 1) is about 193.0 rad/s for L-1001, L-901 and LC-901, but decreases to 139.0 rad/s for L-751 and LC-751 indicating a more elastic behavior when 25% RTF is added to the compounds. On the other hand, composites with 50 wt.% RTF (Figure 4.4a) and increased compounding speed (Figure 4.4b) present two values for ω_c and tan δ. This can be explained by the increased elasticity at 50 wt.% RTF.

As the mixing speed increases, ω_c shifts to lower values. Although this is associated with the smaller rubber particles (Moghaddamzadeh & Rodrigue, 2017a) imparting higher elasticity (Moghaddamzadeh & Rodrigue, 2017b), the addition of SEBS-g-MA decreased even the ω_c indicating lower rigidity for the compatibilized compounds (better stress transfer to the rubber phase having low modulus) (Moghaddamzadeh & Rodrigue, 2017b). For the effect of the temperature profiles, Figure 4.4c shows that ω_c shifts form 7.2 rad/s for LC-502 (LT profile) to 51.8 rad/s (E-250) and 26.8 rad/s (I-250). Once again, this behavior is related to the degradation of LLDPE/GTR for HT profiles resulting in lower elastic behavior for samples E-250 and I-250 (Moghaddamzadeh & Rodrigue, 2017a, 2017b).

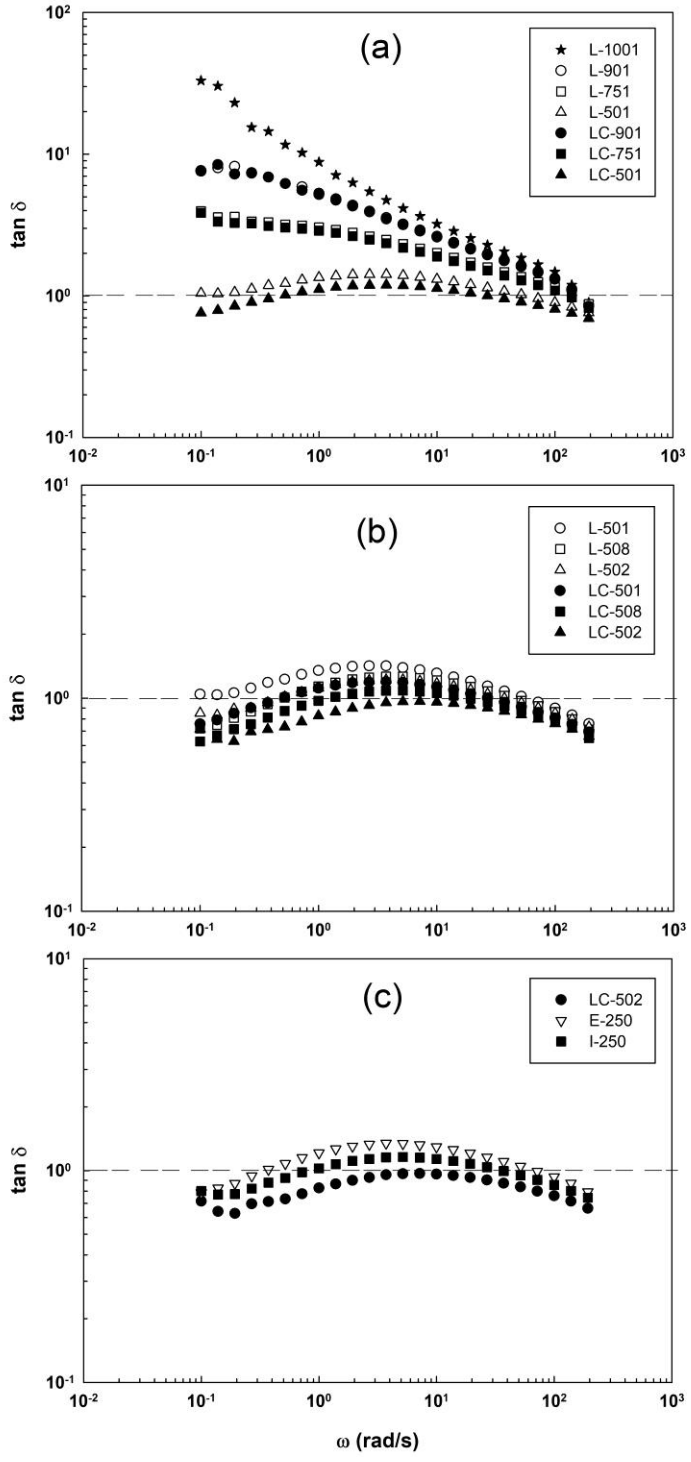

z

Figure 4.4. Damping factor as a function of frequency (180°C) to determine the effect of: a) RTF content, b) extruder screw speed, and c) temperature profiles.

Table 4.6. Crossover frequency (ω_c) of the compounds at different processing parameters (180°C).

Sample	ω_c (rad/s)	Sample	ω_c (rad/s)
L-1001	193.0	L-508	0.4 / 37.3
L-901	193.0	LC-508	0.9 / 13.9
LC-901	193.0	L-502	0.5 / 37.3
L-751	139.0	LC-502	7.2
LC-751	139.0	E-250	0.3 / 51.8
L-501	0.1 / 51.8	I-250	0.7 / 26.8
LC-501	0.4 / 26.8	-	-

4.4.2 Dynamic mechanical analysis (DMA)

The storage modulus (E') curves as a function of temperature in DMA can also help to understand the stiffness of the material due to interfacial bonding (Jacob, Francis, & Thomas, 2006). Figure 4.5 presents the values as a function of temperature for different RTF content (Figure 4.5a), mixing speed (Figure 4.5b) and temperature profiles (Figure 4.5c). As seen in Figures 4.5a and 4.5b, E' initially increased from 30°C up to a maximum around 35 to 50°C and then decreases for all blends. According to Chimeni et al. (Chimeni et al., 2017), this maximum is associated to the β transition of PE, while the decreasing trend is related to material softening from higher segmental mobility of the polymer chains. However, neat LLDPE has the highest E'; i.e. the highest stiffness overall due to the presence of crystallites related to its semi-crystalline structure (Saleesung, Saeoui, & Sirisinha, 2010).

Lower rigidity with increasing RTF content (Figure 4.5a) and decreasing rubber particles size (Moghaddamzadeh & Rodrigue, 2017a) (Figure 4.5b) is also observed. This behavior is associated with stress transfer from the matrix to GTR particles (low modulus) (Moghaddamzadeh & Rodrigue, 2017b). Addition of a compatibilizer led to additional reduction in the storage modulus blends indicating better compatibility between the rubber phase and the matrix (Moghaddamzadeh & Rodrigue, 2017b).

For the effect of the temperature profiles (Figure 4.5c), LC-502 presents lower E' than E-250 and I-250 overall. This trend is in contrast with the values reported for Young's modulus in our previous study (Moghaddamzadeh & Rodrigue, 2017b), but can be related to the direction of the applied forces on the samples (mainly RTF) as the Young's modulus was measured in uniaxial tension, while the DMA tests were performed in flexion (a mixture of compression and tension across thickness). Hence, the material response is different probably due to fibre orientation which is another important parameter for fibre reinforced materials. Nevertheless, due to the matrix degradation at HT profiles (Moghaddamzadeh & Rodrigue, 2017a), no β transition is observed for E-250 and I-250. Table 4.7 presents all the values for the maximum storage modulus and its corresponding temperature for the blends.

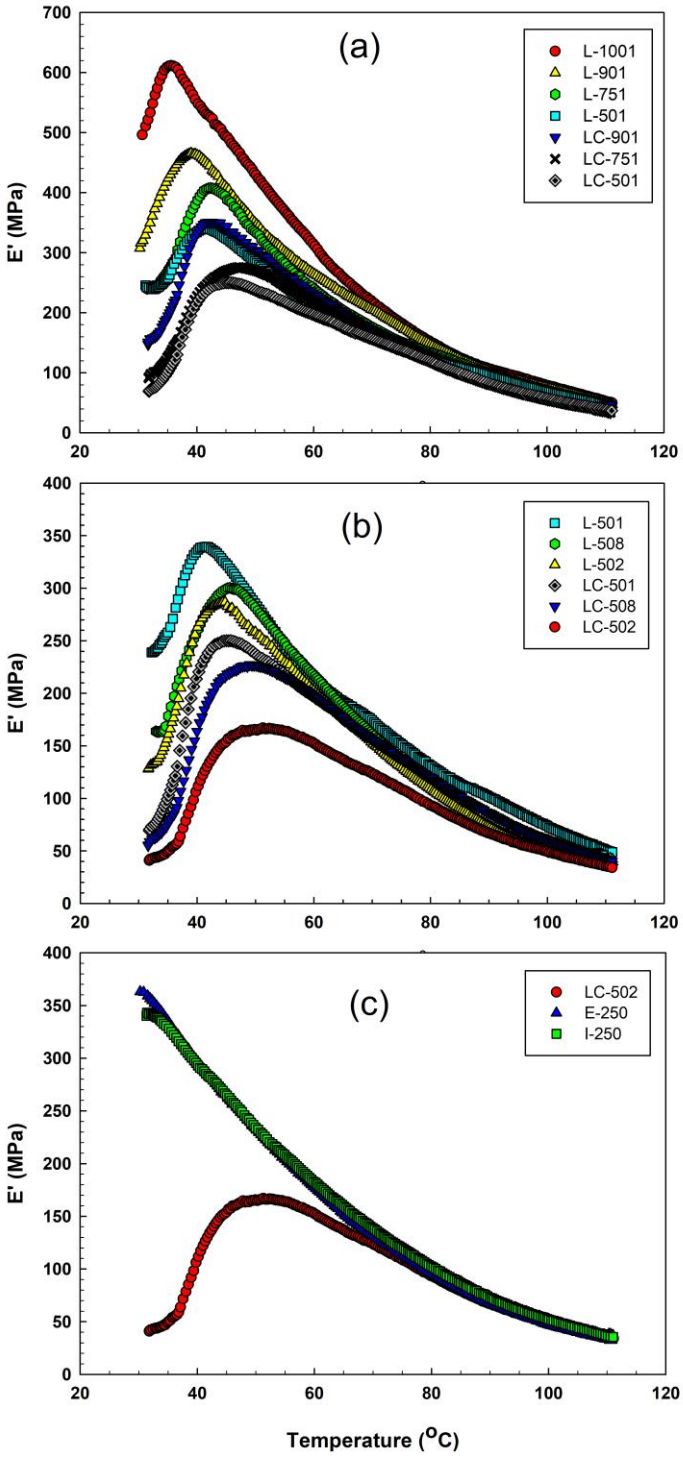

Figure 4.5. Storage modulus as a function of temperature to determine the effect of: a) RTF content, b) extrusion screw speed, and c) temperature profiles.

Table 4.7. Maximum of the storage modulus at its corresponding temperature of the blends in the solid state.

Sample	E' (MPa)	Temperature (°C)	Sample	E' (MPa)	Temperature (°C)
L-1001	611	35.6	L-508	300	45.6
L-901	465	39.0	LC-508	227	49.0
LC-901	350	42.9	L-502	286	44.4
L-751	407	42.3	LC-502	167	51.3
LC-751	275	46.8	E-250	363	30.2
L-501	339	41.8	I-250	343	32.0
LC-501	250	45.0	-	-	-

It is known that three different relaxation peaks for polyethylene (PE), namely α, β and γ, are observed via DMA. The α relaxation deals with reorientation of defects in the crystals associated to chain segment mobility in the crystalline phase, while the γ relaxation occurs in the amorphous phase associated to the glass transition temperature (T_g) of the polymer. Although the origin of the β transition is related to the motion of side branches for polymers like LDPE and LLDPE, it is almost inexistent in HDPE (Chimeni et al., 2016; John, Varughese, Oommen, Pötschke, & Thomas, 2003; Mohanty & Nayak, 2010; Mohanty, Verma, & Nayak, 2006; Sewda & Maiti, 2013). Since the γ transition (T_g) of LLDPE is around -145°C (Khanam & AlMaadeed, 2015), it is easier to focus on the α transition temperature (T_α) which occurs above 0^oC.

Figure 4.6 presents the damping factor (tan δ) of the samples as a function of temperature for different RTF content (Figure 4.6a), compounding screw speed (Figure 4.6b) and temperature profiles (Figure 4.6c). As seen in Figure 4.6a, the damping factor increases with increasing temperature and showed two maxima: a small hump is observed around 35°C (LLDPE) to 45°C (composites) and a second one around 85-96°C. The small shoulder at lower temperature can be associated with the β transition of the samples and is smaller for neat LLDPE compared to the composites due to the linear structure of LLDPE (Chimeni et al., 2017). As temperature increases, a broad peak appears at 84.8°C for neat LLDPE related

to its T_α. Similar results have been reported by Chimeni et al. (Chimeni et al., 2016) for linear medium density polyethylene (LMDPE). Adding RTF to the matrix produced broad peaks at higher temperatures and increased the damping factor values. The presence of GTR in uncompatibilized samples increased the T_α of compounds to 86.1°C (L-901), 90.9°C (L-751) and 94.2°C (L-501), while tan δ was constant (0.24-0.25) for all samples. This indicates higher chain segments mobility in the polymer to slide pass each other resulting in more dissipated vibration energy (viscous heating) (Roche et al., 2011).

Moreover, addition of SEBS-g-MA led to higher T_α for the compatibilized compounds up to 94.3, 95.0 and 96.0°C, as well as increased tan δ up to 0.29, 0.28 and 0.27 for LC-901, LC-751 and LC-501, respectively. This behavior indicates the strong effect of SEBS-g-MA to improve stress transfer from the matrix to the rubber particles resulted in lower rigidity of the compounds (Moghaddamzadeh & Rodrigue, 2017b) and increased polymer chains mobility. As a result, the loss tangent peak value and its position have a direct relation with the polymer chain segment mobility (Chimeni et al., 2017).

When smaller GTR particles (Moghaddamzadeh & Rodrigue, 2017a) are produced (Figure 4.6b), the tan δ curves of the uncompatibilized samples show a small shoulder around 40-55°C (T_β) and broad peaks around 87-94°C (T_α). At the lowest extruder screw speed, L-501 has T_α = 94.2°C and tan δ = 0.25, but increasing the screw speed from 110 to 180 rpm resulted in lower T_α (87.1°C) and higher tan δ (0.26) for sample L-508. At the highest compounding screw speed, L-502 shows higher T_α (88.1°C) and lower tan δ (0.25). This behavior indicates that at a constant RTF content in uncompatibilized blends, different GTR particle sizes (Moghaddamzadeh & Rodrigue, 2017a) behave similarly as to increase the damping factor and T_α of the compounds. But the addition of SEBS-g-MA leads to higher values for tan δ and T_α due to improved interfacial adhesion between the rubber particles and the matrix (Moghaddamzadeh & Rodrigue, 2017b). In fact, T_α and tan δ increased from 94.2 to 96.0°C and 0.25 to 0.27 respectively, for LC-501 compared to L-501.

At higher mixing speed (180 rpm), sample LC-508 exhibits higher T_α (95.2°C) and damping factor (0.28) compared to L-508 (T_α = 87.1°C and tan δ =0.26). Similarly, the highest screw speed (250 rpm) produced finer GTR particles (Moghaddamzadeh & Rodrigue, 2017a) and LC-502 showed the highest values for T_α = 100.0°C and tan δ = 0.28. Once again, in the case

of the temperature profiles effect (Figure 4.6c), a small shoulder around 50-55°C for LC-502 is related to the β transition, while this T_β is not observed for samples produced with HT profiles. This can be associated to LLDPE degradation in E-250 and I-250 (Moghaddamzadeh & Rodrigue, 2017a) leading to T_β disappearance. Moreover, the rigidity of the samples increased with increasing the damping factor at lower temperatures. In fact, tan δ increases from 0.28 (LC-502) to 0.33 (E-250) and 0.29 (I-250), while T_α decreased from 100.0 (LC-502) to 92.4 (E-250) and 93.5°C (I-250) indicating reduced polymer chains mobility and elasticity. However, sample E-250 shows higher tan δ compared to I-250 indicating a less elastic behavior related to more LLDPE and GTR degradation in the extruder (higher material residence time) compared to injection molding (lower material residence time) (Moghaddamzadeh & Rodrigue, 2017a).

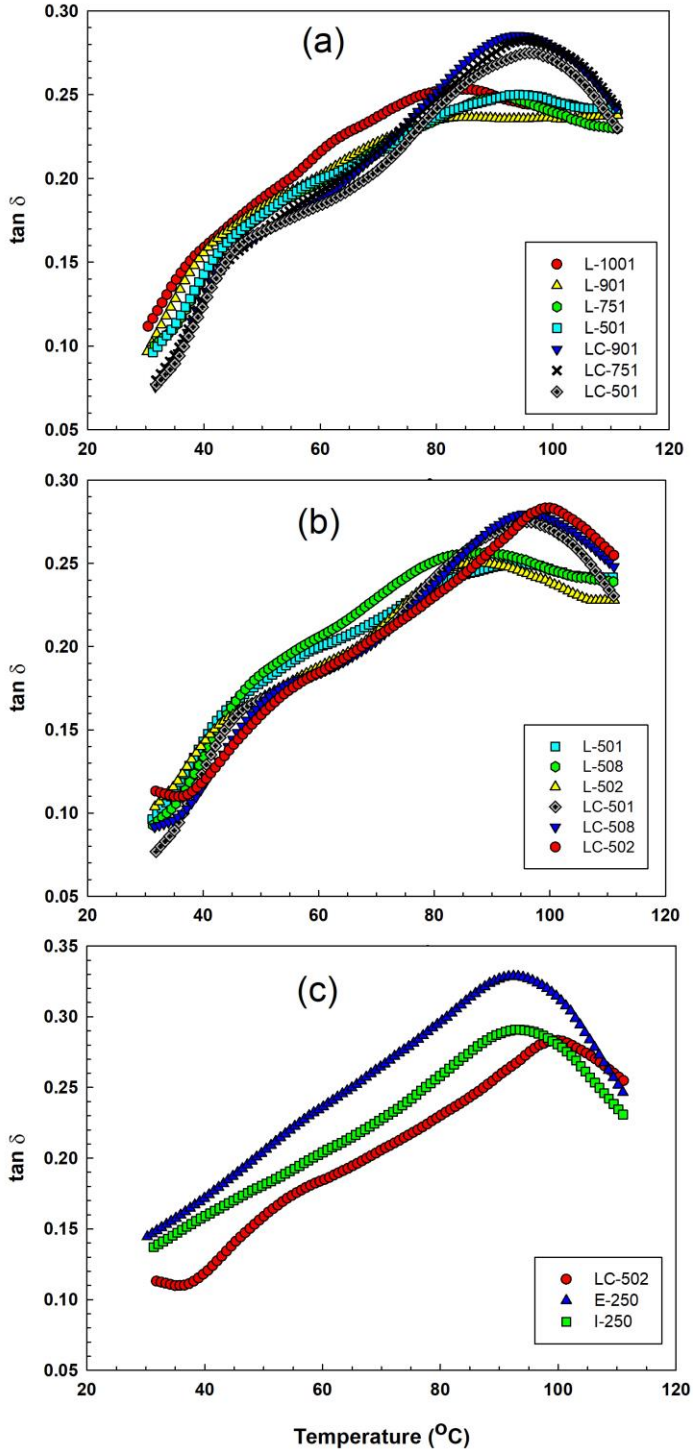

Figure 4.6. Damping factor as a function of temperature to determine the effect of: a) RTF content, b) extruder screw speed, and c) temperature profiles.

4.5 Conclusion

In this work, the rheological behaviors of polyester recycled tire fibers (RTF) mixed with ground tire rubber (GTR) and linear low density polyethylene (LLDPE) with and without styrene-ethylene-butylene-styrene grafted maleic anhydride (SEBS-g-MA) as a compatibilizer were studied in the melt (small amplitude oscillatory shear or SAOS) and solid (dynamic mechanical analysis or DMA) states. In particular, the effect of RTF content (10, 25 and 50 wt.%), extruder screw speed (110, 180 and 250 rpm) and temperature profiles (extrusion and injection molding) was studied. The main results are:

- Data in the melt state showed increased dynamic storage modulus and complex viscosity of the compounds with increasing RTF content (crosslinked structure of GTR) and compounding screw speed (higher surface contact area generated). These effects were even more important for compatibilized blends.
- The van Gurp-Palmen plots showed different behaviors between the neat matrix, the uncompatibilized blends and the compatibilized ones. In particular, the presence of a maximum in the curve and a shift of its position can be directly associated to the presence of an interface and its quality (adhesion and compatibility).
- The processing conditions have a direct effect on the rheological properties as they control the final morphology in terms of interfacial area generated, but also composition is important especially for the interface stress transfer (presence of a compatibilizer).
- The effect of processing temperature (LT vs. HT) is important as it can lead to material degradation and morphology changes (melting or not of the polyester fibres).
- Contrary to the melt state, the DMA results showed a decreasing trend in the storage modulus of all samples with increasing RTF content and mixing speed representing lower rigidity for compatibilized compounds resulting in improved damping factor and T_α compared to neat LLDPE.

Acknowledgements

The authors acknowledge the financial support of the Natural Sciences and Engineering Research Council of Canada (NSERC), the Research Center on Advanced Materials (CERMA), the Quebec Center on Functional Materials (CQMF) and the Research Center for High Performance Polymer and Composite Systems (CREPEC). The technical help of Mr. Yann Giroux was also much appreciated.

.

Chapter 5

Conclusions and recommendations

5.1 General conclusions

As a product of tire recycling to manage discarded tires in the environment, recycled tire fiber (RTF) is a by-product containing imbedded ground tire rubber (GTR) particles. Despite several attempts of using GTR as filler/impact modifier in thermoplastic elastomers with and without natural fibers as reinforcement, almost no effort has been devoted to use RTF mixed with GTR, as a direct product of tire recycling, as filler/reinforcement/impact modifier in polymer composites, where polyester recycled tire fibers can act as a reinforcing agent due to their good tensile strength and modulus while GTR can improve the impact strength of the compounds. For this reason, this work focused on the possibility to introduce polyester RTF mixed with GTR in linear low density polyethylene (LLDPE) based composites to study the effects of RTF content, compatibilizer concentration, compounding screw speed, and temperature profiles below (LT) and above (HT) the melting temperature of RTF (253°C) in extrusion and injection molding on the physical, mechanical, morphological and rheological properties of the produced composites. As a result, this investigation led to the following general conclusions:

1. As the first step of the work, prior to compounding, different characterizations (FTIR, XPS, DSC, SEM, TGA and density) were done to confirm the polyester structure of RTF and presence of GTR imbedded in RTF as there was no datasheet for this material. Then, morphological observations were done for all the fractured surfaces of uncompatibilized and compatibilized compounds melt-blended via twin-screw extrusion followed by injection molding. The results showed better distribution of GTR particles in the matrix with increasing RTF content, but the compatibilized blends presented more homogeneity compared to uncompatibilized ones. Smaller RTF length and GTR particle sizes was observed when the compounding screw speed was increased due to higher shear stresses which was higher for compatibilized composites. However, no interfacial adhesion between the RTF with GTR and/or LLDPE was observed, even in the presence of compatibilizer (SEBS-g-MA). Finally, applying HT profiles for extrusion and injection molding resulted in the degradation of GTR (starting at 210°C) and LLDPE (starting at

260°C) which was more severe in the extrusion step compared to the injection molding step due to the higher material residence time in the extruder.

2. The second part of the work presented a complete series of studies for mechanical (tension, flexion and impact) and physical (hardness and density) properties of all the composites reported in the previous step as to better understand the morphological results. The results showed that despite a decrease in all mechanical properties with increasing RTF content for the compatibilized blends, Charpy impact strength improved by about 18, 29 and 50% at 10, 25 and 50% RTF, respectively. Also, the physical properties showed increased density of both uncompatibilized and compatibilized compounds by about 2, 6 and 12%, while hardness (Shore D) decreased by about 4, 7 and 9% when the RTF content increased from 10 to 25 and 50%. With increasing compounding screw speed from 110 to 180 and 250 rpm, the compatibilized 50% RTF samples had higher tensile strength (14 and 13%) and Charpy impact strength (54 and 56%). Moreover, although density of all the uncompatibilized and compatibilized compounds was almost constant at different extruder screw speed, the hardness (Shore D) of the compatibilized 50% RTF decreased by 4% at 250 rpm compared to 110 rpm. Finally, the samples produced at HT profiles showed decreases in all the mechanical properties as well as density values compared to samples produced at LT profiles due to GTR and LLDPE degradation, where degradation in the injection molding step is less severe due to lower material residence time compared to the extruder. Nevertheless, the hardness of the compounds produced at HT profiles did not significantly change.

3. As the last part of the work, the rheological characterization of all the composites produced in the first part of the work was performed in the melt (small amplitude oscillatory shear or SAOS) and solid (dynamic mechanical analysis or DMA) states to better understand the relationships between processing, morphology and macroscopic properties. The results in the melt state showed that increasing shear storage modulus (G') was observed with increasing RTF content and extruder screw speed due to strong interfacial adhesion between the GTR and LLDPE, especially when SEBS-g-MA was added. As the most important result in the melt state, the van Gurp-Palmen plots presented higher elasticity with increasing RTF content and compounding screw speed, with higher

values for the compatibilized blends compared to uncompatibilized ones. Based on the results, the best compound was reported for the compatibilized 50% RTF sample produced at the highest screw speed (250 rpm) showing $|G^*_{\delta max}|$ = 65 kPa at δ_{max} = 44.1°, while all the other compounds showed lower $|G^*_{\delta max}|$ at higher phase angle maximum presenting less elasticity. Also, compared to the LT profile, the HT profile decreased the compounds elasticity due to LLDPE and GTR degradation for the same reasons as mentioned above. But contrary to the melt state, the results in the solid state (DMA) presented lower storage modulus (E') with increasing RTF and compatibilizer contents, as well as compounding screw speed leading to less rigidity resulting in higher damping factor (tan δ) at higher values and temperatures compared to neat LLDPE (tan δ = 0.25 at 84.8°C), while the compatibilized 50% RTF compound presented the highest tan δ = 0.28 at 100°C. However, HT profile exhibited more rigidity compared to LT profile.

4. Overall, considering the increased elasticity of the compatibilized compounds with increasing RTF content and compounding screw speed for a LT profile in extrusion and injection molding, some possible applications of these composites having recycled materials can be in automobile (wheel cap) and containers (public and industrial recycling bins) areas.

5.2 Recommendations for future work

Based on the results obtained, several questions are still open to be answered. The following recommendations are presented for future work:

1. In the present work, the presence of SEBS-g-MA as a compatibilizer showed a strong effect at improving the final properties of the composites in different aspects, especially for the highest RTF content (50 wt.%) and compounding screw speed (250 rpm) for LT profiles. It is expected that with optimized processing conditions, the final properties of the compounds can be improved by optimizing the SEBS-g-MA concentration.

2. In this study, SEBS-g-MA was used as a compatibilizer to improve the final properties of the composites. As mentioned earlier in chapter 1, there are other coupling agents/compatibilizers such as E-GMA with higher number and stronger functional groups such as epoxy that can better react with PET to improve the mechanical properties of the composites.

3. Since most of the literature focused on the final application of RTF in building and construction, studying the thermal properties (thermal insulation, expansion, etc.) as well as creep behavior (rheology) of the produced composites could be interesting.

4. Although a PE based matrix was selected for this work, substitution of LLDPE with other thermoplastics such as PP and PET or even a bio-based matrix like PLA with a similar structure to polyester fibers and GTR could also be of interest.

5. Efforts to produce thermoplastic elastomer foams based on RTF and GTR could also be of interest to investigate the combined effects of synthetic fibers (PET) and GTR on the final properties of polyolefin based foamed composites as some studies have been done previously to produce similar materials based on polyolefins/GTR (or EPDM) and polyolefins/natural fibers.

6. As mentioned in chapter one, another synthetic fiber in tire structure as tire cord is polyamide (Nylon 66) which is highly used in truck/bus/heavy duty tires. A similar study to the one presented here can be done by substituting polyester RTF with Nylon 66 RTF with different matrices and coupling agents/compatibilizers. This would help to explore a wider range of final properties and/or the production of new composites.

References

2013 U. S. Scrap Tire Management Summary. (2013).

2015 U. S. Scrap Tire Management Summary. (2015).

Acevedo, B., Fernández, A. M., & Barriocanal, C. (2015). Identification of polymers in waste tyre reinforcing fibre by thermal analysis and pyrolysis. *Journal of Analytical and Applied Pyrolysis*, *111*, 224–232. http://doi.org/10.1016/j.jaap.2014.11.005

Adhikari, B., De, D., & Maiti, S. (2000). Reclamation and recycling of waste rubber. *Progress in Polymer Science*, *25*(7), 909–948.

Akiba, M. (1997). Vulcanization and crosslinking in elastomers. *Progress in Polymer Science*, *22*(3), 475–521. http://doi.org/10.1016/S0079-6700(96)00015-9

Al-Malki, Z. T., Al-Nasir, E. A., Khalaf, M. N., & Zidan, R. K. (2013). Study the Effect of Recycled Tire Rubber on the Mechanical and Rheological Properties of TPV (HDPE/Recycled Tire Rubber). *Open Journal of Polymer Chemistry*, *3*, 99–103. http://doi.org/10.4236/ojpchem.2013.34017

Anthony, W. S. (2005). Separation of Crumb and Fiber in Tire Recycling Operations. In *ASAE Annual International Meeting* (pp. 1–24). Tampa, Florida.

Arockiasamy, A., Toghiani, H., Oglesby, D., Horstemeyer, M. F., Bouvard, J. L., & King, R. L. (2013). TG–DSC–FTIR–MS study of gaseous compounds evolved during thermal decomposition of styrene-butadiene rubber. *Journal of Thermal Analysis and Calorimetry*, *111*(1), 535–542. http://doi.org/10.1007/s10973-012-2559-0

Asgari, M., & Masoomi, M. (2012). Thermal and impact study of PP/PET fibre composites compatibilized with Glycidyl Methacrylate and Maleic Anhydride. *Composites: Part B*, *43*(3), 1164–1170. http://doi.org/10.1016/j.compositesb.2011.11.035

Asgari, M., & Masoomi, M. (2015). Tensile and flexural properties of polypropylene/short poly (ethylene terephthalate) fibre composites compatibilized with glycidyl methacrylate and maleic anhydride. *Journal of Thermoplastic Composite Materials*, *28*(3), 357–371. http://doi.org/10.1177/0892705713484748

Bignozzi, M. C., Saccani, A., & Sandrolini, F. (2000). New polymer mortars containing polymeric wastes. Part 1. Microstructure and mechanical properties. *Composites: Part A*, *31*(2), 97–106.

Cañavate, J., Casas, P., Colom, X., & Nogués, F. (2011). Formulations for thermoplastic vulcanizates based on high density polyethylene, ethylene-propylene-diene monomer,

and ground tyre rubber. *Journal of Composite Materials*, *45*(11), 1189–1200. http://doi.org/10.1177/0021998310369596

Chimeni, D. Y., Dubois, C., & Rodrigue, D. (2017). Polymerization Compounding of Hemp Fibers to Improve the Mechanical Properties of Linear Medium Density Polyethylene Composites. *Polymer Composites*. http://doi.org/10.1002/pc.24279

Chimeni, D. Y., Toupe, J. L., Dubois, C., & Rodrigue, D. (2016). Effect of surface modification on the interface quality between hemp and linear medium-density polyethylene. *Journal of Applied Polymer Science*, *133*, 43802. http://doi.org/10.1002/app.43802

Colom, X., Andreu-Mateu, F., Cañavate, F. J., Mujal, R., & Carrillo, F. (2009). Study of the Influence of IPPD on Thermo-Oxidation Process of Elastomeric Hose. *Journal of Applied Polymer Science*, *114*(4), 2011–2018. http://doi.org/10.1002/app.30746

Daneshvar, M., & Masoomi, M. (2012). Synthesis and Application of MDPE-g-GMA as Reactive Compatibilizer in Blends of MDPE/PET and MDPE/PA6 Mohsen. *Journal of Applied Polymer Science*, *124*, 2048–2054. http://doi.org/10.1002/app.35235

De, S. K., Isayev, A. I., & Khait, K. (2005). *Rubber Recycling*. Boca Raton: CRC Press.

Dobrovszky, K., & Ronkay, F. (2015). Effects of SEBS-g-MA on Rheology, Morphology and Mechanical Properties of PET/HDPE Blends. *International Polymer Processing*, *30*(1), 91–99.

Ezzati, P., Ghasemi, I., Karrabi, M., & Azizi, H. (2008). Rheological Behaviour of PP/EPDM Blend: The Effect of Compatibilization. *Iranian Polymer Journal*, *17*(9), 669–679. Retrieved from http://journal.ippi.ac.ir

Ferrão, P., Ribeiro, P., & Silva, P. (2008). A management system for end-of-life tyres: A Portuguese case study. *Waste Management*, *28*(3), 604–614. http://doi.org/10.1016/j.wasman.2007.02.033

Ferreira, C. T., Perez, C. A. B., Hirayama, D., & Saron, C. (2013). Recycling of polyamide (PA) from scrap tires as composites and blends. *Journal of Environmental Chemical Engineering*, *1*(4), 762–767. http://doi.org/10.1016/j.jece.2013.07.016

Formela, K., Korol, J., & Saeb, M. R. (2015). Interfacially modified LDPE/GTR composites with non-polar elastomers: From microstructure to macro-behavior. *Polymer Testing*, *42*, 89–98. http://doi.org/10.1016/j.polymertesting.2015.01.003

Fukumori, K., Matsushita, M., Okamoto, H., Sato, N., Suzuki, Y., & Takeuchi, K. (2002). Recycling technology of tire rubber. *JSAE Review*, *23*(2), 259–264. http://doi.org/10.1016/S0389-4304(02)00173-X

Gent, A. N., & Walter, J. D. (2006). *Pneumatic Tire*. Akron: Mechanical Engineering Faculty Research.

Girija, B. G., Sailaja, R. R. N., & Madras, G. (2005). Thermal degradation and mechanical properties of PET blends. *Polymer Degradation and Stability*, *90*(1), 147–153. http://doi.org/10.1016/j.polymdegradstab.2005.03.003

Grigoryeva, O. P., Fainleib, A. M., Tolstov, A. L., Starostenko, O. M., Lievana, E., & Karger-Kocsis, J. (2005). Thermoplastic Elastomers Based on Recycled High-Density Polyethylene, Ethylene–Propylene–Diene Monomer Rubber, and Ground Tire Rubber. *Journal of Applied Polymer Science*, *95*(3), 659–671. http://doi.org/10.1002/app.21177

Han, C. D., Van Den Weghe, T., Shete, P., & Haw, J. R. (1981). Effects of Coupling Agents on the Rheological Properties, Processability, and Mechanical Properties of Filled Polypropylene. *Polymer Engineering & Science*, *21*(4), 196–204. http://doi.org/10.1002/pen.760210404

He, J., Shao, W., Zhang, L., Deng, C., & Li, C. (2009). Crystallization Behavior and UV-Protection Property of PET-ZnO Nanocomposites Prepared by In Situ Polymerization. *Journal of Applied Polymer Science*, *114*(2), 1303–1311. http://doi.org/10.1002/app.30614

Heino, M., Kirjava, J., Hietaoja, P., & Seppala, J. (1997). Compatibilization of Polyethylene Terephthalate/Polypropylene Blends with Styrene–Ethylene/Butylene– Styrene (SEBS) Block Copolymers. *Journal of Applied Polymer Science*, *65*(2), 241–249. http://doi.org/10.1002/(SICI)1097-4628(19970711)65:2<241::AID-APP4>3.0.CO;2-O

Hoffman, W. (1988). *Synthetic Rubber, Rubber Technology Handbook*. Munich: Hanser Publisher.

Holland, B. J., & Hay, J. N. (2002). The thermal degradation of PET and analogous polyesters measured by thermal analysis–Fourier transform infrared spectroscopy. *Polymer*, *43*(6), 1835–1847. http://doi.org/10.1016/S0032-3861(01)00775-3

Hrdlička, Z., Cebriá, P. M. M., Štefan, V., & Kuta, A. (2016). Thermoplastic Elastomeric Blends Based on Waste Tires and Polyethylene: The Role of Rubber Particle Size. *Progress in Rubber, Plastics and Recycling Technology*, *32*(3), 129–142.

Huang, X., Ke, Q., Kim, C., Zhong, H., Wei, P., Wang, G., … Jiang, P. (2007). Nonisothermal Crystallization Behavior and Nucleation of LDPE/Al Nano- and Microcomposites. *Polymer Engineering and Science*, *47*(7), 1052–1061. http://doi.org/10.1002/pen.20784

Imamura, N., Sakamoto, H., Higuchi, Y., Yamamoto, H., Kawasaki, S., Yamada, K., … Nishino, T. (2014). Effectiveness of Compatibilizer on Mechanical Properties of Recycled PET Blends with PE, PP, and PS. *Materials Sciences and Applications*, *5*,

548–555. http://doi.org/10.4236/msa.2014.58057

Jacob, C., De, P. P., Bhowmick, A. K., & De, S. K. (2001). Recycling of EPDM Waste. II. Replacement of Virgin Rubber by Ground EPDM Vulcanizate in EPDM/PP Thermoplastic Elastomeric Composition. *Journal of Applied Polymer Science*, *82*(13), 3304–3312. http://doi.org/10.1002/app.2189

Jacob, M., Francis, B., & Thomas, S. (2006). Dynamical Mechanical Analysis of Sisal/Oil Palm Hybrid Fiber-Reinforced Natural Rubber Composites. *Polymer Composites*, *27*, 671–680. http://doi.org/10.1002/pc.20250

Jain, A. K., Gupta, N. K., & Nagpal, A. K. (2000). Effect Of Dynamic Cross-Linking On Melt Rheological Properties Of Polypropylene/Ethylene-Propylene-Diene Rubber Blends. *Journal of Applied Polymer Science*, *77*(7), 1488–1505. http://doi.org/10.1002/1097-4628(20000815)77:7<1488::AID-APP10>3.0.CO;2-K

Jalilvand, A. R., Ghasemi, I., Karrabi, M., & Azizi, H. (2007). A Study of EPDM Devulcanization in a Co-rotating Twin-screw Extruder. *Iranian Polymer Journal*, *16*(5), 327–335.

Jang, J.-W., Yoo, T.-S., Oh, J.-H., & Iwasaki, I. (1998). Discarded tire recycling practices in the United States, Japan and Korea. *Resources, Conservation and Recycling*, *22*(1), 1–14. http://doi.org/10.1016/S0921-3449(97)00041-4

John, B., Varughese, K. T., Oommen, Z., Pötschke, P., & Thomas, S. (2003). Dynamic Mechanical Behavior of High-Density Polyethylene/Ethylene Vinyl Acetate Copolymer Blends: The Effects of the Blend Ratio, Reactive Compatibilization, and Dynamic Vulcanization. *Journal of Applied Polymer Science*, *87*(13), 2083–2099. http://doi.org/10.1002/app.11458

Joseph, P. V., Joseph, K., & Thomas, S. (1999). Effect of processing variables on the mechanical properties of sisal-fiber-reinforced polypropylene composites. *Composites Science and Technology*, *59*(11), 1625–1640. http://doi.org/10.1016/S0266-3538(99)00024-X

Kakroodi, A. R., Bainier, J., & Rodrigue, D. (2012). Mechanical and Morphological Properties of Flax Fiber Reinforced High Density Polyethylene/Recycled Rubber Composites. *International Polymer Processing*, *27*(2), 196–204.

Kakroodi, A. R., Kazemi, Y., & Rodrigue, D. (2013). Mechanical, rheological, morphological and water absorption properties of maleated polyethylene/hemp composites: Effect of ground tire rubber addition. *Composites Part B: Engineering*, *51*, 337–344.

Kakroodi, A. R., & Rodrigue, D. (2013). Highly filled thermoplastic elastomers from ground tire rubber, maleated polyethylene and high density polyethylene. *Plastics, Rubber and*

Composites, *42*(3), 115–122. http://doi.org/10.1179/1743289812Y.0000000042

Karger-Kocsis, J. (1995). *Polypropylene structure, blends and composites: composites*. Springer Science+Business Media Dordrecht.

Karger-Kocsis, J., Mészáros, L., & Bárány, T. (2013). Ground tyre rubber (GTR) in thermoplastics, thermosets, and rubbers. *Journal of Materials Science*, *48*(1), 1–38. http://doi.org/10.1007/s10853-012-6564-2

Kayaisang, S., Amornsakchai, T., & Saikrasun, S. (2013). Potential utilization of recycled PET in comparison with liquid crystalline polymer as an additive for HDPE based composite fibers: Comparative investigation on mechanical performance of cross-ply laminates. *Journal of Polymer Engineering*, *33*(9), 793–802. http://doi.org/10.1515/polyeng-2013-0155

Ke, F., Jiang, X., Xu, H., Ji, J., & Su, Y. (2012). Ternary nano-$CaCO_3$/poly(ethylene terephthalate) fiber/polypropylene composites: Increased impact strength and reinforcing mechanism. *Composites Science and Technology*, *72*(5), 574–579. http://doi.org/10.1016/j.compscitech.2012.01.001

Khanam, P. N., & AlMaadeed, M. A. A. (2015). Processing and characterization of polyethylene-based composites. *Advanced Manufacturing: Polymer & Composites Science*, *1*(2), 63–79. http://doi.org/10.1179/2055035915Y.0000000002

Kim, J. I., Ryu, S. H., & Chang, Y. W. (2000). Mechanical and Dynamic Mechanical Properties of Waste Rubber Powder/HDPE Composite. *Journal of Applied Polymer Science*, *77*, 2595–2602. http://doi.org/10.1002/1097-4628(20000919)77:12<2595::AID-APP60>3.0.CO;2-C

Kim, J. K., Lee, S. H., & Balasubramanian, M. (2006). A Comparative Study of Effect of Compatibilization Agent on Untreated and Ultrasonically Treated Waste Ground Rubber Tire and Polyolefin Blends. *Ciência e Tecnologia*, *16*(4), 263–268.

Kim, J. K., Lee, S. H., Paglicawan, M. a., & Balasubramanian, M. (2007). Effects of Extruder Parameters and Compositions on Mechanical Properties and Morphology of Maleic Anhydride Grafted Polypropylene/Waste Tire Blends. *Polymer-Plastics Technology and Engineering*, *46*(1), 19–29. http://doi.org/10.1080/03602550600916233

Klyosov, A. A. (2007). *Wood-plastic composites*. Hoboken: John Wiley & Sons.

Kumaran, G. S., Lakshmipathy, M., & Mushule, N. (2011). Analysis of the Transport Properties of Tyre Fiber Modified Concrete. *American Journal of Engineering and Applied Sciences*, *4*(3), 400–404.

Lee, S. H., Balasubramanian, M., & Kim, J. K. (2007a). Dynamic Reaction inside Co-Rotating Twin Screw Extruder. I. Truck Tire Model Material/Polypropylene Blends.

Journal of Applied Polymer Science, *106*, 3193–3208. http://doi.org/10.1002/app.26489

Lee, S. H., Balasubramanian, M., & Kim, J. K. (2007b). Dynamic Reaction inside Co-Rotating Twin Screw Extruder. II. Waste Ground Rubber Tire Powder/Polypropylene Blends. *Journal of Applied Polymer Science*, *106*(5), 3209–3219. http://doi.org/10.1002/app.26490

Lei, Y., & Wu, Q. (2012). High density polyethylene and poly(ethylene terephthalate) in situ sub-micro-fibril blends as a matrix for wood plastic composites. *Composites: Part A*, *43*(1), 73–78. http://doi.org/10.1016/j.compositesa.2011.09.012

Lei, Y., Wu, Q., Clemons, C. M., & Guo, W. (2009). Phase Structure and Properties of Poly(ethylene terephthalate)/High-Density Polyethylene Based on Recycled Materials. *Journal of Applied Polymer Science*, *113*, 1710–1719. http://doi.org/10.1002/app.30178

Li, R., Yu, W., & Zhou, C. (2006a). Phase Behavior and its Viscoelastic Responses of Poly(methyl methacrylate) and Poly(styrene-co-maleic anhydride) Blend Systems. *Polymer Bulletin*, *56*, 455–466. http://doi.org/10.1007/s00289-005-0499-6

Li, R., Yu, W., & Zhou, C. (2006b). Rheological Characterization of Droplet-Matrix versus Co-Continuous Morphology. *Journal of Macromolecular Science, Part B: Physics*, *45*(5), 889–898. http://doi.org/10.1080/00222340600777496

Li, Y., Zhang, Y., & Zahang, Y. (2003). Mechanical Properties of High-Density Polyethylene/Scrap Rubber Powder Composites Modified with Ethylene–Propylene–Diene Terpolymer, Dicumyl Peroxide, and Silicone Oil. *Journal of Applied Polymer Science*, *88*(8), 2020–2027. http://doi.org/10.1002/app.11907

Li, Y., Zhang, Y., & Zhang, Y. (2004). Morphology and mechanical properties of HDPE/SRP/elastomer composites: Effect of elastomer polarity. *Polymer Testing*, *23*(1), 83–90. http://doi.org/10.1016/S0142-9418(03)00065-5

Liang, H. (2015). Characterization and Surface Modification of Rubber from Recycled Tires.

Liang, H., Hardy, J.-M., Rodrigue, D., & Brisson, J. (2014). EPDM Recycled Rubber Powder Characterization: Thermal and Thermogravimetric Analysis. *Rubber Chemistry and Technology*, *87*(3), 538–556.

Liang, H., Rodrigue, D., & Brisson, J. (2015). Characterization of recycled styrene butadiene rubber ground tire rubber: Combining X-ray fluorescence, differential scanning calorimetry, and dynamical thermal analysis for quality control. *Journal of Applied Polymer Science*, *132*, 42692. http://doi.org/10.1002/app.42692

Lima, P., Magalhães Da Silva, S. P., Oliveira, J., & Costa, V. (2015). Rheological properties of ground tyre rubber based thermoplastic elastomeric blends. *Polymer Testing*, *45*, 58–67. http://doi.org/10.1016/j.polymertesting.2015.05.006

Lu, X., Wang, W., & Yu, L. (2014). Waste Ground Rubber Tire Powder/Thermoplastic Vulcanizate Blends: Preparation, Characterization, and Compatibility. *Journal of Applied Polymer Science*, *131*(3), 39868. http://doi.org/10.1002/app.39868

Ma, L., Wang, M., & Ge, X. (2013). Surface treatment of poly (ethylene terephthalate) by gamma-ray induced graft copolymerization of methyl acrylate and its toughening effect on poly (ethylene terephthalate)/elastomer blend. *Radiation Physics and Chemistry*, *90*, 92–97. http://doi.org/10.1016/j.radphyschem.2013.04.004

Maderuelo-Sanz, R., Nadal-Gisbert, A. V, Crespo-Amorós, J. E., & Parres-García, F. (2012). A novel sound absorber with recycled fibers coming from end of life tires (ELTs). *Applied Acoustics*, *73*(4), 402–408. http://doi.org/10.1016/j.apacoust.2011.12.001

Magioli, M., Sirqueira, A. S., & Soares, B. G. (2010). The effect of dynamic vulcanization on the mechanical, dynamic mechanical and fatigue properties of TPV based on polypropylene and ground tire rubber. *Polymer Testing*, *29*(7), 840–848. http://doi.org/10.1016/j.polymertesting.2010.07.008

Mahallati, P., Hassanabadi, H. M., Wilhelm, M., & Rodrigue, D. (2016). Rheological Characterization of Thermoplastic Elastomers (TPE) Based on PP and Recycled EPDM. *Applied Rheology*, *26*, 33503. http://doi.org/10.3933/APPLRHEOL-26-33503

Mahallati, P., & Rodrigue, D. (2014). Effect of feeding strategy on the mechanical properties of PP/Recycled EPDM/PP-g-MA blends. *International Polymer Processing*, *29*(2), 280–286.

Mahallati, P., & Rodrigue, D. (2015). Effect of Feeding Strategy on the Properties of PP/Recycled EPDM Blends. *International Polymer Processing*, *30*(2), 276–283. http://doi.org/10.3139/217.3008

Mandal, A. K., Chakraborty, D., & Siddhanta, S. K. (2014). Effect of the Compatibilizer, on the Engineering Properties of TPV Based on Hypalon and PP Prepared by Dynamic Vulcanization. *Journal of Applied Polymer Science*, *131*(11), 40312. http://doi.org/10.1002/app.40312

Martínez-Cruz, E., Martínez-Barrera, G., & Martínez-López, M. (2013). Polymer concrete reinforced with recycled-tire fibers: Mechanical properties. *IOP Conference Series: Materials Science and Engineering*, *45*(1), 12026. http://doi.org/10.1088/1757-899X/45/1/012026

Mehrabzadeh, M., & Nia, K. H. (1999). Impact Modification of Polypropylene by Ethylene Propylene Copolymer-Grafted Maleic Anhydride. *Journal of Applied Polymer Science*, *72*(10), 1257–1265. http://doi.org/10.1002/(SICI)1097-4628(19990606)72:10<1257::AID-APP4>3.0.CO;2-7

Miller, F. A., & Wilkins, C. H. (1952). Infrared Spectra and Characteristic Frequencies of

Inorganic Ions. *Analytical Chemistry*, *24*(8), 1253–1294.

Moghaddamzadeh, S., & Rodrigue, D. (2017a). The effect of polyester recycled tire fibers mixed with ground tire rubber on polyethylene composites Part I: Morphological analysis. *Progress in Rubber, Plastics and Recycling Technology*.

Moghaddamzadeh, S., & Rodrigue, D. (2017b). The effect of polyester recycled tire fibers mixed with ground tire rubber on polyethylene composites Part II: Physical-Mechanical analysis. *Progress in Rubber, Plastics and Recycling Technology*.

Mohanty, S., & Nayak, S. K. (2010). Short Bamboo Fiber-reinforced HDPE Composites: Influence of Fiber Content and Modification on Strength of the Composite. *Journal of Reinforced Plastics and Composites*, *29*(14), 2199–2210. http://doi.org/10.1177/0731684409345618

Mohanty, S., Verma, S. K., & Nayak, S. K. (2006). Dynamic mechanical and thermal properties of MAPE treated jute/HDPE composites. *Composites Science and Technology*, *66*, 538–547. http://doi.org/10.1016/j.compscitech.2005.06.014

N. Mostofi, Nazockdast, H., & Mohammadigoushki, H. (2009). Study on Morphology and Viscoelastic Properties of PP/PET/SEBS Ternary Blend and their Fibers. *Journal of Applied Polymer Science*, *114*, 3737–3743. http://doi.org/10.1002/app.30612

Naskar, A. K., De, S. K., & Bhowmick, A. K. (2002). Thermoplastic elastomeric composition based on maleic anhydride–grafted ground rubber tire. *Journal of Applied Polymer Science*, *84*(2), 370–378.

Nishida, H. (2011). Development of materials and technologies for control of polymer recycling. *Polymer Journal*, *43*(5), 435–447. http://doi.org/10.1038/pj.2011.16

Oliphant, K., & Baker, W. E. (1993). The Use of Cryogenically Ground Rubber Tires as a Filler in Polyolefin Blends. *Polymer Engineering & Science*, *33*(3), 166–174. http://doi.org/10.1002/pen.760330307

Oliphant, K., Rajalingam, P., & Baker, W. E. (1993). *Ground Rubber Tire-Polymer Composites*. Toronto: ChemTec Publishing.

Pehlken, A., & Essadiqi, E. (2005). *Scrap Tire Recycling in Canada*.

Pei, X., Evstatiev, M., & Friedrich, K. (2012). Mechanical and Tribological Properties of PET/HDPE MFCs. *International Journal of Polymeric Materials*, *61*(12), 963–977. http://doi.org/10.1080/00914037.2011.610065

Phinyocheep, P., Axtell, F. H., & Laosee, T. (2002). Influence of Compatibilizers on Mechanical Properties , Crystallization , and Morphology of Polypropylene/Scrap Rubber Dust Blends. *Journal of Applied Polymer Science*, *86*, 148–159.

http://doi.org/10.1002/app.10917

Pracella, M., & Chionna, D. (2004). Functionalization of styrene-olefin block copolymers by melt radical grafting of glycidyl methacrylate and reactive blending with PET. *Macromolecular Symposia*, *218*, 173–182. http://doi.org/10.1002/masy.200451418

Pracella, M., Rolla, L., Chionna, D., & Galeski, A. (2002). Compatibilization and properties of poly (ethylene terephthalate)/polyethylene blends based on recycled materials. *Macromolecular Chemistry and Physics*, *203*, 1473–1485.

Prut, E., Kuznetsova, O., Karger-Kocsis, J., & Solomatin, D. (2012). Rheological properties of ground rubber tire filled isotactic polypropylenes of different molecular weight characteristics. *Journal of Reinforced Plastics and Composites*, *31*(24), 1758–1771. http://doi.org/10.1177/0731684412449700

Rajalingam, P., & Baker, W. E. (1992). The Role of Functional Polymers in Ground Rubber Tire-Polyethylene Composite. *Rubber Chemistry and Technology*, *65*(5), 908–916. http://doi.org/10.5254/1.3538650

Rajalingam, P., Sharpe, J., & Baker, W. E. (1993). Ground Rubber Tire/Thermoplastic Composites: Effect of Different Ground Rubber Tires. *Rubber Chemistry and Technology*, *66*(4), 664–677. http://doi.org/10.5254/1.3538337

Rajan, V. V, Dierkes, W. K., Joseph, R., & Noordermeer, J. W. M. (2006). Science and technology of rubber reclamation with special attention to NR-based waste latex products. *Progress in Polymer Science*, *31*(9), 811–834. http://doi.org/10.1016/j.progpolymsci.2006.08.003

Ramarad, S., Khalid, M., Ratnam, C. T., Chuah, A. L., & Rashmi, W. (2015). Waste tire rubber in polymer blends: A review on the evolution, properties and future. *Progress in Materials Science*, *72*, 100–140. http://doi.org/10.1016/j.pmatsci.2015.02.004

Robertson, G. L. (2006). *Food packaging principles and practice*. Boca Raton: CRC Press.

Roche, N., Ichchou, M. N., Salvia, M., & Chettah, A. (2011). Dynamic damping properties of thermoplastic elastomers based on EVA and recycled ground tire rubber. *Journal of Elastomers and Plastics*, *43*(4), 317–340. http://doi.org/10.1177/0095244311398631

Rodgers, B., & Waddell, W. (2011). *Science and technology of Rubber*. *Tire engineering*. United States of America: Elsevier Academic Press.

Sahajwalla, V., Zaharia, M., Rahman, M., Khanna, R., Saha-Chaudhury, N., O'Kane, P., … Knights, D. (2011). Recycling Rubber Tyres and Waste Plastics in EAF Steelmaking. *Steel Research International*, *82*(5), 566–572. http://doi.org/10.1002/srin.201100047

Saleesung, T., Saeoui, P., & Sirisinha, C. (2010). Mechanical and thermal properties of

thermoplastic elastomer based on low density polyethylene and ultra-fine fully-vulcanized acrylonitrile butadiene rubber powder (UFNBRP). *Polymer Testing*, *29*(8), 977–983. http://doi.org/10.1016/j.polymertesting.2010.08.008

Satapathy, S., Nando, B., Jose, J., & Nag, A. (2008). Mechanical Properties and Fracture Behavior of Short PET Fiber-Waste Polyethylene Composites. *Journal of Reinforced Plastics and Composites*, *27*(9), 967–984. http://doi.org/10.1177/0731684407086626

Scaffaro, R., Dintcheva, N. T., Nocilla, M. A., & La Mantia, F. P. (2005). Formulation, characterization and optimization of the processing condition of blends of recycled polyethylene and ground tyre rubber: Mechanical and rheological analysis. *Polymer Degradation and Stability*, *90*(2), 281–287. http://doi.org/10.1016/j.polymdegradstab.2005.03.022

Sewda, K., & Maiti, S. N. (2013). Dynamic mechanical properties of high density polyethylene and teak wood flour composites. *Polymer Bulletin*, *70*(10), 2657–2674. http://doi.org/10.1007/s00289-013-0941-0

Shanmugharaj, A. M., Kim, J. K., & Ryu, S. H. (2005). UV surface modification of waste tire powder: Characterization and its influence on the properties of polypropylene/waste powder composites. *Polymer Testing*, *24*(6), 739–745. http://doi.org/10.1016/j.polymertesting.2005.04.006

Si, H., Chen, T., & Zhang, Y. (2013). Effects of High Shear Stress on the Devulcanization of Ground Tire Rubber in a Twin-Screw Extruder. *Journal of Applied Polymer Science*, *128*(4), 2307–2318. http://doi.org/10.1002/app.38170

Sienkiewicz, M., Kucinska-Lipka, J., Janik, H., & Balas, A. (2012). Progress in used tyres management in the European Union: a review. *Waste Management*, *32*(10), 1742–1751. http://doi.org/10.1016/j.wasman.2012.05.010

Sircar, A. K. (1992). Analysis of elastomer vulcanizate composition by TG-DTG techniques. *Rubber Chemistry and Technology*, *65*(3), 503–526.

Smith, W. C. (1994). Automotives: A major textile market. *Textile World*, *144*, 68–69.

Sonnier, R., Leroy, E., Clerc, L., Bergeret, A., & Lopez-Cuesta, J. M. (2006). Compatibilisation of polyethylene/ground tyre rubber blends by γ irradiation. *Polymer Degradation and Stability*, *91*(10), 2375–2379. http://doi.org/10.1016/j.polymdegradstab.2006.04.001

Sripornsawat, B., Saiwari, S., Pichaiyut, S., & Nakason, C. (2016). Influence of ground tire rubber devulcanization conditions on properties of its thermoplastic vulcanizate blends with copolyester. *European Polymer Journal*, *85*, 279–297. http://doi.org/10.1016/j.eurpolymj.2016.10.031

Sunthonpagasit, N., & Duffey, M. R. (2004). Scrap tires to crumb rubber: feasibility analysis for processing facilities. *Resources, Conservation and Recycling*, *40*(4), 281–299. http://doi.org/10.1016/S0921-3449(03)00073-9

Tantayanon, S., & Juikham, S. (2004). Enhanced Toughening of Poly(propylene) with Reclaimed-Tire Rubber. *Journal of Applied Polymer Science*, *91*(1), 510–515. http://doi.org/10.1002/app.13182

Tolstov, A., Grigoryeva, O., Fainleib, A., Danilenko, I., Spanoudaki, A., Pissis, P., & Grenet, J. (2007). Reactive Compatibilization of Polyethylene/Ground Tire Rubber Inhomogeneous Blends via Interactions of Pre-Functionalized Polymers in Interface. *Macromolecular Symposia*, *254*(1), 226–232. http://doi.org/10.1002/masy.200750834

Torres, N., Robin, J. J., & Boutevin, B. (2001). Chemical Modification of Virgin and Recycled Poly(ethylene terephthalate) by Adding of Chain Extenders during Processing. *Journal of Applied Polymer Science*, *79*(10), 1816–1824.

Trinkle, S., Walter, P., & Friedrich, C. (2002). Van Gurp-Palmen Plot II - classification of long chain branched polymers by their topology. *Rheologica Acta*, *41*, 103–113. http://doi.org/10.1007/s003970200010

van Beukering, P. J. H., & Janssen, M. A. (2001). Trade and recycling of used tyres in Western and Eastern Europe. *Resources, Conservation and Recycling*, *33*(4), 235–265. http://doi.org/10.1016/S0921-3449(01)00082-9

van Bruggen, E. P. A., Koster, R. P., Picken, S. J., & Ragaert, K. (2016). Influence of processing parameters and composition on the effective compatibilization of polypropylene-poly(ethylene terephthalate) blends. *International Polymer Processing*, *31*(2), 179–187. http://doi.org/10.3139/217.3124

Vasile, C., & Pascu, M. (2005). *Practical guide to polyethylene*. Shawbury: Rapra Technology Limited.

Veilleux, J., & Rodrigue, D. (2016). Properties of recycled PS/SBR blends: Effect of SBR pretreatment. *Progress in Rubber, Plastics and Recycling Technology*, *32*(3), 111–128.

Wall, D. (1989). The processing of fiber reinforced thermoplastics using co-rotating twin screw extruders. *Polymer Composites*, *10*(2), 98–102.

Wang, L., Lang, F., Li, S., Du, F., & Wang, Z. (2014). Thermoplastic elastomers based on high-density polyethylene and waste ground rubber tire composites compatibilized by styrene-butadiene block copolymer. *Journal of Thermoplastic Composite Materials*, *27*(11), 1479–1492. http://doi.org/10.1177/0892705712473628

Wang, W.-K., Yang, W., Bao, R.-Y., Xie, B.-H., & Yang, M.-B. (2011). Effect of repetitive processing on the mechanical properties and fracture toughness of dynamically

vulcanized iPP/EPDM blends. *Journal of Applied Polymer Science*, *120*(1), 86–94. http://doi.org/10.1002/app.33072

Wang, Z., Zhang, Y., Du, F., & Wang, X. (2012). Thermoplastic elastomer based on high impact polystyrene/ethylene-vinyl acetate copolymer/waste ground rubber tire powder composites compatibilized by styrene-butadiene-styrene block copolymer. *Materials Chemistry and Physics*, *136*(2–3), 1124–1129. http://doi.org/10.1016/j.matchemphys.2012.08.063

Yang, G. C. C. (1993). Recycling of discarded tires in Taiwan. *Resources, Conservation and Recycling*, *9*(3), 191–199. http://doi.org/10.1016/0921-3449(93)90003-X

Yazdani, H., Karrabi, M., Ghasmi, I., Azizi, H., & Bakhshandeh, G. R. (2011). Devulcanization of Waste Tires Using a Twin-Screw Extruder: The Effects of Processing Conditions. *Journal of Vinyl & Addittive Technology*, *17*, 64–69. http://doi.org/10.1002/vnl.20257

Yilmazer, U., & Cansever, M. (2002). Effects of Processing Conditions on the Fiber Length Distribution and Mechanical Properties of Glass Fiber Reinforced Nylon 6. *Polymer Composites*, *23*(1), 61–71.

Yin, Y., Liu, M., Zheng, X., Shen, S. Z., & Deng, P. (2013). Improvement of Compatibility of Poly(ethylene terephthalate) and Poly(ethylene octene) Blends by γ-Irradiation. *Journal of Applied Polymer Science*, *127*(1), 200–207. http://doi.org/10.1002/app.37863

Zhang, H., Guo, W., Yu, Y., Li, B., & Wu, C. (2007). Structure and properties of compatibilized recycled poly (ethylene terephthalate)/linear low density polyethylene blends. *European Polymer Journal*, *43*(8), 3662–3670.

Zhang, S. L., Zhang, Z. X., Kang, D. J., Bang, D. S., & Kim, J. K. (2008). Preparation and characterization of thermoplastic elastomers (TPEs) based on waste polypropylene and waste ground rubber tire powder. *E-Polymers*, (160), 1–6.

Zhang, X., Lu, C., & Liang, M. (2011). Preparation of Thermoplastic Vulcanizates Based on Waste Crosslinked Polyethylene and Ground Tire Rubber Through Dynamic Vulcanization. *Journal of Applied Polymer Science*, *122*(3), 2110–2120.

Zhang, X., Zhu, X., Liang, M., & Lu, C. (2009). Improvement of the Properties of Ground Tire Rubber (GTR)-Filled Nitrile Rubber Vulcanizates Through Plasma Surface Modification of GTR Powder. *Journal of Applied Polymer Science*, *114*(2), 1118–1125. http://doi.org/10.1002/app.30626

Zhang, Y., Guo, W., Zhang, H., & Wu, C. (2009). Influence of chain extension on the compatibilization and properties of recycled poly (ethylene terephthalate)/linear low density polyethylene blends. *Polymer Degradation and Stability*, *94*(7), 1135–1141.

http://doi.org/10.1016/j.polymdegradstab.2009.03.010

Zhu, Y., Li, Z., Zhang, D., & Tanimoto, T. (2006). Thermal Behaviors of Poly(ethylene terephthalate)/SiO_2 Nanocomposites Prepared by Cryomilling. *Journal of Polymer Science Part B: Polymer Physics*, *44*(9), 1351–1356. http://doi.org/10.1002/polb.20788

Appendix (A): Extruder Screw Configuration

A.1 Extruder screw design

The extruder screw configuration design is shown as below. The numbers above elements indicate the screw profile orders.

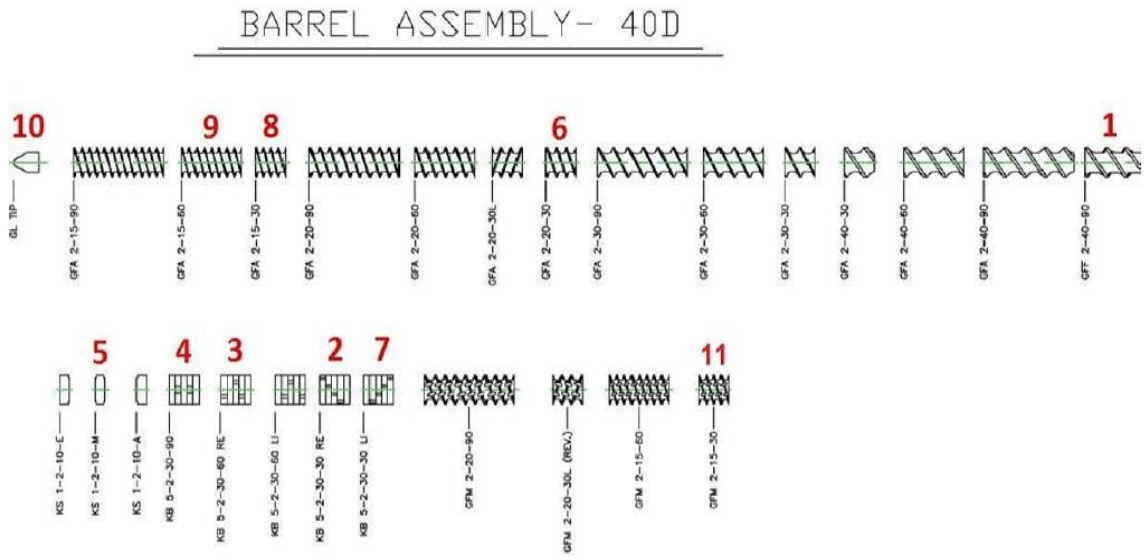

A.2 Screw profiles

It can be seen that the same screw profile was designed by using different elements for the extruder screw configurations as:

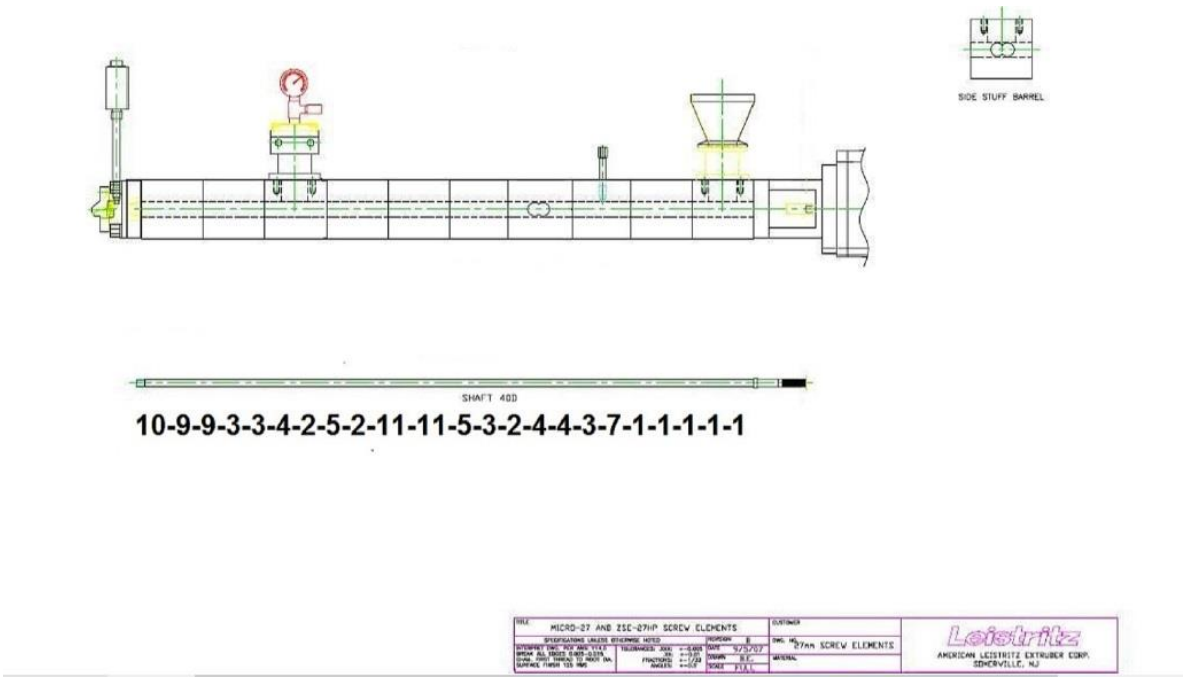

Scheme of the screw configuration design when using zone #1 (hopper) as the feeding zone. The presence of side stuffer can be seen in zone #4 which was not used during compounding for this research work. The numbers are related to the screw elements presented in section A.1.

Appendix (B): Injection molding conditions

Injection time: 4 s		Curing time: 25 s	
SM: 35 mm	SD: 3 mm	VS: 45%	PB: 15 MPa
V1: 80 mm/s	V2: 40 mm/s	V3: 60 mm/s	V4: 20 mm/s
S1: 21 mm	S2: 18 mm	S3: 7 mm	S4: 5 mm

LLDPE/RTF	P1 (MPa)	P2 (MPa)	P3 (MPa)
100/0	50	50	40
90/10	60	60	50
75/25	80	80	70
50/50	95	95	90